DEVELOPMENT OF DEGRADABLE POLYPROPYLENE BY RADIATION GRAFTING AND BLENDING WITH POLYLACTIC ACID

Thesis

Submitted for fulfillment of the Degree

of

Doctor of Philosophy

By

Dev Kumar Mandal
(Registration No.: 901401012)

Under the guidance of

Dr. Haripada Bhunia
Professor
Department of Chemical Engineering,
Thapar Institute of Engineering &
Technology (Deemed to be University), Patiala

Dr. Pramod K. Bajpai
Ex-Distinguished Professor
Department of Chemical Engineering,
Thapar Institute of Engineering &
Technology (Deemed to be University), Patiala

Department of Chemical Engineering
Thapar Institute of Engineering & Technology
(Deemed to be University)
Patiala – 147004, Punjab (India)
www.thapar.edu

February 2018

Dedicated

To

My Parents

Mr. Sugan Mandal & Mrs. Kalpana Mandal

And

My sisters and brother

Ms. Khema Rani Mandal, Ms. Ranu Mandal and Master Himanshu Mandal

Certificate

This is to certify that the thesis entitled **"Development of degradable polypropylene by radiation grafting and blending with polylactic acid"** being submitted by **Mr. Dev Kumar Mandal** to Department of Chemical Engineering, Thapar Institute of Engineering & Technology (Deemed to be University), Patiala in fulfillment of the degree of **Doctor of Philosophy**, is a record of bonafide research work carried out by him under our guidance and supervision and is worthy of consideration for the award of the degree of Doctor of Philosophy of the University.

The results embodied in the thesis have not been submitted in part or full to any other University or Institute for the award of any degree or diploma.

25-02-2018

(Haripada Bhunia)
Professor
Department of Chemical Engineering,
Thapar Institute of Engineering & Technology (Deemed to be University), Patiala

25-02-2018

(Pramod K. Bajpai)
Ex-Distinguished Professor
Department of Chemical Engineering,
Thapar Institute of Engineering & Technology (Deemed to be University), Patiala

Acknowledgements

I would like to express my sincere regard and gratitude to my supervisors **Dr. Pramod K. Bajpai,** Ex-Distinguished Professor and **Dr. Haripada Bhunia**, Professor, Department of Chemical Engineering, Thapar Institute of Engineering & Technology (Deemed to be University) for providing me such a valuable research opportunity. They provided me with motivation, knowledge and the tools to carry out this research and for future success. I am thankful for their constant encouragement, intellectual generosity and valuable contribution of their time throughout the course of this work.

I am extremely thankful to **Prof. Prakash Gopalan**, Director, Thapar Institute of Engineering & Technology (Deemed to be University), **Shri Gurbinder Singh, Registrar,** Thapar Institute of Engineering & Technology (Deemed to be University), **Prof. O. P. Pandey**, Dean of Research & Sponsored Projects, Thapar Institute of Engineering & Technology (Deemed to be University) and **Dr. Raj K. Gupta**, Professor (Head), Department of Chemical Engineering, Thapar Institute of Engineering & Technology (Deemed to be University) for giving the necessary approvals and kind support to perform this research work.

I would like to express the utmost thank to my doctoral committee members **Dr. Rajeev Mehta**, Professor, Department of Chemical Engineering, Thapar Institute of Engineering & Technology (Deemed to be University); **Dr. Avinash Chandra**, Assistant Professor, Department of Chemical Engineering, Thapar Institute of Engineering & Technology (Deemed to be University) and **Dr. B. N. Chudasama,** Associate Professor, School of Physics & Material Science, Thapar Institute of Engineering & Technology (Deemed to be University) for providing their expertise and vast experience throughout the course of this research in a patient and encouraging manner. The generous support of all the staff members

of Department of Chemical Engineering, Thapar Institute of Engineering & Technology (Deemed to be University) is greatly appreciated.

I am also grateful to **Dr. Golok B. Nando**, Ex-Professor, Rubber Technology Centre, **IIT Kharagpur**, West Bengal for his kind support and guidance in performing some part of the experimental work in his research laboratory. His constructive comments have been of immense value in improving the quality of my research work.

Also, my sincere thanks to **Dr. Lalit Varshney, Dr. Abhinav Dubey** and **Mr. Chandrasekhar V. Chaudhari,** Radiation Technology Development Division, BARC, Mumbai for their kind support and guidance in performing some part of the experimental work in their research laboratory.

I express deep sense of gratitude to my senior **Dr. Gaurav Madhu, Dr. Chitrakshi Goel,** and **Dr. Kimi Jain**, my colleagues **Mr. Deepak Tiwari, Mrs. Meenakshi Sheoran Nandal, Ms. Metali Sarkar, Mrs. Balpreet Kaur, Mr. Jasminder Singh, Ms. Simarjot Kaur and Mr. Sunil Sable** for providing all the encouragement and support at various stages of work. I express my deepest gratitude to my parents **Mr. Sugan Mandal** and **Mrs. Kalpana Mandal** and my sisters and brother **Khama Rani Mandal, Ranu Mandal and Master Himanshu Mandal** for their love, never ending support, and encouragement and would like to dedicate this thesis to them.

Finally, I would like to gratefully acknowledge the financial support from **Department of Atomic Energy (DAE) - Board of Research in Nuclear Sciences (BRNS) and Bhabha Atomic Research Centre (BARC),** Government of India, Mumbai, through research project.

Above all, I express my indebtedness to the "**ALMIGHTY**" for all his blessing and kindness.

Dev Kumar Mandal

Abstract

Simultaneous radiation grafting was optimized to graft acrylic acid monomer on the polypropylene (PP) films to make them hydrophilic and enhance their biodegradability. Experiments were designed based on full factorial central composite design (response surface methodology) and influence of monomer concentration, radiation dose, inhibitor concentration, sulfuric acid concentration on degree of grafting was investigated. The extent of grafting was found to increase with increasing monomer concentration, inhibitor concentration and radiation dose. Different degrees of grafted PP were used for different applications. 35% grafted PP was chosen as our optimum grafted material due to desirable tensile strength (above 20 MPa) for packaging application. The targeted 35% grafting could be achieved at the optimum conditions - monomer concentration 12.09 wt%, radiation dose 12.40 kGy, inhibitor concentration 0.07 M and sulfuric acid concentration 0.12 M. The grafted PP films at different degrees of grafting were tested for tensile properties and characterized by swelling test, Fourier transform infrared spectroscopy (FTIR), thermogravimetric analysis (TGA), differential scanning calorimetry (DSC) and scanning electron microscopy (SEM). Successful grafting of acrylic acid onto PP films was indicated by FTIR and confirmed quantitatively by determination of carboxylic groups on the film surface. Tensile strength of grafted PP films decreased with increase in degree of grafting. The crystallinity of the grafted films was lower than that of PP film as indicated by DSC studies. Grafting of acrylic acid increased the roughness on the surface of PP films indicated by SEM studies. Thermal stability and degradation behavior of acrylic acid grafted polypropylene (PP-g-AAc) films were investigated by using thermogravimetric analysis (TGA) at four different heating rates 5, 10, 15 and 20 °C/min over a temperature range of 40 to 550 °C in nitrogen atmosphere. The kinetic parameters namely activation energy (E_a),

reaction order (n) and frequency factor (Z) were calculated by three multiple heating rate methods. The thermal stability of PP-g-AAc films is found to decrease with increase in degree of grafting. The TGA data and thermal kinetic parameters were also used to predict the lifetime of grafted PP films. The estimated lifetime of neat PP as well as grafted PP decreased with increase in temperature by all the three methods. Studies also indicated that E_a and lifetime of PP-g-AAc films decreased with increase in degree of grafting, which may also be helpful in biodegradation of grafted PP films. The maximum biodegradability of the 35% grafted film was ~ 6%. Residue after biodegradation of grafted samples were evaluated for ecotoxicological impact by microbes and plants (corn and tomato) growth test as per OECD 208 guidelines. Ecotoxicological test indicated that biodegradation intermediates were non-toxic in nature.

Melt blending technique was used to prepare blends of PP and PLA with or without compatibilizer, and pro-oxidant and composites of PP and compatibilized blend with nanoclay. Compression molding was used to prepare the films of blend and composite materials. The optimum weight of pro-oxidants and nanoclay was selected 0.2 and 2 wt% on the basis of tensile test results. Blends PP85PL15 and PP85PL15MA4 are the optimum from tensile strength point of view. CoSt and CaSt (0.2 wt%) were added separately to PP85PL15MA4 blend. Nanoclay was added separately to PP85PL15MA4 blend in 2 wt%. The optimized blends and composites were further characterized by FTIR, TGA, DSC, XRD, rheological studies, SEM, biodegradability test and ecotoxicological evaluation. Pseudo-plastic nature of all the blended and composite films was confirmed by rheological studies. Thermal stability of polypropylene films decreased with addition of polylactic acid as confirmed by TGA analysis. The thermal degradation kinetic parameters namely activation energy, order of reaction and frequency factor of the samples were determined over a temperature range of 30 to 550 °C under nitrogen atmosphere at four different heating rates

(5, 10, 15 and 20 °C/min). The activation energy was calculated by Kissinger, Kim-Park and Flynn-Wall methods. The activation energy value of PP was much higher than that of PLA. Whereas, addition of polylactic acid, pro-oxidant and nanoclay in PP decreased the activation energy. Addition of compatibilizer increased the compatibility and activation energy of blended films upto some extent. The lifetime of PP was found to decrease with addition of polylactic acid, pro-oxidant and nanoclay. This study indicated that the thermal degradation behavior and lifetime of the investigated samples depend on the fractions of constituents and heating rates. The maximum biodegradation of around 9% could be achieved for PP85PL15MA4CoSt0.2 blend. Biodegraded intermediates were non-toxic in nature as confirmed by ecotoxicological test.

Figure 1 shows schematic of the overall thesis work.

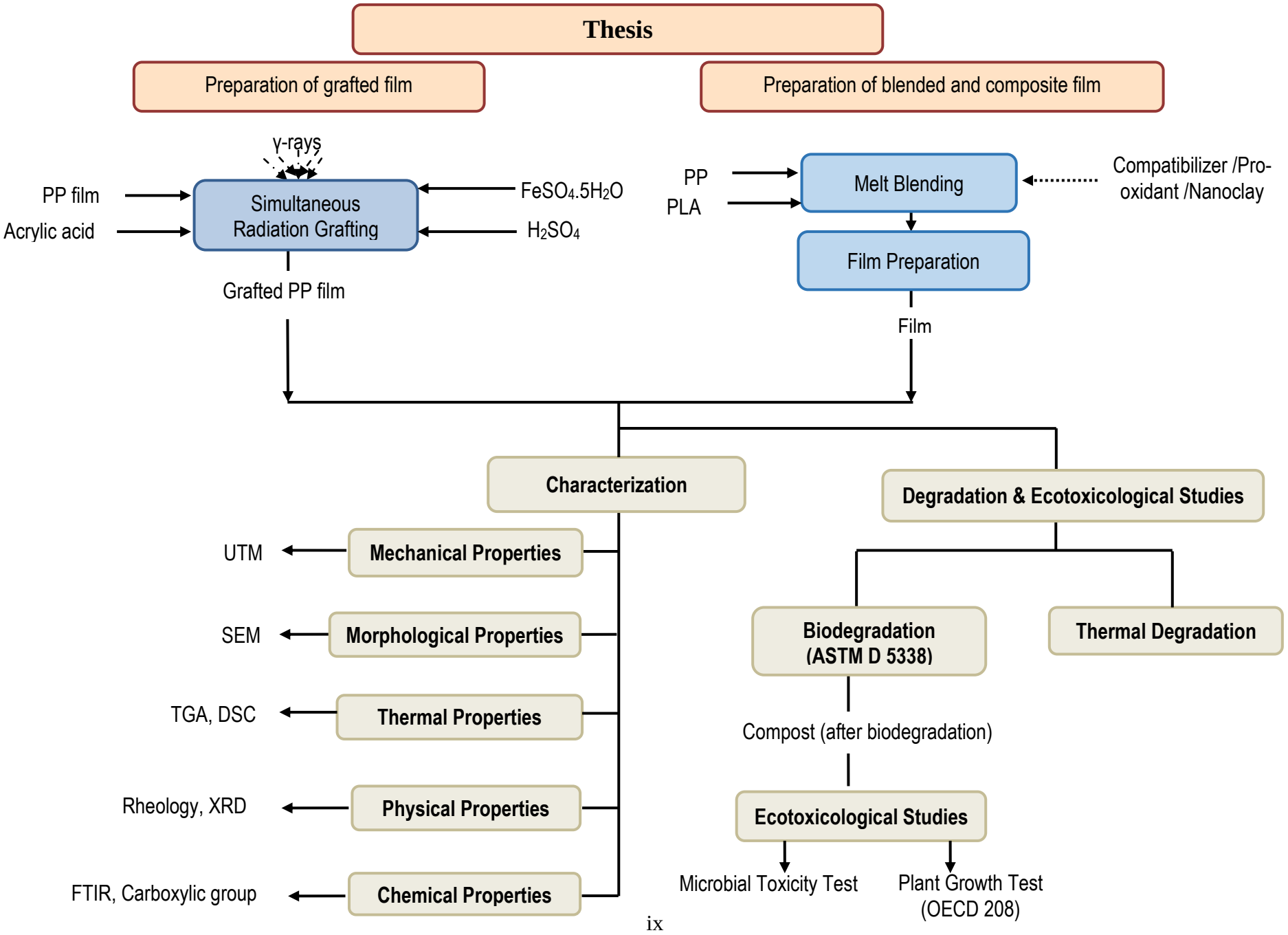

Figure 1 Schematic overall thesis work

Table of Contents

List of Figures

List of Tables

List of Symbols

CO_2	Carbon dioxide
$Co_2(Th)$	Theoretical carbon dioxide
Da	Dalton
E_a	Activation energy
$f(\alpha)$	Differential function of the kinetic model
G'	Storage modulus
G''	Loss modulus
ΔH_c	Enthalpy of crystallization
ΔH_f	Enthalpy of fusion
M_n	Number average molecular weight
M_w	Weight average molecular weight
MPa	Mega pascal
R	Universal gas constant
T	Absolute temperature
T_c	Crystallization temperature
T_g	Glass transition temperature
T_i	Initial degradation temperature
T_m	Melting temperature
T_{max}	Maximum degradation temperature
T_f	Final degradation temperature
t_f	Time of failure
X_c	Degree of crystallinity
Z	Frequency factor

Greek letters

α	Weight loss
β	Heating rate
γ	Shear strain
ω	Angular frequency
η^*	Complex viscosity
μ_m	Micrometer
A^o	Angstrom

List of Abbreviations

ASTM	American Society for Testing and Materials
CAGR	Compound annual growth rate
CaSt	Calcium stearate
CoSt	Cobalt stearate
DDR	Draw-down ratio
DSC	Differential scanning calorimetry
DTA	Differential thermal analysis
DTG	Differential themogravimetry
EB	Elongation at break
FTIR	Fourier transform infrared
PP	Polypropylene
HDPE	High density polyethylene
LDPE	Low density polyethylene
LLDPE	Linear low density polyethylene
MA	Maleic anhydride
AAc	Acrylic acid
PP-g-AAc	Polypropylene grafted acrylic acid
MA-g-PP	Maleic anhydride grafted polypropylene
MFI	Melt flow index
MWD	Molecular weight distribution
PCL	Poly(ε-caprolactone)
PE	Polyethylene
PHA	Poly(hydroxyalkanoates)
PHB	Poly(3-hydroxybutyrate)
phr	Parts per hundred of resin
PLA	Polylactic acid/polylactide

SEM	Scanning electron microscopy
TG	Thermogravimetry
TGA	Thermogravimetric analysis
TOC	Total organic carbon
XRD	X-ray Diffraction
OECD	Organisation for Economic Cooperation and Development
ISO	International Organization for Standardization
ANOVA	Analysis of variance
CFU	Colony forming units
FMGC	Fast moving consumer goods
MSW	Municipal solid waste
WEF	World economic forum

Chapter 1-Introduction

Polymers are macromolecule, or large molecule collection of many repeated subunits. These subunits can be extremely simple, where a simple molecule adds on to itself or other simple molecules. The word 'polymer' was although coined in 1833 by Jons Jacob Berzelius, but the polymers are in use since 15th century long before anyone understood what they were. When natural polymer was first discovered in 1496 by Columbus, the European explorer, as a material obtained from the exudates of a tree (*Heavea brasiliensis*). Polymers, both natural and synthetic, are created via polymerization of many small molecules, known as monomers. Many common classes of polymers are composed of hydrocarbons, compounds of carbon and hydrogen. These polymers are specifically made of carbon atoms bonded together, one to the next, into long chains that are called the backbone of the polymer. Polymers that contain carbon and hydrogen atoms are polyethylene, polypropylene, polybutylene and polystyrene. Polymers are classified in a number of ways such as their origin, line structure, physical properties & applications, method of formation, crystallinity, thermal behavior and degradability.

1.1 Polymers in flexible packaging

The flexible packaging market is one of the most dynamic packaging markets exhibiting diversified type of packaging and materials used across the regions. The global market value for flexible packaging is reach $99,621.9 million in 2018, grown at a compound annual growth rate (CAGR) of 5.1% from 2013 to 2018 driven by rising demand in major Asian markets such as India and China [1]. Worldwide production of plastics was 407 million tons in 2015. A major portion (~ 44%) of the globally plastics produced was used in the packaging industry [2]. The growth of packaging industry in India will be influenced by changing demographics such as increasing urbanization and growing of middle class consumers. During the period of 2016-2021

food industries and soft drinks industries will be the highest packaging market share (in units) with share growth rate of 3.4% and 1.3%, respectively. In case of packaging application, rigid plastics will be the major share gainers, with share growth rate of 0.6% during the period of 2016-2021. Whereas, flexible packaging will be leading the Indian packaging market with their share and will grow at a healthy compound annual growth rate (CAGR) of 8.9% during 2016-2021. The major contributions of flexible packaging are in the household care, food packaging and cosmetics & toiletries industries. This growth is largely driven by its low cost and flexibility to suit multiple shapes and sizes, convenience (zip-locks, plastic closures) [3]. Today, plastics are the material of choice in packaging for the sectors such as fast-moving consumer goods (FMCG), food and beverages, pharmaceuticals etc. Globally, plastics comprise of 42 percent of packaging with the combination of rigid and flexible plastics in packaging. Plastics are used heavily for packaging due to innovative visual appeal for customer attraction and convenience. Additionally, they improve the hygiene quotient and shelf-life of the products especially in food and beverages segment. Prominent polyolefins used in the packaging industries are polypropylene (PP) and polyethylene (PE) such as high density polyethylene (HDPE), low density polyethylene (LDPE), linear low density polyethylene (LLDPE). Each of these polymers exhibit unique characteristics and thus has distinct packaging applications. PP has excellent mechanical properties as well as good water barrier properties and thus is used in containers for milk, detergents, bleach, shampoo, deodorants, caps for bottles as well as flexible packaging for crackers, cereals, and snacks [4]. In India, industries are dominated by flexible plastic packaging. There has been a gradual shift from rigid to flexible packaging due to flexible packaging being visually appealing, cheaper and durable. Polyethylene and polypropylene account for 62% of polymer usage in flexible packaging Industry (Figure 1.1) [5].

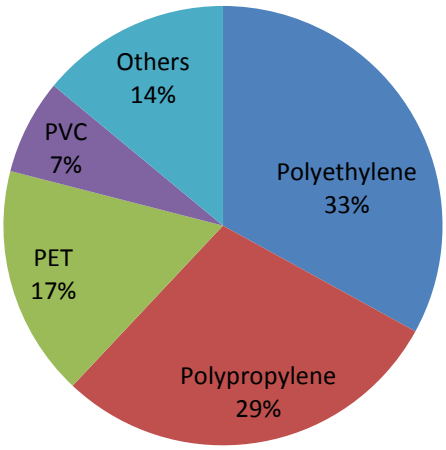

Figure 1.1. End use share of plastic product (%) [5]

1.1.1 Waste generation from packaging plastics

Several tonnes of polyolefin goods are thrown to landfill site every day, increasing the amount of municipal waste [6]. According to World Bank [7], plastic waste accounted for 8–12% of total municipal solid waste (MSW) generated in different countries all over the world. The actual percentage varies according to the income level of the people in the country. It was also estimated that global plastic waste generation in 2025 will increase to 9–13% of total MSW, which again varies according to country. In order to reduce the adverse effects brought by plastic waste, efforts have been made in promoting recovery of plastic waste for recycling [8]. On an average, 50% of the plastic waste generated in Europe is recovered, while the rest is sent to landfills.

The generation of plastic waste in India was 5.6 million metric tons per annum in 2012 [9]. As per estimation, the generation of plastic waste would be about 16.5 million metric ton by 2030 and trebling every 10 years. Plastic goods consumption in India is 12.5 million metric tons per

annum. In 2012-13, India's per capita plastics consumption was estimated 9.7 kg. Out of the total plastic waste, approx. 40% contribution is from the packaging industry. Each year, an estimated 500 billion to 1 trillion plastic bags are consumed worldwide, i.e., over 1 million plastic bags used per minute [10]. Building and construction is the second largest source with 20.3% of the total plastic waste. Automotive is the third sector with a share of 8.5%; electrical and electronic applications represent 5.6% of the plastic waste and are closely followed by agricultural applications which have a share of 4.3%. Other application sectors such as appliances, household and consumer products, furniture and medical products comprise a total of 21.7% of the plastic waste [11]. One of the worst consequences of plastic waste is a lot of it ends up in the ocean. Around 8 million tons of plastic waste enters the ocean every year, with Asian countries responsible for four-fifths of it, and at present there are 150 million tons in seas. The World Economic Forum (WEF) report says in 2014 there was 1 kg of plastic in the ocean for every 5 kg of fish; by 2025 the ratio will worsen to one to three; and by 2050 plastic will exceed fish by weight. In the terrestrial and marine coastal environment, the synthetic plastics accumulate at a rate of 25 million tons per year. A recent study conservatively estimated that 2,68,940 tons plastic particles are currently in the world's oceans [12]. India's contribution to plastic waste that is dumped into the world's oceans every year is a massive 60%. India generates around 56 lakh tons of plastic waste annually, where Delhi alone accounts for 9,600 metric tons per day.

1.1.2 Environmental implications from plastic waste

Plastic pollution involves the accumulation of plastic products in the environment that adversely affects wildlife, wildlife habitat, or humans [13]. Plastics that act as pollutants are categorized into micro-, meso-, or macro debris, based on size [14]. The prominence of plastic pollution is correlated with plastics being inexpensive and durable, which leads to high levels of plastics

used by humans [15]. However, it is slow to degrade. Plastic pollution can unfavorably affect lands, waterways and oceans. Living organisms, particularly marine animals, can also be affected through entanglement, direct ingestion of plastic waste, or through exposure to chemicals within plastics that cause interruptions in biological functions. The distribution of plastic debris is highly variable as a result of certain factors such as wind and ocean currents, coastline geography, urban areas, and trade routes. Human population in certain areas also plays a large role in this. Plastics are more likely to be found in enclosed regions such as the Caribbean.

Almost 90% of plastic debris that pollutes ocean water, which translates to 5.6 million tons, comes from ocean-based sources. Merchant ships expel cargo, sewage, used medical equipment, and other types of waste that contain plastic into the ocean. These plastic items can also accidentally end up in the water through negligent handling. The largest ocean-based source of plastic pollution is discarded fishing gear, responsible for up to 90% of plastic debris in some areas. This equipment includes a variety of traps and nets. A little over 10% of plastic debris in ocean water comes from land-based sources, responsible for 0.8 million tons every year. A source that has caused concern is landfills. Most waste in the form of plastic in landfills is single-use items such as packaging. Discarding plastics this way leads to accumulation [16]. Although disposing of plastic waste in landfills has less of a gas emission risk than disposal through incineration, the former has space limitations. A 2017 study found that 83% of tap water samples taken around the world contained plastic pollutants. This was the first study to focus on global drinking water pollution with plastics, and showed that with a contamination rate of 94%, tap water in the United States was the most polluted, followed by Lebanon and India. European countries such as the United Kingdom, Germany and France had the lowest contamination rate,

though still as high as 72%. This means that people may be ingesting between 3,000 and 4,000 micro particles of plastic from tap water per year. Sea turtles are affected by plastic pollution. Some species are consumers of jelly fish, but often mistake plastic bags for their natural prey.

Some of the tiniest bits of plastic are being consumed by small fish, in a part of the pelagic zone in the ocean called the mesopelagic zone, which is 200 to 1000 meters below the ocean surface, and completely dark. Not much is known about these fish, other than that there are many of them. They hide in the darkness of the ocean, avoiding predators and then swimming to the ocean's surface at night to feed. Plastics found in the stomachs of these fish were collected during malaspina's circumnavigation, a research project that studied the impact of global change on the oceans [17]. The most popular mesopelagic is the lantern fish. It resides in the central ocean gyres, a large system of rotating ocean currents. Since lantern fish serves as a primary food source for the fish that consumers purchase, including tuna and swordfish, the plastics they ingest become part of the food chain.

Plastic pollution does not only affect animals that live solely in oceans. Seabirds are also greatly affected. In 2004, it was estimated that gulls in the North Sea had an average of thirty pieces of plastic in their stomachs [18]. Seabirds often mistake trash floating on the ocean's surface as prey. Their food sources often have already ingested plastic debris, thus transferring the plastic from prey to predator. Ingested trash can obstruct and physically damage a bird's digestive system, reducing its digestive ability and can lead to malnutrition, starvation, and death.

1.2 Apparent solutions for plastic waste management

The 4 Rs, for plastic waste management are reduce, reuse, recycle and redevelop (Figure 1.2). We all know the reduce, reuse and recycle as a proposed plan to control the use of plastics and other wastes. Where redevelop is develop degradable plastic, when the plastic biodegrades down to humus or fertilizer and rejuvenates to the ground. In reduce, if people refuse plastic as a packaging material, the industry will decrease production for that purpose, and the associated problems such as energy use, pollution, and adverse health effects will diminish. In reuse, refillable plastic containers can be reused for many times, container reuse can lead to a substantial reduction in the demand for disposable plastic and reduced use of materials and energy, with the consequent reduced environmental impacts. In recycle, plastic waste is recycled in other valuable products. But, number of factors can complicate the recycling of plastics waste, such as the collection of the plastics waste, separation of different types of plastics, cleaning of the waste and possible pollution of the plastics. A further complicating factor is the low-value nature of most of the products that can be manufactured from recycled plastics.

In the rejuvenate, plastic biodegrades down to humus or fertilizer and rejuvenates the ground. The degradation of polyolefin material depends on the end-of-life options and the physico-chemical conditions (e.g. the presence of oxygen, temperature, light and specific microorganisms). The main end-of-life options for biodegradable polyolefins include.

- recycling (and reprocessing);
- incineration (and the other recovery options);
- biological waste treatments: composting and anaerobic digestion;
- landfill.

In the most cases, the nature of the degradable material would determine suitable end-of-life management practice. The most favorable final disposition, from an environmental point of view, for biodegradable plastics is represented by the composting process, taking into account that the process conditions in terms of humidity, oxygen, etc., must be strictly controlled in order to achieve appreciable results in terms of final products. Degradability of the polyolefins can be enhanced by (1) grafting with hydrophilic monomer such as acrylic acid, methacrylic acid acrylamide etc. and (2) blending with natural polymers such as cellulose [19], starch [20-23], PLA [24, 25], poly(ε-caprolactone) [26] etc., pro-oxidants viz. calcium stearate, magnesium stearate, etc [27], and nanoclay.

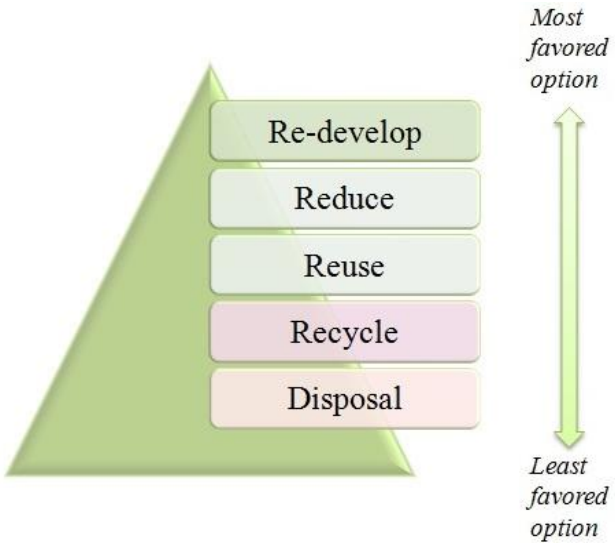

Figure 1.2 Options for handling plastic waste [28]

Biodegradable polymers

Biobased polymers include natural polymers (synthesized by living species such as plants, animals and microorganisms and extracted as polymers) and polymers synthesized from biobased monomers in laboratories or by industry. Natural polymers derived from biomass

(excluding microorganisms) are abundant and renewable in nature [29]. They are also biodegradable (capable of being converted/decomposed into simple/basic molecules by microorganisms), and thus they can reduce the strain on our landfills. These polymers exist in the form of polysaccharides (e.g. cellulose, starches and their derivatives, seaweed extracts such as carrageenan and alginates, chitosan [30] and pectin), proteins (whey protein, gelatin, corn zein, soy protein, collagen and wheat gluten) and lipids. The most prominent biodegradable plastic is poly-lactic acid (PLA) derived from plant material, typically corn (maize). It is increasingly being used for food applications, and is promoted as being compostable.

Polylactic acid (PLA)

Polylactic acid (PLA) is aliphatic polyester prepared from biomass through bioconversion and polymerization. It is biopolymer and easily degradable with the action of bacteria, algae, fungi etc. [31]. PLA is a well-known bio-based plastic that has attracted immense attention over the past few decades. An extensive range of experimental studies have been performed on this family of polymers and these findings have been highlighted in numerous useful review articles and books. In particular, the synthetic aspects [32], processing [33], structure [34], physical properties [34, 35], and degradation processing [36], of PLA and its copolymers have been thoroughly reviewed. Although PLA and their blends has many applications in the medical and textile fields, this section will focus exclusively on the packaging-related properties of PLA [37, 38].

Figure 1.3 shows the production of bioplastics worldwide. Owing to its semi-crystalline nature, PLA has reasonably good oxygen barrier properties. For example, PLA has 10 times better oxygen barrier properties than petroleum-based PP [39]. Auras et al. [40] reported the effect of temperature on the oxygen permeability of PLA films. The oxygen permeability increased with

rising temperature due to the faster diffusion of the oxygen at higher temperatures. Interestingly, in contrast with water-soluble polymers such as chitosan and starch, the oxygen permeability of PLA decreases with increasing water content, possibly because the water absorbed by PLA occupies the site that blocks the pathway through oxygen molecules diffuse through the plastic. However, PLA has a poor barrier property for water vapor.

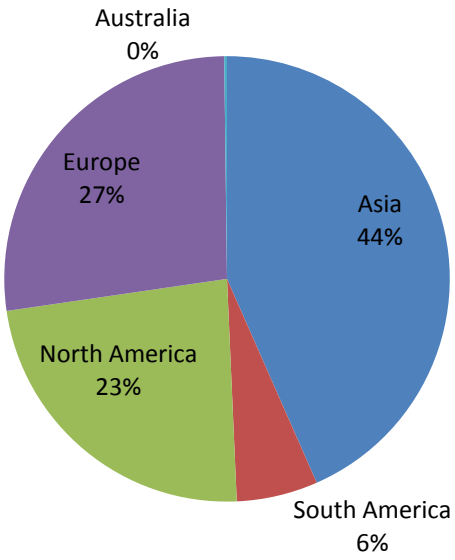

Figure 1.3 Global production of bioplastic in 2016

1.3 Accelerating the degradation of polyolefins

Polyolefin degradation can be defined as "a deleterious change in the chemical structure, physical properties, or appearance of a polymer, which may result from chemical cleavage of the macromolecules forming a polymeric item, regardless of the mechanism of chain cleavage" [41]. Such degradation produces changes in: mechanical, electrical or optical characteristics, through cracking, crazing, discoloration, phase separation and erosion. Polyolefins degradation can take place by two ways – (1) abiotic and (2) biotic. Abiotic degradation includes the physical and chemical processes that exert intermolecular degradation in the polymer [42, 43]. Degradation of

polyolefins can be classified as thermo-oxidative, photo-oxidative, hydrolytic, ozone-induced, mechanochemical, catalytic and/or biodegradation, depending on the mechanism [44]. Polyolefins undergo photo-oxidation or thermo-oxidation upon exposure to UV or heat, respectively. The synthetic polymers such as LDPE and PP generally contain pro-oxidant (a photo sensitizer) compounds which can activate the degradation. The degradation of PP provides the sole source of carbon and energy in soil microorganisms specifically, showed that small fragments were consumed faster than larger ones. To facilitate the biodegradation of the polymers, the first step is photo-oxidation or thermo-oxidation. The oxidation of polymers results in the formation of carbonyl residues that can be consumed by non-specific microbial populations.

Mechanical criteria for failure

Polyolefins should meet the mechanical criteria of failure; their fracture energy has to fall to a pre-determined fraction of the starting value. In the literature on service lifetimes of polymers, this predetermined set-point varies. For example, in case of PP, mechanical failure is frequently taken as the point at which fracture energy has reached 50% of the initial value [45], although in practice this may be beyond the point at which the polymer is still serviceable. Another approach for assessing failure in thermoplastic polymers is to measure elongation at break. When this has fallen to 5% of the initial ultimate elongation on measuring under tension, the polymer can no longer yield and as such will fail in a brittle mode on the application of force. The direct measurement of the actual fracture toughness is also useful, if it is possible, since this enables the tracking of the dissipation of energy at the crack tip [45]. In practice, however, the total loss of toughness is most commonly indicated by the polymer fracturing when tapped or otherwise handled.

Polymer lifetime estimation

An estimation of polymer lifetime is made, in most cases, through the use of accelerated ageing using increased temperature and/or higher radiation intensity. This approach measures the rate of degradation under controlled conditions, such that the time taken to reach an extent of degradation corresponding to failure under these conditions can be determined [46]. Extrapolation back to service conditions is then made through the use of a reciprocity relationship (whereby it is assumed, for example, that there is an equal radiation dose to failure regardless of the dose rate).

Interconnection of macroscopic, microscopic and chemical changes on degradation

The first key measurable stage of polymer degradation is loss of physical properties, particularly toughness, such that the polymer material becomes mechanically embrittled. As already described, it is the changes to the polymer molecular weight, intermolecular forces and crystallinity that underpin loss of physical properties for both oxo-degradable and biodegradable polymers. The change frequently varies and depends on the type of polymer used for the degradation.

Photo-oxidative degradation

Photo-oxidative degradation is considered as important process, in which decomposition of polymeric materials takes place by the action of light in ambient condition. Visible light and UV radiation easily start the degradation of polyolefins, due to the sufficient energy to cleavage the backbone chain of polymer. Polymer degradation mainly occurs in the soft-segment parts. During the photo-oxidative degradation, aldehyde, ester and different end groups are generated [44]. In photodegradation, the natural tendency for the most polymers is to undergo a gradual reaction with atmospheric oxygen in the presence of light. A photosensitizing agent is employed

to accelerate this natural tendency. Photodegradation involves the absorption of UV light which then leads to the generation of free radicals [47]. An auto-oxidation process then occurs which leads to the eventual disintegration of the plastic. The instability of polyolefins is believed to be brought about by the presence of impurities (such as carbonyl and hydroperoxide groups), which may form during the fabrication or processing of the polyolefin products. The primary oxidation product, the hydroperoxide group, is both thermally and photolytically unstable [48].

Thermal degradation

The degradation mechanism and products formed by heat are similar to the photo-oxidation. However, ketone products are stable to heat but not to light [48, 49]. The temperature has direct effect on the rate of thermal degradation, with higher values achievable at higher temperatures[50, 51]. Pro-oxidants, such as cobalt stearate (CoSt), can also accelerate both the thermal and thermo oxidative degradation of polyolefins.

Chemical degradation

In the abiotic degradation, chemical transformation is the other most important parameter. Agrochemicals and atmospheric pollutants may interact with polymers changing the macromolecule properties [52]. Oxygen is the most powerful among the chemicals provoking the degradation of materials. The atmospheric form of oxygen (i.e. O_2 or O) attacks covalent bonds producing free radicals. The oxidative degradation depends on the polymer structure (e.g. unsaturated links and branched chains). These oxidations can be concomitant or synergic to light degradation to produce free radicals.

Mechanical degradation

Sometimes, mechanical degradation also occurs in polymers if they are subjected to mechanical stress higher than permissible. For example, during processing in a screw extruder, the polymers are subjected to high shear stress due to which micro alkyds are formed leading to accelerated oxidation [53, 54].

During biodegradation process, mechanical factors are not very important but mechanical damages can activate it or accelerate it [52]. In field conditions, mechanical stresses act in synergy with the other abiotic parameters (temperature, solar radiations and chemicals).

Radiation induced degradation

Radiation such as γ-rays and X-ray are the highest energy radiations. They degrade the polymers to a larger extent in comparison of UV radiation. γ-rays are electromagnetic radiations like UV rays, but the energy level of γ-rays is much higher than UV rays which is helpful for the polymer degradation [55].

Degradation through environmental stress cracking

When a polymer degrades and cracks develop due to the presence of stress through the external environment like in the presence of polar vapors of liquids, detergent chemicals, etc., it is termed as environmental stress cracking (ESC).

Biodegradation

Biodegradation is one of the important types of degradation in which polyolefins are degraded by the action of microorganisms either in anaerobic or aerobic environment. Biodegradation is the process which come into play after photodegradation or thermal degradation and chemical degradation [49]. Polyolefins are hydrophobic in nature and their high molecular weight make

them resistant to biodegradation due to the absence of microbial attacks [56-58]. Several steps are involved in the biodegradation of polymers. In the first step, microorganisms are attached to the surface of the polymer then they grow and utilize the polymer as a carbon source. In the second step, the scission of main chain takes place, and this follows to the formation of low molecular weight products such as dimmers or monomers. In the final step, mineralization of polymer results into biomass, water, and CO_2 [59, 60]. To achieve the biodegradation in significant time period, the average molecular weight of an oxidized polyolefin should be <5000 Da [61]. Thus, the development of biodegradation system according to ASTM D 5338 would be a good method to evaluation of degradation of polyolefins.

Eco-toxicological impact of degraded polymers

Evaluation of environmental impacts of biodegradation intermediates is important to know if they are non-toxic to the environment. Ecotoxicological test generally used for the evaluation of toxicity of biodegradation intermediates are microbial and plant growth tests [62, 63]. Plant growth tests are preformed according to the guideline of OCED 208 in which different types of plants are used to study the ecotoxicity [58, 64-66].

Polypropylene extensively used in plastic packaging industries. But, they are non biodegradable and create plastic waste management problem. There are several researches on the development of biodegradable polymers and blends of synthetic polymers with biodegradable polymers to enhance the biodegradability. Several researches also present on the development of degradable polymer by grafting method. But, there is lack of studies on the degradability and ecotoxicological impact of biodegradable intermediates of grafted films.

1.4 Thesis motivation and objectives

It was seen that researchers tried to solve the plastic packaging waste management problem by development of biodegradable polymers and improving degradability of plastic material by blending with biodegradable polymers. But, biodegradable polymers are costly and have lower mechanical properties. Less attention has been given to the preparation of degradable polymer by grafting technique. After degradation, it is necessary to study the ecotoxicological impact of biodegraded intermediates. To overcome this gap, acrylic acid grafted polypropylene has been developed and their biodegradation and ecotoxicological impact of biodegraded intermediates were studied. PP/PLA blends filled with pro-oxidant and PP/PLA composites with nanoclay were also tried. The biodegradation and ecotoxicological impact are also studied.

The overall objective of the research is to develop degradable polypropylene films which maintain its functional properties during its lifespan and at the same time be able to breakdown quickly & effectively after utilization. The specific objectives are:

i. To develop degradable polypropylene by grafting with acrylic acid (PP-g-AAc) having optimum performance properties for flexible packaging.

ii. To develop degradable blend of polypropylene and polylactic acid with pro-oxidant and nanoclay as filler.

iii. To study the degradation kinetics of grafted and blended polypropylene films.

iv. To study the eco-toxicity (after biodegradation) of the grafted and blended polypropylene films.

1.5 Thesis overview

This thesis has been divided into **six chapters**. In this thesis, simultaneous radiation grafting method is used to graft acrylic acid on polypropylene films. Pro-oxidant filled PP/PLA blends filled with pro-oxidant and PP/PLA composites with nanoclay are prepared by melt blending method. Characterization has been done to investigate the mechanical, chemical and surface properties. Biodegradation of grafted PP, pro-oxidant filled PP/PLA blend and nanoclay filled PP/PLA composite are evaluated by following the standard ASTM D 5338. Ecotoxicological test (microbial and plant growth) has been preformed to evaluate the toxicity effect of biodegradation intermediates.

Chapter one (Introduction) presents the current environmental issues and the brief description of problem and solution related to plastic waste management. It covers the various applications of plastic packaging especially polypropylene film and its impact on environment. Approaches to reduce the plastic waste have also been addressed in this chapter.

Chapter two (literature review) discusses the grafting, blending methods and preparation of degradable polyolefins. More emphasis has been given to preparation of degradable polypropylene by grafting and blending methods.

Chapter three (Materials and methods) shows the outline of the **experimental** works in this research. The materials, chemicals and experimental methods used for the characterization of acrylic acid grafted PP and PLA blended PP films are given.

Chapter four (Acrylic acid grafted polypropylene) discusses the preparation, characterization, thermal degradation, biodegradation and ecotoxicological studies of acrylic acid grafted polypropylene (AAc-g-PP) films. Simultaneous grafting technique has been used for the

grafting of AAc on PP films. Characterization has been performed to evaluate the physico-chemical properties. Thermal degradation kinetic parameters have been evaluated to estimate the lifetime of PP and grafted PP films. Biodegradation studies have been performed to evaluate the degradation of grafted PP films. Ecotoxicological (microbial and plant growth) studies have been performed to evaluate the toxicity effect of degradable intermediates of grafted PP films.

Chapter five (PP blends and composites) covers the development and characterization, thermal degradation, biodegradation and ecotoxicological studies PP/PLA blend, pro-oxidant filled PP/PLA blend and nanoclay filled PP/PLA composite. Tensile test was used to optimize the blended and nanocomposite films. The optimized blended and nanocomposite films have been characterized by FTIR, TGA, rheology and SEM. Biodegradation studies have been performed to evaluate the degradation of blended and nanocomposite films. Ecotoxicological (microbial and plant growth) studies have been performed to evaluate the toxicity effect of degradable intermediates of blended and nanocomposite films.

Finally, chapter six (Conclusions and recommendations) summarizes the data reported and also gives some recommendations for future research.

At the end, the references cited in this synopsis have been listed

Chapter 2-Literature Review

It is estimated that worldwide, 60 million metric ton waste per year is accumulated in the environment [67]. The present annual quantity of solid waste generation in Indian cities has increased from 6 million tons in 1947 to 48 million tons in 1997 with an annual growth rate of 4.25%, and it is expected to increase to 300 million tons by 2047 [68]. Total 1000 tons of plastic waste was daily handling and trading in India's National Capital Delhi [69]. This undesirable plastic waste pollutes the environment. Thus, there is a need of biodegradable polymer to replace these oil based synthetic polymers, which can be easily biodegraded.

Blending of synthetic polymers with biodegradable polymers and grafting of PP are the methods for preparation of biodegradable polymer packaging materials for packaging applications. The main advantage of grafting and blending is that the polymer material maintains well physical and mechanical properties during the life long use and biodegraded under biological environment after its use.

2.1 Polypropylene based biodegradable system

PP is extensively used in packaging application, when the products of PP complete their service life, most of them are disposed in open dumps, landfills, or as simple litter, but they do not decompose by themselves. Moreover, recycling of PP produces inferior quality products [70]. To solve this problem, biodegradable PP is needed, having shorter lifetime, and minimum environmental impact. Blending and grafting are the effective methods to improve the biodegradability of PP. Blending of PP with biodegradable polymers such as starch [71], cellulose, PLA, PHB, PCL etc. accelerates the degradation process. Some complex transition

metals such as cobalt stearate (CoSt) and calcium stearate (CaSt) are helpful for the improvement of degradation of PP matrix [72]. Grafting of PP with hydrophilic monomer is also an important method to improve the biodegradability of PP.

2.1.1 Polypropylene blending with natural biodegradable polymers

There are several natural polymers for the blending and direct incorporation into polyolefins, such as starch, cellulose, chitosan etc. They are widely used to maximize the degradability of polymers. The microbial assimilation of natural polymers in blends was observed to increase the surface area of synthetic bulk materials and to render them more susceptible to degradation [73]. Blending of polyolefins with various polymers is described below.

Starch

Starch is a highly studied polymer used as a biodegradable polymer [74]. It has largely been used for the preparation of partially biodegradable polymers, blending with petroleum-derived polyolefins [75]. Starch consists of two types of molecules; one is amylopectin (normally 70–80%) and the second is amylose (normally 20–30%). Both of these polysaccharides are composed of D-glucose units [74]. Griffin was the first, to develop a partially degradable blend of polyolefins with starch using starch granules as a filler [6].

There are several research studies in which starch has been used as biodegradable filler in polyolefins. Al-Salem et al. [76] studied the thermal degradation kinetics of PP and compared it with polypropylene/starch blend (PP/S) (70/30 (wt %)), with the effect of photodegradation caused by natural weathering. There is a change in the degradation mechanism due to the effect of starch addition and weathering condition [77]. Addition of starch and weathering condition affected the kinetic parameters of the degradation reaction and thermal stability.

Obasi and Igwe [78] have investigated the effects of starch content in the starch filled PP blends. The blends were prepared by the addition of starch between 0 and 50 wt. % into PP using an injection molding machine within temperature range of 160 - 190°C at a screw speed of 50 rpm. Tensile strength and elongation at break decreased, while Youngs modulus, water absorption and weight loss percent increased with increasing starch content. The morphological studies of fractured surfaces using SEM showed the deterioration in the properties.

Chitosan

Chitosan is a high-molecular-weight natural polymer. It can be used for the formation of transparent films [79-82]. Chitosan plays two important roles in the blends; act as biodegradable additive and develops antimicrobial properties.

Chitosan blending improved the impact strength and Youngs modulus but lowered the tensile properties of polyolefins. It was observed that chemically treated PP/chitosan composites have higher mechanical properties as compared to virgin PP. This may be due to the enhanced interfacial adhesion and better dispersion of the chitosan in PP matrix [83].

Sunilkumar et al. [84] studied the biodegradability of chitosan filled LDPE films, in which films were inoculated with *Aspergillus niger* on a potato dextrose agar media and incubated at 25°C for 21 days. Studies showed that the biodegradation increased with increase in chitosan concentration in the films.

Cellulose

Cellulose is a linear polysaccharide made up of number of glucose monosaccharide units. Cellulose was first discovered by Anselme Payen, a French chemist in 1838. He identified it within plant matter and also determined its chemical formula. The cellulose structure mainly

consists of long chain of glucose units connected with each other through beta acetyl linkage. The properties of cellulose mainly depends on its degree of polymerization and the chain length [85].

Kaczmarek et al. [86] studied the degradation of polypropylene compositions containing 5 to 30% cellulose after pre-irradiation and then composted in garden soil. They found that photo- and bio-induced changes in PP/cellulose compositions accelerated as compared to pure PP. The mechanical properties of sample tested are lower than those of PP.

Polylactic acid (PLA)

Polylactic acid is a linear aliphatic thermoplastic polyester, produced from renewable resources and is readily biodegradable. PLA is produced by ring-opening polymerization of lactides and the lactic acid monomers, obtained from the fermentation of sugar feed stocks. Commercial PLA grades are generally copolymers of poly(L-lactic acid) (PLLA) and poly(D,L-lactic acid) (PDLLA), which are produced from L-lactides and D,L-lactides, respectively [87].

Blends of polyolefins with PLA are also being developed for various household applications in recognition of the environmental appeal of the carbon neutral feature of PLA [70, 88]. PP/PLA blends are suffering from the very serious disadvantage of compatibilization, due to which blends have low mechanical properties. Improvements in the mechanical properties of the PLA/PP blend have been achieved by the use of effective compatibilizers suited for the requirements of particular application [25, 89]. The application of blends is limited due to the immiscibility between polymers. Compatibilizers are often used as additives to solve this problem and to improve the compatibility. Polypropylene-grafted-maleic anhydride (PP-g-MA) is an important compatibilzer generally used to improve the compatibility. For blending PP with

polar polymers, PP-g-MA has been established as an effective compatibilizer in which the PP part of the PP-g-MA is compatible with PP, and the anhydride part reacts with the polar component [88, 90, 91].

Ploypetchara et al. [90] studied the effect of PLA concentration and effect of compatibilizer on the properties of PP/PLA blends. The interaction between compatibilizer and polymers confirmed by FTIR. Increase of PLA content from 40 to 60 wt% resulted in decreased melting temperature and crystallinity from 158 °C to 154 °C and 38% to 31%, respectively. The tensile modulus, increased with increase in the PLA content, while elongation at break drastically decreased from 500% (for PP) to less than 50% (for blends). From the results, the PP/PLA blends showed a typical immiscible polymer blend.

Effects of compatibilizers and hydrolysis on the tensile and impact strength, interfacial tension and morphology of the PP/PLA (80/20) blends were studied by Yoo et al. [92]. Before hydrolysis, the tensile strength of the PP/PLA (80/20) blends reached a maximum when the polypropylene-g-maleic anhydride (PP-g-MAH) copolymer was added at 3 phr. The tensile strength did not change appreciably with the PP-g-MAH content in PP/PLA (80/20) blends after hydrolysis. The tensile strength of the blends with the styrene-ethylene-butylene-styrene-g-maleic anhydride (SEBS-g-MAH) before or after hydrolysis decreased with increasing SEBS-g-MAH content. The interfacial tension of the PP/PLA (80/20) blend was determined from the relaxation time using the Pelerine and Choi-Schowalter models, and showed a minimum value at a PP-g-MAH content of 3 phr in each model. The increase in impact strength of PP/PLA (80/20) blends with the SEBS-g-MAH was more significant for the blends after hydrolysis. This suggests that PLA becomes less brittle after hydrolysis. The SEBS-g-MAH is an effective impact modifier to improve the impact strength of the PP/PLA (80/20) blends.

2.1.2 Polypropylene blending with synthetic biodegradable polymers

Synthetic biodegradable polymers such as aliphatic polyesters have become more attractive alternatives for preparation of degradable polymer blends due to the easier chemical modification than natural biodegradable polymers. Several articles [32, 72, 93] have been published on the usefulness of blend of biodegradable polymers with conventional polyolefin (from environment point of view). These blends are partially miscible or immiscible and suitably compatibilized to increase the interfacial adhesion and miscibility. Blending of PLA with conventional polymers such as polypropylene, poly(ethylene glycol), poly(ethylene oxide), poly(4-vinylphenol), poly(vinyl acetate) and polyacrylates can modify the thermal and mechanical properties, degradation rate and permeability [94-96].

2.1.3 Enhancing degradability of polyolefins with pro-oxidants

Pro-oxidants as the additives are extensively used to increase the biodegradability of polyolefins. Transition metal ion complexes are the most active pro-oxidant added into polyolefins. They are mostly used in the form of stearates complexes for example Mn^{2+} and Mn^{3+} [97, 98]. Transition metals are having stearates complexes such as cobalt stearate (CoSt) [99, 100], manganese stearate (MnSt) [101], chromium stearate, zinc stearate [102, 103] and titanium stearate, or alkaline earth metals, such as calcium stearate (CaSt) [72, 101] and magnesium stearate [104, 105]. The most used transition metals are cobalt, iron, and manganese and can increase the rate of oxidation by air/oxygen and cleavage of PP chains under the influence of light and/or heat. These metals can act as a thermal catalyst and photocatalyst. Whereas, Fe^{3+} is used for accelerating photodegradation and Mn^{2+} and Co^{2+} are used for thermal degradation [68, 106, 107]. Pro-oxidant effect on the degradation of high density polyethylene (HDPE) and low density polyethylene (LDPE) has been reported by Koutny et al. [108]. Some of the microbial

strains tested, particularly *R. rhodochrous* and closely related *N. asteroids*, were able to form biofilm on the material surface. Fontanella et al. [109] reported that the main factor controlling the biodegradability of the polyethylene film was the nature of the pro-oxidant additive with HDPE and LDPE. Finally, the above process results in PP films fragmentation and resolves the problem of visible pollution. Pro-oxidants, when exposed to heat/light in the presence of oxygen, can promote the oxidation of the polyolefins. These pro-oxidants are usually based on transition metals added in the form of long chain carboxylates or as acetyl lacetonates.

2.1.4 Enhancing degradability of polyolefins with nanoclay

In recent years, significant efforts have been made in the development of melt-compounded PP with organically modified natural clay (montmorillonite). The coupling agent, such as MA-g-PP were used to improve the dispersion of clay particle in PP matrix [110, 111]. The best properties were obtained with high loadings of clay and coupling agents in the PP films. Enhanced properties were obtained at a significantly higher price, which reduces their range of application, for example, in the automotive sector [112, 113]. The impact resistance of the PP/clay composite decreased, in most cases, when an effective coupling agent was used, especially at high clay concentrations.

2.1.5 Enhancing degradability of polyolefins with radiation grafting

Grafting polymerization is a method for the modification of shape, size and structure of polymeric materials. Grafting copolymerization can be achieved by various methods, viz. chemical means [114], photo-radiation [115], γ-radiation [116], and thermal action [117]. Among these techniques, γ-radiation grafting copolymerization is one of the most important techniques due to its rapid formation of free radicals and effective penetration in the polymer matrix. There are two ways of radiation grafting methods: first is simultaneous and second is pre-

irradiation grafting method [118]. Simultaneous radiation grafting method is highly efficient than pre-irradiation one. This is due to the higher radical availability by the direct method where both components were irradiated simultaneously. On the other hand, the lower availability of pre-irradiated radical was a result of the very short lifetime of PP macroradicals in the amorphous phase. Probably, all reacting radicals in the pre-irradiation method were the trapped radicals from the crystals, moving to the interface of the amorphous phase. [119]. Simultaneous radiation grafting suffers from a serious disadvantage of homopolymer formation during grafting, resulting in loss of monomer and requires extraction of homopolymers from the grafted co-polymer. Mohr's salt (inhibitor) suppresses the production of undesirable homopolymer during the radiation grafting, thus leaving more monomers available for grafting and hence enhance the degree of grafting. This has been attributed mainly to scavenging of ˙OH radical (generated due to radiolysis of water in the bulk of the mixture) by metal ions thereby reducing the homopolymerization in the bulk [116]. There has been some effort on the degradability study of polymers produced by grafting polymerization methods. Polyethylene film grafted acrylamide/methacrylic acid (AAm)/(MAAc) showed degradability up to 47% within 50 days in soil burial test [120]. Soil burial test confirmed that the degradability of acrylic acid/acrylonitrile grafted low density polyethylene (LDPE-*g*-AAc/AN) was due to the high concentration of AAc [121].

2.2 Gaps identified

There are vast opportunities to explore the development of biodegradable polymers of low cost and non-toxic in nature. Biodegradable polymers are gaining higher attention for the research in academic and industry due to their environmental benefits. Blending of polymers with biodegradable additive/polymer is highly studied but very less attention has been given to

the preparation of biodegradable polymer by grafting techniques. On the basis of literature survey following gaps have been identified:

(i) Several studies are reported on the degradation of grafted PE and LDPE but, none of the researcher(s) have reported the biodegradability behavior of grafted PP.

(ii) The rate of degradation (i.e. kinetics) of nano-filler composite (for packaging application) has not been validated till date.

(iii) After biodegradation of PP blend, the resulting compost material must be non-toxic. Hence, it is necessary to study eco-toxicity, which has not been considered by the researcher(s).

Chapter 3-Materials and Methods

3.1 Materials

Homopolymer PP pellets (Grade F110) were received from Haldia Petrochemicals Limited, India with melt flow index (MFI) of 11 g/10 min, melting point (T_m) = 165 °C and density 0.9 g/cm^3. Acrylic acid monomer (purity > 99%) was purchased from Sigma-Aldrich. PLA (4032D) pellets of density 1.24 g/cm^3 and D-isomer content of 2% w/w were procured from NatureWorks LLC, USA. Compatibilizer – maleic anhydride modified PP (Optim P406) of density 0.908 g/cm^3, MFI = 110g/10 min and T_m = 161°C was procured from Pluss Polymers Pvt. Ltd., Gurgaon, India. Calcium stearate (6.6-7.4% Ca) of molecular weight (M_w) = 607.02 was provided by Sigma-Aldrich. Cobalt stearate (Co, 9-10%) of M_w = 625.89 pellets were purchased in pellet from Alfa Aesar, Johnson Matthey Chemical India Pvt. Ltd. Nanoclay (Cloisite 30B) was supplied by the Connell Bros. Company Pvt. Ltd., Mumbai, India. Micro crystalline cellulose powder (particle size ≤ 20 μm), H_2SO_4 (purity > 98 %) and $Ba(OH)_2$ (M_w = 315.47) were purchased from S-D Fine Chemicals Limited. Methylene Blue (M_w = 319.86) was purchased from Loba Chemie Pvt. Ltd. Mumbai, India. Mohr's salt (purity > 99%) was used as analar grade. Nutrient agar and hydrochloric acid (35% concentration) were obtained from Hi-Media Laboratories Pvt. Ltd., India. Seeds of corn and tomato plants were procured from Arman Seed Farm, Patiala. Pure ethanol was purchased from Changshu Yangyuan Chemical, China.

For biodegradability test, compost (municipal solid waste) was provided by Delhi Jal Board at Okhla, New Delhi, India. The properties of compost were determined as per the American Public Health Association [122]. Coarse matter of glass, metal, stone etc. was separated out through screening of 1 mm mesh. The total organic carbon of the compost was 34% and total Kjeldahl nitrogen was 2.2%. The water holding capacity was 60-65%. The C:N ratio of compost was 15.3.

The volatile solids and total dry solids were 18% and 81%, respectively. The pH of the compost, measured as per reported procedure was 7.2 [38].

3.2 Methods

3.2.1 Swelling studies

Swelling studies of PP and grafted PP films was performed by immersing the grafted films in excess of distilled water. The experiment was performed for the different time intervals at room temperature. Filter paper was used to remove the excess of water from the grafted films and swelling was determined gravimetrically by equation 3.1:

$$\text{Swelling (\%)} = \frac{W_s - W_g}{W_g} \times 100 \qquad 3.1$$

where W_s and W_g are the weight of wet and dry grafted PP films, respectively.

3.2.2 Moisture content

Moisture content in all the samples was determined by an instrument Moisture Analyser (PRESISA XM60 Switzerland) using IR drying method.

3.2.3 Carboxylic group analysis

Colorimetric analysis was used to determine the amount of carboxylic groups present on the AAc grafted PP films. Methylene Blue staining was used. The molar ratio between dye and carboxyl groups was assumed unity. Grafted films of 0.01 g were put in a dye solution of 6.1 ppm at a pH of 10 for 6 h at 30 °C. Any dye adhering to the surface was removed by thoroughly washing with NaOH solution of pH 9. Acetic acid solution of 50% V/V and 10 ml was used for desorption of dye from the grafted films. The carboxylic groups present on the grafted PP films were measured

by the optical density of solution at 665 nm using Perkin Elmer Lambda 35 UV-visible spectrophotometer [123]. A calibration curve of Methylene Blue solutions was obtained from the optical density of known concentrations at 665 nm.

3.2.4 Mechanical testing

Tensile strength and elongation of the films were measured according to the ASTM D 882-91 standard [32] using Universal Testing Machine (Z010, Zwick-Roell, Germany). The rectangular specimens were prepared by strip - sample cutter for tensile test. The clamp separation was maintained 100 mm with cross head speed of 12.5 mm/min. The average value of five specimens of each film sample is reported.

3.2.5 Fourier transforms infrared (FTIR) spectroscopy

FTIR measurements of all the film samples were performed by using a spectrometer Agilent Pro Cary 660. It was carried out within the wave number range of 500-4000 cm^{-1}. A total of 16 scans/sample were taken, with a resolution of 4 cm^{-1}.

3.2.6 X-ray diffraction (XRD)

X-ray diffractometer Philips Xpert (Almelo, Netherlands) was used to obtain XRD patterns of the sample. The instrument was operated at 40 kV and 20 mA with a Cu-Kα radiation of 1.54 A° wavelength (λ). The scanning speed was 5° min^{-1} in the diffraction angle range of 5–35°.

3.2.7 Differential scanning calorimetry (DSC)

Differential scanning calorimetry (DSC) was performed by the instrument 200F3, Netzsch-Geratebau GmbH, Germany to evaluate the thermal behavior of all the samples using 5-10 mg material in nitrogen atmosphere. The thermal history of the samples were removed by heated from room temperature to 200 ºC at heat rate of 10 ºC/min and then held for 1 min.

Subsequently, the samples were cooled to -30 ºC at a cooling rate of 10 ºC/min. Then, second heating was preformed for analysis to 200 ºC at heating rate 10 ºC/min. The area under the melting thermograms was used to measure the melting enthalpy (ΔH_m). The percentage crystallinity (X_c%) of the samples was calculated by using equation 3.2 [124]:

$$X_c\ (\%) = \frac{\Delta H_m}{\Delta H_{m\,(crys)}} \times 100 \qquad 3.2$$

Where, ΔH_m(crys) is the melting enthalpy of 100% crystalline PP (163 J/g) [124]. The melting enthalpy of 100% crystalline polylactic acid was considered as 93 J/g [90].

3.2.8 Thermogravimetric analysis (TGA)

Thermogravimetric analysis (TGA) of all the samples was performed by a TGA Q-500 series analyzer from TA Instruments, USA. The measurements were done at a heating rate of 20 °C/min in nitrogen atmosphere with a flow rate of 50 ml/min. About 5-10 mg samples was taken and thermal profiles were recorded from 30 to 550 °C.

3.2.9 Scanning electron microscopy (SEM)

A SEM instrument JEOL (JSM 6510- LV, Tokyo, Japan) was used to the assessment of surface morphology and fracture surface morphology of all the samples. A gold film of 15 nm was used as coating under an electron beam in a high vacuum automatic sputter coater model JFC-1600, Japan to avoid the charging.

3.2.10 Rheological testing

An instrument Anton Paar parallel plate rheometer (MCR 102) was used to studied the rheological behavior of the blended and nanocomposite sample in nitrogen atmosphere. The

instrument is equipped with 25 mm diameter plates with 1 mm gap and operated at 190 °C. The linear viscoelastic (LVE) region was determined by running the samples from the initial strain value of 0.01 to the final value of 1000% at a constant frequency of 1 rad/s. Then, frequency sweep test was performed in the LVE region (γ=1%) in the frequency range of 0.01 to 500 rad/s.

3.2.11 Thermal degradation kinetics

TGA method is an excellent way to study the thermal degradation kinetics. It provides information on activation energy (E_a), reaction order (n) and frequency factor (Z) by using various kinetic models such as Friedman [125], Kissinger [126], Flynn-Wall [127], Kim-Park [128] and Freeman-Carroll [129]. The kinetic parameters obtained from these kinetic models can be used to calculate the lifetime of polymers at various temperatures. Several methods for the calculation of kinetic parameters of thermal degradation by TGA have been developed. They can be classified into three categories: differential, integral and direct methods on the basis of Arrhenius equation. Another way of classification of methods for calculating the kinetic parameters is: single heating rate methods and multiple heating rate methods. Friedman, Freeman-Carroll and Coats-Redfern [130] are single heating rate methods, whereas Flynn-Wall, Ozawa [131], Kim-Park and Kissinger are multiple heating rate methods. The third classification of methods for the analysis of kinetic parameters is either model fitting or model free methods. Freeman-Carroll and Coats-Redfern are model fitting methods and Flynn-Wall, Kim-Park and Kissinger are model free methods. On the basis of thermal condition, thermal degradation kinetic methods can be classified into isothermal and non-isothermal methods. The conventional and standard method is isothermal method whereas Friedman, Freeman-Carroll, Kissinger and Flynn-Wall are non-isothermal methods. The model-fitting methods were widely used for solid-state reaction because of their ability to directly determine the kinetic parameters from a single TGA

thermogram, but in recent years, the use of model-free methods have been reported [132-134]. Model-fitting methods produce unreliable and sometimes nonsensical results. For more accurate measurement, model-free methods may be applied to assess the dependence of activation energy on the degree of conversion, which can be correlated with the investigated process mechanism. The advantage of the model-free analysis is found in its simplicity and avoidance of errors connected with the choice of a kinetic model and assumptions. The only disadvantage of these methods is a series of measurements at different heating rates, which must be made at the same sample mass and the same volumetric flow of inert gas and their fluctuations can cause errors. Keeping in view the above mentioned information, we performed the kinetic analysis of the PP and grafted PP films with the application of model-free methods suggested by Kissinger, Flynn-Wall and Kim-Park.

Thermogravimetric analysis is an important method to know the rate of degradation of polymers. In TG analysis, the rate of degradation reaction (α) can be defined as the ratio of actual weight loss at time (t) to total weight loss corresponding to the decomposition process.

$$\alpha = \frac{w_0 - w_t}{w_0 - w_f} \qquad 3.3$$

where w_t, w_0 and w_f are the actual weight of sample at time t, initial weight and final weight of a test sample, respectively. The rate of degradation ($d\alpha/dt$) is a function of temperature and weight of the sample:

$$r = \frac{d\alpha}{dt} = kf(\alpha) \qquad 3.4$$

Here, $f(\alpha)$ is the rate of conversion and r is the reaction rate. k is the rate constant and a function of temperature described by the Arrhenius equation.

$$k = Ze^{\frac{-E_a}{RT}} \quad 3.5$$

where E_a is the activation energy, Z is the frequency factor, T is the absolute temperature and R is the gas constant. The reaction rate can be expressed by combining the equation 3.4 and 3.5 as:

$$r = Ze^{\frac{-E_a}{RT}} f(\alpha) \quad 3.6$$

By introducing heating rate in rate of degradation (dα/dt), the modified equation is:

$$\frac{d\alpha}{dt} = \frac{d\alpha}{dT} \times \frac{dT}{dt} = \beta \frac{d\alpha}{dT} \quad 3.7$$

The combining of equations 3.4, 3.6 and 3.7 yields the following expression:

$$\frac{d\alpha}{dT} = \frac{Z}{\beta} e^{\frac{-E_a}{RT}} f(\alpha) \quad 3.8$$

And, the integral function of α is g(α) as follows:

$$g(\alpha) = \int_0^{\alpha} \frac{d\alpha}{f(\alpha)} = \frac{Z}{\beta} \int_0^{T} e^{\frac{-E_a}{RT}} dT \quad 3.9$$

3.2.11.1 Kissinger method

The kinetic parameters of degradation E_a, n and Z were determined using the Kissinger method [126] :

$$n = (1-\alpha_m) E_a [(I)] \frac{\{\exp(-E_a / RT_{\max})\}}{\beta R(d\alpha / dt)} \quad 3.10$$

where n is the reaction order, E_a is the activation energy, R is the universal gas constant, T_{max} is the maximum degradation temperature, β is the heating rate, α_m is the conversion at maximum degradation and Z is the frequency factor. The value of ln(Z) can be obtained from the intercept I. I is calculated from the following equation:

$$I = \ln\left[\frac{n(1-\alpha_m)^{n-1}}{E_a} ZR\right] \qquad 3.11$$

Activation energy E_a of thermal degradation is determined by the following expression:

$$\ln\left(\frac{\beta}{T_{\max}^2}\right) = \ln\left[\frac{n(1-\alpha_m)^{n-1}}{E} ZR\right] - \frac{E_a}{RT_{\max}} \qquad 3.12$$

3.2.11.2 Kim-Park method

The kinetic parameters of degradation E_a, n and Z are determined using the Kim-park method [135]:

$$\ln\beta = \ln Z + \ln\left(\frac{E_a}{R}\right) + \ln\left[1-n+\frac{n}{0.944}\right] - 5.3305 - 1.0516\left(\frac{E_a}{RT_{\max}}\right) \qquad 3.13$$

where

$$n = \frac{(1-\alpha_m)}{RT_{\max}^2 (d\alpha/dt)} \qquad 3.14$$

3.2.11.3 Flynn-Wall method

The kinetic parameters of degradation was estimated by Flynn-Wall method [127]. It is a logarithm of the integrated results expressed as follows:

$$\ln \beta = \ln\left(\frac{ZE_a}{R}\right) - \ln(\alpha) - 0.4567\frac{E_a}{RT} \qquad 3.15$$

A straight line is obtained from the plot of ln β and $1/T$ at the given conversion α. The activation energy E_a is calculated from the slope 0.457 E_a/R.

3.2.11.4 Lifetime estimation

The lifetime of PP and grafted PP films was estimated by using equations 3.16, 3.17 and 3.18 derived by Toop [136] in the temperature range of 50-140 °C.

$$X_f = E_a/RT_i \qquad 3.16$$

$$\log p(X_f) = -2.315 - 0.457X_f \qquad 3.17$$

$$\ln t_f = \left(\frac{E_a}{RT_f}\right) + \ln\left[\frac{E_a}{\beta R}\, p\left(X_f\right)\right] \qquad 3.18$$

Where X_f is E_a/RT_i and T_i (K) is the temperature at 5% weight loss [137]. T_f (K) is the failure temperature, t_f is approximate time of failure (min) and log $p(X_f)$ is a linear function of X_f.

3.2.12 Biodegradability

Biodegradation of polymer generally follows two steps: first one is abiotic degradation and second is biotic degradation. In abiotic degradation, degradation mainly occurs due to the chain scission of the ester groups in the form of hydrolysis, oxidative reaction, heat, light, etc. Chain scission reduces the molecular weight of polymer by breakdown of large chain into several shorter chains. In biotic degradation, the low molecular weight polymers after abiotic degradation are consumed by microorganisms and give by-products, i.e. carbon dioxide, biomass, water and residue.

There are some standards for the assessment of the biodegradability of biodegradable plastic materials under different environments, developed by American Society for Testing and Materials (ASTM) and International Organization for Standardization (ISO). ASTM D 5338 is an important standard method used for the assessment of biodegradability of plastic materials under controlled composting conditions [138].

3.2.12.1 Preparation and standardization of $Ba(OH)_2$ and HCl solutions

4g of $Ba(OH)_2.8H_2O$ was dissolved in 1 liter distilled water to prepare 0.024N barium hydroxide solution. The solution normality was verified by standardizing it against HCl. Sodium carbonate (Na_2CO_3) is primary standard used for the standardization HCl because HCl is a secondary standard.

3.2.12.2 Positive, negative and blank controls

The positive control consisted of microcrystalline cellulose powder in compost material and negative control consisted of PP film in compost material. Whereas, blank control consisted of compost material in the composting vessel (bioreactor).

3.2.12.3 Biodegradation procedure

The bioreactors were filled up with four different mixtures (a) blank (only compost material), (b) positive reference (compost + cellulose), (c) negative reference (compost + reference polymer) and (d) test material (compost + test polymer), each in triplicate. The biodegradation was performed under controlled conditions: air (CO_2-free) flow rate of 60-80 ml/min and 50-60% relative humidity (RH). The weight of the sample was taken 1 g and incubated in bioreactor of 1 liter at 58±2 °C for 45 days using a temperature profile as mentioned in the protocol to ensure the proper growth of microorganisms, which is helpful for biodegradation process. The uniform distribution of air throughout the compost material in all the bioreactors was maintained by shaking the bioreactor twice a week. The evolved CO_2 from bioreactor was absorbed in conical flasks containing 0.024 N barium hydroxide solution. The retrieved $Ba(OH)_2$ solution was titrated with 0.05 N HCl and the amount of CO_2 produced was determined by calculating the difference (in ml of titrant) between the test substance and blank $Ba(OH)_2$ traps. The measurement was taken in intervals of 5 days for 45 days.

3.2.12.4 Calculations

The total theoretical CO_2 produced by the test sample was calculated by using equation 3.19.

$$CO_2(Th) = W_{sample} \times C_{sample} \times \frac{44}{12} \qquad 3.19$$

Where W_{sample} is the weight of total dry solids in the test sample (g); C_{sample} is the proportion of total organic carbon (TOC) in the sample (g/g); 44 and 12 are the molecular weights of carbon dioxide and carbon, respectively (g/mol).

A TOC analyser, TOC-V_{CPH} (solid module) from Shimadzu, Japan was used to determine the theoretical amount of carbon dioxide (CO_2th) in samples. The TOC-V_{CPH} analyzer involves heating 900°C. The carbon dioxide is detected by a non-dispersive infrared (NDIR) gas analyzer. The NDIR outputs in the form of analog signal forms a peak; the peak area is calculated using the TOC-Control V software.

The cumulative quantity of CO_2 produced from the sample was determined by acid-base titration. The biodegradation was calculated by the equation 3.20.

$$\text{Biodegradation}\,(\%) = \frac{CO_2t - CO_2b}{CO_2th} \times 100 \qquad 3.20$$

Where, CO_2t is the mass of CO_2 evolved from the test sample in grams; and CO_2b is the mass of CO_2 evolved from the blank sample in grams.

3.2.12.5 Statistical analysis

Each measurement was done in triplicate and the mean and standard deviation of the experimental results were calculated using Origin 8.0.

3.2.13 Ecotoxicological studies

Microbial test and plant growth test were performed to study the toxicological effects of biodegradation intermediates.

3.2.13.1 Microbial toxicity test

3.2.13.1.1 Procedure

In the microbial toxicity test, 1 g of each biodegraded compost sample was immersed in 10 ml of sterilized distilled water, vortexed for 1 min and kept undisturbed for 30 min. The compost

suspension was serial diluted to a factor of 10^{-3} and 100 µl of each of 10^{-1}, 10^{-2} and 10^{-3} dilution [139] factor was inoculated on nutrient agar plate. The inoculated plates were incubated at 37 °C in an incubator (Model NSW-152 of Narang Scientific Works Pvt. Ltd., India) for 24 hours. The number of bacterial colony-forming units (CFUs) on agar plate was calculated to estimate the number of colonies per ml [62, 140].

3.2.13.1.2 Calculation

The microbial population on the compost was determined as number of bacterial colony-forming units (CFUs) per ml of suspension as given below:

CFU/ml = number of colonies per ml plated/ Total dilution factor 3.21

Only municipal solid waste (without degraded polymer) was used as control.

3.2.13.2 Plant growth test

3.2.13.2.1 Medium preparation

For the plant growth test, the medium composition of soil, perlite and compost (after biodegradation) was in the ratio of 2:1:1.

3.2.13.2.2 Procedure

The guidelines of Organization for Economic Cooperation and Development (OECD 208) for Terrestrial Plant Growth test have been used for the plant growth test on tomato (*Solanum lycopersicon*) and corn (*Zea mays*)) [64]. Thirty tomato plants and 90 corn seeds were sown in the medium. Experiments were conducted in three replicate. The condition maintained during plant growth test are 22 ± 10 °C, 70% ± 25% humidity and 16 h light/8 h dark cycle for 3 weeks. The grown seedlings were counted after 21 days.

3.2.14 Softwares used

OriginPro 8 software was used for fitting various kinetic data and draws of curves of PP and all modified film samples in FTIR, TGA, SEM, XRD etc.. The Design Expert software was used for the statistical design of experiments and data analysis in RSM optimization method.

Chapter 4-Acrylic acid Grafted Polypropylene

4.1 Preparation of PP films

PP films of 80-85 μm thickness were prepared from PP pellets on aluminum sheet. The temperature and pressure maintained during the compression molding was 180 °C and 400 kN/m^2. Cooling was performed by water.

4.2 Grafting method

Simultaneous radiation grafting method was used for the grafting of AAc on PP films. PP films of size 15 cm × 7.5 cm were immersed in solution having different amounts of AAc monomer, inhibitor (Mohr's salt) and sulfuric acid in 200 ml glass vials at 30 °C. Homopolymerization of AAc monomer is inhibited by adding different amounts of inhibitor in the solution. Different concentrations of sulfuric acid were added to enhance the degree of grafting. Gamma radiation chamber GC-5000 having ^{60}Co as a radiation source was used for irradiation of sealed glass vials, supplied by M/s BRIT, India. The dose rate was 0.75 kGy measured by Fricke dosimetry. Homopolymers of AAc from grafted films were removed by washing with hot distilled water after soaking overnight. The grafted films were rested overnight at 40 °C in oven for drying and then weighed. Equation 4.1 was used for the determination of degree of grafting.

$$\text{Degree of grafting } (\%) = \frac{W_g - W_o}{W_o} \times 100 \qquad 4.1$$

where W_g and W_o denote the weights of grafted and ungrafted PP films, respectively.

4.2.1 Optimization of grafting

Four factors and five level central composite design (CCD) based on response surface methodology (RSM) was used in this study to optimize the grafting conditions viz. monomer concentration, radiation dose, inhibitor concentration and sulfuric acid concentration. RSM may be summarized as a collection of mathematical and statistical techniques that have been successfully used for developing, improving and optimizing processes [141]. In RSM method, second-order quadratic models are widely used due to their several advantages. They can be taken on a wide variety of functional forms and are very flexible. They would work well as an approximation to the true response surface. Moreover, it is very easy to estimate the parameters in a second-order model using the method of least squares. Central composite design (CCD) is one of the most important experimental designs and is extensively used in the building of second order response surface models and optimization process studies [142-144]. Monomer concentration (0-16 wt%), radiation dose (0-16 kGy), inhibitor concentration (0-0.12 M) and sulfuric acid concentration (0-0.4 M) were the input parameters, and degree of grafting was the response of the system. The operating range and coded levels of experimental variables are shown in Table 4.1, and experimental design matrix is shown in Table 4.2. Total 30 experiments (Table 4.2) suggested by RSM were conducted in this study. For statistical calculations, the levels for the four parameters X_i (X_1(A), X_2(B), X_3(C), X_4(D)) were coded as x_i according to the following relationship:

$$x_i = \frac{X_i - X_0}{\delta X} \qquad 4.2$$

where x_i is coded (dimensionless) value of parameter; X_i, X_0 are values of the parameter x_i at the center point and δX represents the step change. Based on this, the levels were designated as -2, -1, 0, +1, +2 (Table 4.1)

The experiments were run in random order to give randomly distributed variables. The experimental data obtained as per Table 4.2 were analysed using Design-Expert software, and second order quadratic equation (equation 4.3).

$$Y = \beta_0 + \sum_{i=1}^{k} \beta_i x_i + \sum_{i=1}^{k} \beta_{ii} x_i^2 + \sum_{1 \subseteq i \subseteq j}^{k} \beta_{ij} x_i x_j + \varepsilon \qquad 4.3$$

where β_0, β_i, β_{ii} and β_{ij} are the regression coefficients for intercept, linear, quadratic and independent variables, k is the number of variables, x_i represent the variables, Y is the response (degree of grafting) and ε represents the noise or random error in the response Y.

Table 4.1 Process parameters and their levels for grafting of AAc on PP

Variable	Units	Factors	Level, x_i				
			-2	-1	0	1	2
Monomer concentration, A	(wt%)	X_1	0	4	8	12	16
Radiation dose, B	(kGy)	X_2	0	4	8	12	16
Inhibitor concentration, C	(M)	X_3	0	0.03	0.06	0.09	0.12
Sulfuric acid concentration, D	(M)	X_4	0	0.1	0.2	0.3	0.4

Table 4.2 Run conditions for central composite design

Run order	Grafted films	Monomer conc. (wt%)	Radiation dose (kGy)	Inhibitor conc. (M)	Sulfuric acid conc. (M)
1	PP1	4	4	0.03	0.1
2	PP2	12	4	0.03	0.1
3	PP3	4	12	0.03	0.1
4	PP4	12	12	0.03	0.1
5	PP5	4	4	0.09	0.1
6	PP6	12	4	0.09	0.1
7	PP7	4	12	0.09	0.1
8	PP8	12	12	0.09	0.1
9	PP9	4	4	0.03	0.3
10	PP10	12	4	0.03	0.3
11	PP11	4	12	0.03	0.3
12	PP12	12	12	0.03	0.3
13	PP13	4	4	0.09	0.3
14	PP14	12	4	0.09	0.3
15	PP15	4	12	0.09	0.3
16	PP16	12	12	0.09	0.3
17	PP17	0	8	0.06	0.2
18	PP18	16	8	0.06	0.2
19	PP19	8	0	0.06	0.2
20	PP20	8	16	0.06	0.2
21	PP21	8	8	0	0.2
22	PP22	8	8	0.12	0.2
23	PP23	8	8	0.06	0
24	PP24	8	8	0.06	0.4
25	PP25	8	8	0.06	0.2
26	PP26	8	8	0.06	0.2
27	PP27	8	8	0.06	0.2
28	PP28	8	8	0.06	0.2
29	PP29	8	8	0.06	0.2
30	PP30	8	8	0.06	0.2

In order to check the adequacy of model, sequential model sum of squares and model summary statistics were used. The model terms are selected significant on the basis of P-value with 95% probability level. A probability P value less than 0.05 (P< 0.05) was taken as the level of significance [142]. The coefficients of determination (R^2) were determined to check the quality of fit of experimental data into the model. Analysis of variance (ANOVA), quality of fit of the model (F-test) was used for the statistical analysis of the estimated sets of data for this study. Three dimensional plots were used to study the interaction of independent variables on dependent variable.

4.2.1.1 Regression model equation development

The regression equations were obtained by fitting the experimental data into the linear, quadratic and cubic models as shown in Table 4.3. The most suitable model was described by test of sequential model sum of squares, model summary statistics and subsequent ANOVA. It is found that quadratic model most suitably described the degree of grafting and higher polynomial order and model is not aliased [145]. Based on the CCD method using the quadratic model of equation (4.3), the approximated quadratic equation is obtained in terms of coded factors as follows:

$$Y = 13.64 + 9.69X_1 + 9.09X_2 + 2.21X_3 + 4.56X_4 + 0.74X_1^2 + 0.42X_2^2 - 1.23X_3^2 + 0.025X_4^2 + 7.77X_1X_2 + 0.4X_1X_3 + 3.31X_1X_4 + 0.77X_2X_3 + 4.15X_2X_4 + 0.5X_3X_4 \quad 4.4$$

Table 4.3 ANOVA results of fitting the experimental data to various models

Source model	*Sum of squares*	*Df*	*Mean square*	*F value*	*P value Prob>F*	*Std. Dev.*	*R-squared*	*Adj R-squared*	*Pred. R-squared*	
Linear	4852.1	4	1213.0	16.7	0.0001	8.50	0.729	0.685	0.576	Suggested
2FI	1432.9	6	238.8	12.1	0.0001	4.43	0.944	0.914	0.776	Suggested
Quadratic	71.82	4	17.9	0.8	0.4917	4.48	0.955	0.913	0.740	Suggested
Cubic	293.5	8	36.69	33.1	0.0001	1.05	0.999	0.995	0.855	Aliased

Coefficient of determination was used to check the quality of the model. The higher coefficient of determination of model 0.955 is close to unity. This indicates that 95.5% of the total variation in the degree of grafting was attributed to the experimental variable studied. "Adeq Precision" is used to measure the signal to noise ratio. Signal to noise ratio value for this model is 18.584, higher than the minimum desirable value 4, indicating an adequate signal [123]. ANOVA results are shown in Table 4.4. The F-value and prob>F for this model were 22.6 and 0.0001, respectively, which is a high F-value and prob>F less than 0.05 indicating that this model is significant.

Table 4.4 ANOVA results of the established model for responses

Source model	*Sum of squares*	*Df*	*Mean square*	*F value*	*P value Prob>F*	
Model	6356.97	14	1213.0	22.60	<0.0001	Significant
A	2255.44	1	2255.44	112.27	<0.0001	Significant
B	1981.62	1	1981.62	98.64	<0.0001	Significant
C	116.77	1	116.77	5.81	0.0292	Significant
D	498.317	1	498.317	24.80	0.0002	Significant
A^2	15.011	1	15.011	0.74	0.4010	
B^2	4.776	1	4.776	0.23	0.6329	
C^2	41.764	1	41.764	2.07	0.1699	
D^2	0.017	1	0.017	0.001	0.9773	
AB	966.27	1	966.27	48.09	<0.0001	Significant
AC	2.51	1	2.51	0.12	0.7285	
AD	175.69	1	175.69	8.74	0.0098	Significant
BC	9.61	1	9.61	0.47	0.4997	
BD	274.89	1	274.89	13.68	0.0021	Significant
CD	4.00	1	4.00	0.19	0.6618	
Residual	301.33	15	20.08			
Lack of fit	300.25	10	30.02	139.30	<0.0001	
Pure error	1.07	5	0.216			
Cor. total	6658.30	29				

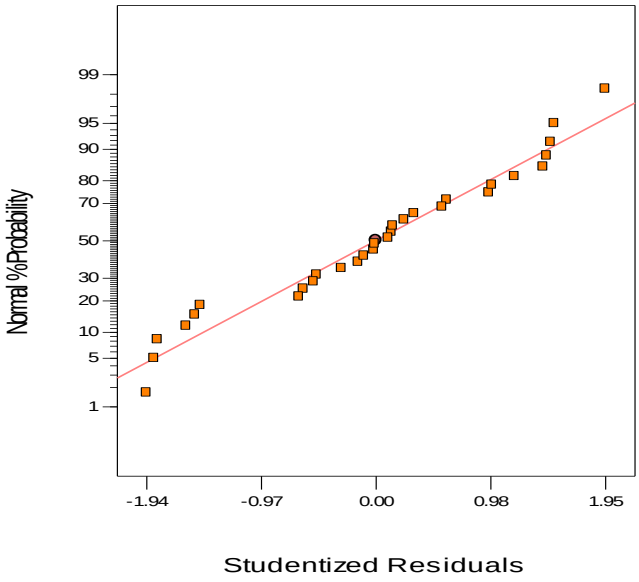

Figure 4.1 Plots of normal probability of residuals

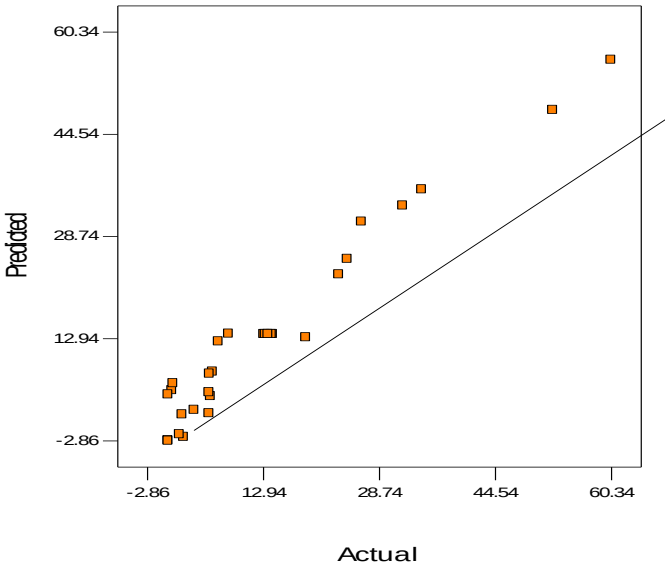

Figure 4.2 Plots of predicted degree of grafting obtained from the model in comparison with the measured degree of grafting

Figure 4.1 shows that the normality assumption was satisfied since all the residuals were linear forming a straight line. Residual data is very important for judging the model accuracy. Therefore, to validate the accuracy, normal probability of the residuals data was plotted with the normality assumption. Figure 4.2 presents the model predicted and actual degree of grafting. It is confirmed that the predicted degree of grafting is in general agreement with the observed data, in the whole range of the operating variables.

4.2.1.2 Effect of operating parameters on grafting and optimization

The effects of four parameters namely radiation dose, sulfuric acid concentration, monomer concentration and inhibitor concentration are shown in three dimension plot in Figure 4.3. Effects of radiation dose and monomer concentration on degree of grafting are shown in Figure 4.3(a). Generation of free radicals on the surface of the film increased with increase in radiation dose and length of grafting chain increased with increase in radiation dose. Increasing monomer concentration increased grafting percentage at lower radiation dose, increasing monomer concentration has no effect on degree of grafting due to formation of less free radicals on the surface of monomer. This is true also for increasing radiation dose at lower monomer concentration but at higher value of radiation dose, increasing monomer concentration sharply increases degree of grafting due to formation of more free radicals on the surface of the monomer. More than 100% degree of grafting is achieved at monomer concentration 16 wt% and 16 kGy radiation dose. Effects of sulfuric acid concentration and monomer concentration on degree of grafting are shown in Figure 4.3 (b). The degree of grafting increased with increase in sulfuric acid concentration at lower monomer concentration. This is due to the partitioning of monomer into the backbone polymer [114]. This is true also for increasing monomer concentration at lower sulfuric acid concentration but at higher value of monomer concentration,

increasing sulfuric acid concentration sharply increases degree of grafting due to the good solubility of acrylic acid in solvent, which provide good accessibility of acrylic acid to free radical sites. The degree of grafting 70% is achieved at 0.4 M sulfuric acid concentration and 16 kGy radiation dose. Effects of sulfuric acid concentration and radiation dose are shown in Figure 4.3 (c). The grafting has increased with increase in sulfuric acid concentration and dose. The grafting has also increased with increase in sulfuric acid concentration at lower radiation dose, increasing sulfuric acid concentration has no effect on degree of grafting. This is true also for increasing radiation dose at lower solvent concentration but at higher value of radiation dose, increasing solvent concentration sharply increases degree of grafting due to the formation of higher free radical sites on the back bone of PP and solvent provides easy accessible path for acrylic acid to graft on the surface of PP. The degree of grafting 85% is achieved at 0.4 M sulfuric acid concentration and 16 wt% monomer concentration. Table 4.5 shows the degree of grafting under different values of the parameters studied. The maximum degree of grafting 60.34% is achieved at run order 16 and minimum degree of grafting 0.52% is achieved at run order 1.

As there was not much improvement of biodegradability beyond 35% degree of grafting (Figure 4.20) with respect to increases in degree of grafting, 35% degree of grafting was taken as the targeted response [146]. The Design Expert software was used to optimize the conditions for obtaining targeted degree of grafting. Table 4.6 shows all the input factors in range and targeted response value. The optimized conditions for targeted degree of grafting of AAc on PP are shown in Table 4.7 (desirability = 1). These results have shown that targeted degree of grafting 35% could be achieved by varying the monomer concentration (6.88-13.52 wt%), radiation dose

(6.74-13.42 kGy), inhibitor concentration (0.01-0.11M) and sulfuric acid concentration (0.12-0.36 M).

The targeted degree of grafting at the optimized conditions suggested by RSM were supported by further experiments conducted with the most favorable condition: monomer concentration 12.09 wt%, radiation dose 12.40 kGy, inhibitor concentration 0.07 M and sulfuric acid concentration 0.12 M (Table 4.8). The experiments with this condition were performed in triplicate and average degree of grafting achieved was around 34%, which is very close to the targeted degree of grafting 35%. Hence, the conditions (i.e. monomer concentration 12.09 wt%, radiation dose 12.40 kGy, inhibitor concentration 0.07 M and sulfuric acid concentration 0.12 M) are considered as optimized conditions for the targeted degree of grafting 35%.

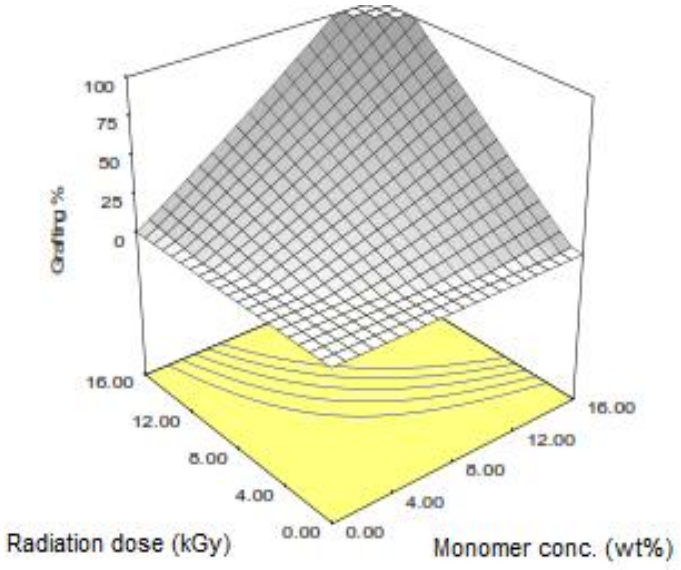

(a)

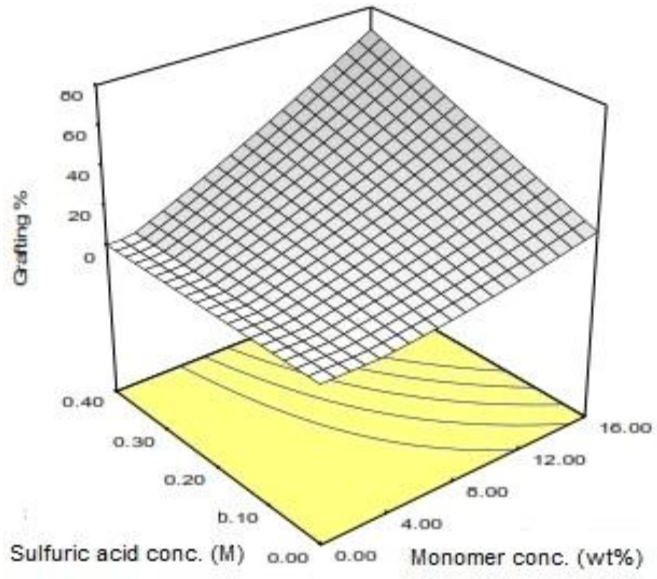

(b)

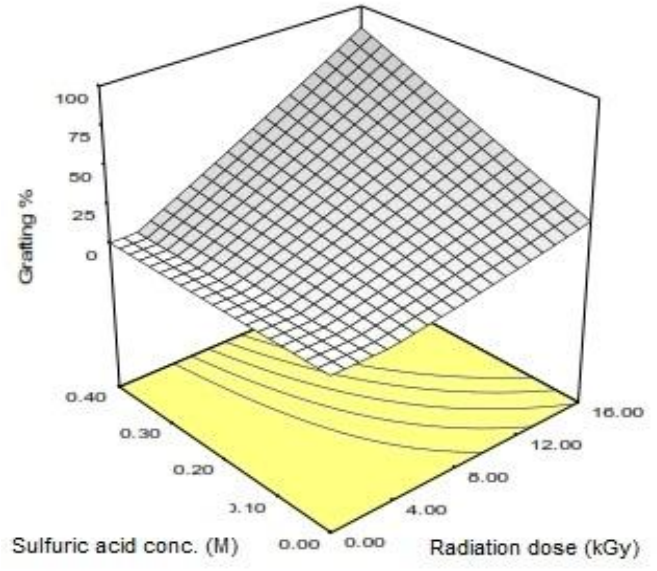

(c)

Figure 4.3 Response surface plots showing the effects of each parameter on degree of grafting of samples (a) radiation dose and monomer concentration (b) sulfuric acid concentration and monomer concentration (c) sulfuric acid concentration and radiation dose

Table 4.5 Degree of grafting under different operating parameters

Run order	Monomer conc. (wt%)	Radiation dose (kGy)	Inhibitor conc. (M)	Sulfuric acid conc. (M)	Degree of grafting (%)
1	4	4	0.03	0.1	0.5
2	12	4	0.03	0.1	6
3	4	12	0.03	0.1	2
4	12	12	0.03	0.1	24
5	4	4	0.09	0.1	0.6
6	12	4	0.09	0.1	6
7	4	12	0.09	0.1	4
8	12	12	0.09	0.1	26
9	4	4	0.03	0.3	2
10	12	4	0.03	0.3	6
11	4	12	0.03	0.3	6
12	12	12	0.03	0.3	52
13	4	4	0.09	0.3	2
14	12	4	0.09	0.3	7
15	4	12	0.09	0.3	8
16	12	12	0.09	0.3	60
17	0	8	0.06	0.2	No grafting
18	16	8	0.06	0.2	35
19	8	0	0.06	0.2	No grafting
20	8	16	0.06	0.2	32
21	8	8	0	0.2	Gel formation
22	8	8	0.12	0.2	19
23	8	8	0.06	0	6
24	8	8	0.06	0.4	23
25	8	8	0.06	0.2	13
26	8	8	0.06	0.2	14
27	8	8	0.06	0.2	14
28	8	8	0.06	0.2	13
29	8	8	0.06	0.2	14
30	8	8	0.06	0.2	14

Table 4.6 Range of input parameters and response

Parameter	*Goal*	*Lower limit*	*Upper limit*	*Lower weight*	*Upper weight*	*Importance*
Monomer concentration (wt%)	in range	0	16	1	1	3
Radiation dose (kGy)	in range	0	16	1	1	3
Inhibitor concentration (M)	in range	0	0.12	1	1	3
Sulfuric acid concentration (M)	in range	0	0.4	1	1	3
Degree of grafting (%)	target = 35	0	100	1	1	3

Table 4.7 Solution to reach the targeted degree of grafting

Number	*Monomer conc. (wt%)*	*Radiation dose (kGy)*	*Inhibitor conc.(M)*	*Sulfuric acid conc. (M)*	*Degree of grafting (%)*	*Desirability*
1	12.09	12.40	0.07	0.12	35	1
2	6.88	13.42	0.05	0.36	35	1
3	14.84	6.74	0.11	0.29	35	1
4	9.83	11.49	0.01	0.35	35	1
5	9.02	13.35	0.10	0.21	35	1
6	13.52	9.78	0.05	0.18	35	1

Table 4.8 Optimum conditions to reach the targeted degree of grafting

Monomer conc. (wt%)	Radiation dose (kGy)	Inhibitor conc.(M)	Sulfuric acid conc. (M)	Predicted degree of grafting (%)	Experimental degree of grafting (%)
12.09	12.40	0.07	0.12	35	34

4.3 Tensile properties

Grafting affects the mechanical properties of the PP films. To investigate this effect, tensile strength and elongation at break of PP and grafted PP films were examined. The results are shown in Table 4.9. PP had tensile strength of 39 MPa and elongation of 3.6%, which decreased with increase in degree of grafting. PP18 has the tensile strength 21 MPa, is higher than 20 MPa applicable for packaging application [147]. Elongation at break curve confirms that increasing grafting percentage decreases the elongation (Figure 4.4). This decrease in tensile strength and elongation at break with increase in grafting was observed due to the chain scission of the polymer chain occurring on irradiation. The 8 grafted samples PP15, PP30, PP22, PP24, PP4, PP8, PP20 and PP18 having tensile strength more than 20 MPa for further characterization such as FTIR, XRD, SEM, biodegradability etc.

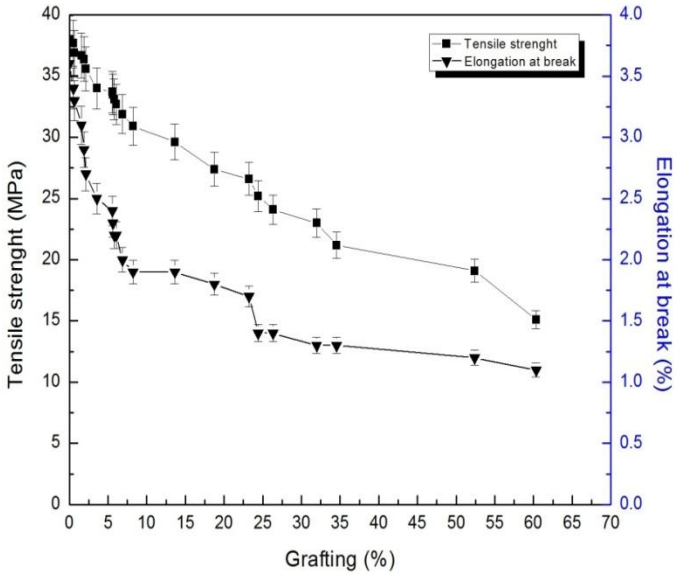

Figure 4.4 Change in tensile strength and elongation at break of the films with increase in degree of grafting

Table 4.9 Mechanical properties of PP and grafted PP films

Run order	Grafted films	Tensile strength at yield (MPa)	Elongation at break (%)
1	PP1	38±2	2.1±0.1
2	PP2	34±2	2.1±0.1
3	PP3	36±2	1.7±0.1
4	PP4	25±2	1.4±0.1
5	PP5	37±2	3.1±0.2
6	PP6	33±2	2.5±0.1
7	PP7	34±2	2.4±0.1
8	PP8	24±2	1.2±0.1
9	PP9	37±2	1.6±0.1
10	PP10	33±2	1.9±0.1
11	PP11	34±2	2.2±0.1
12	PP12	20±2	1.4±0.1
13	PP13	36±2	2.2±0.1
14	PP14	32±1	3.3±0.2
15	PP15	31±1	2.1±0.1
16	PP16	15±1	1.1±0.1
18	PP18	21±1	1.3±0.1
20	PP20	23±1	1.3±0.1
22	PP22	28±1	2.2±0.1
23	PP23	34±2	2.2±0.1
24	PP24	27±1	2±0.1
30	PP30	30±2	1.8±0.1

4.4 Characterization

4.4.1 Swelling studies

Swelling of the PP and grafted PP films in water was studied. Swelling of all the grafted films increased with increase in time and came to equilibrium within 24 h. Swelling increases due to the incorporation of carboxylic groups on the PP films. Effect of time on swelling results is shown in Figure 4.5. PP shows negligible swelling. Whereas, swelling increases with increase in degree of grafting up to 12.82% for PP18. Swelling percentage was calculated using equation 3.1 and the results are shown in Figure 4.6 as function of grafting degree.

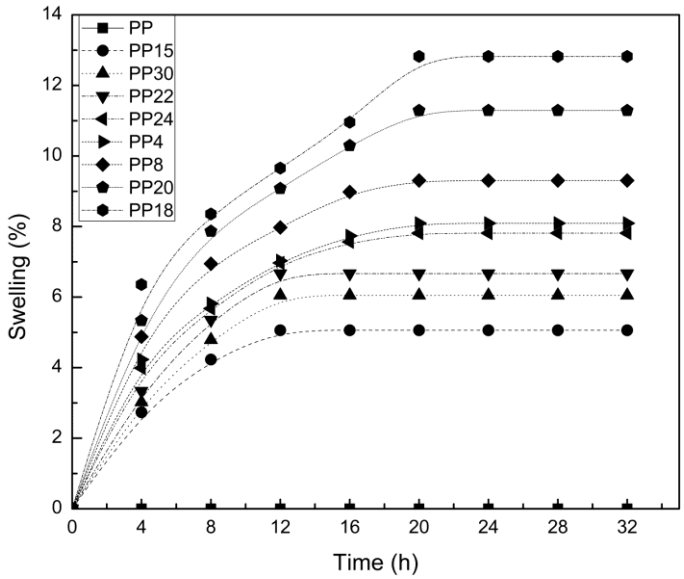

Figure 4.5 Effect of time on swelling of PP and grafted PP films

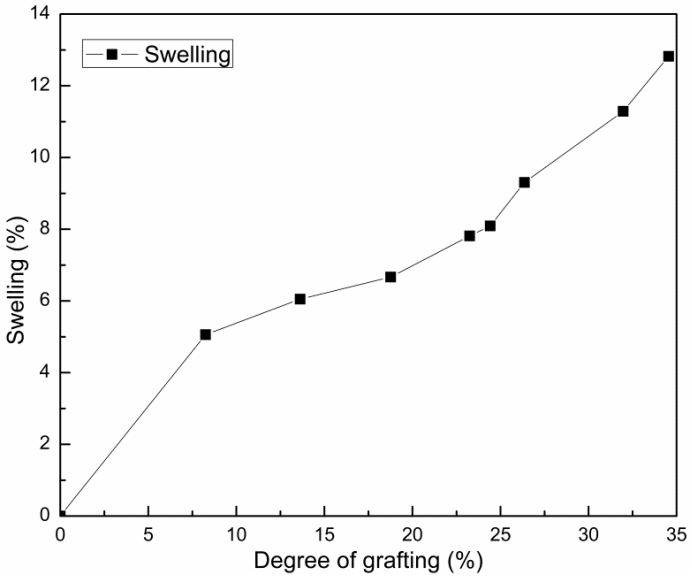

Figure 4.6 The water retention value of grafted PP film as function of degree of grafting

4.4.2 Moisture content

The Moisture contain in the grafted sample increased with increase in degree of grafting. The moisture content of PP18 is 3.25% in comparison to PP (0%). The moisture content increases with increase in degree of grafting due to the increase in hydrophilic nature of grafted PP films. Whereas, the moisture content of PP22, PP8 and PP18 are 1.98%, 2.58% and 3.25%, respectively.

4.4.3 Fourier transform infrared (FTIR) spectroscopy

To confirm that grafting has really taken place, FTIR spectra of PP and grafted PP films were investigated. Figure 4.7 shows the FTIR spectra of PP and grafted PP films. The bands in between 2700 cm^{-1} and 3000 cm^{-1} are due to the –CH stretching of the –CH group of PP [148]. The peaks near 1450 and 1380 cm^{-1} are the CH_2 and CH_3 deformation bands, respectively. The strongest peak in between 1700 cm^{-1} and 1705 cm^{-1} in figure refers to the stretching of the C=O group of carboxylic acid and C-O band at 1100-1250 cm^{-1} of acrylic acid grafted on PP films

[149]. The amount of carboxylic groups on the grafted PP films also confirms the grafting of acrylic acid on to PP films as discussed in subsequent section.

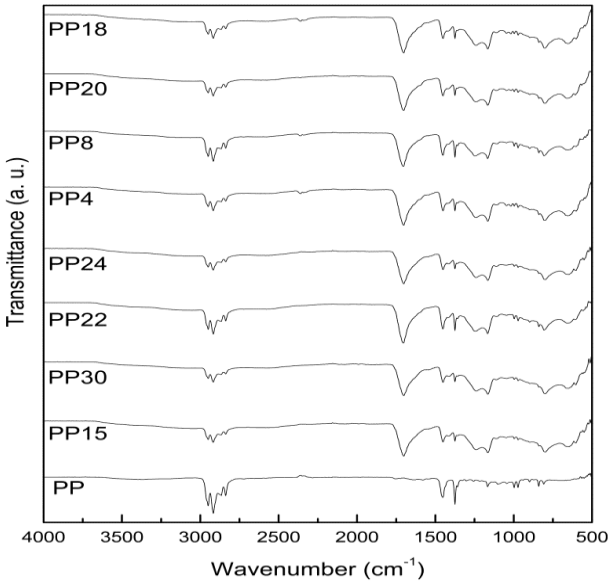

Figure 4.7 Infrared spectra of PP and grafted PP films

4.4.4 Carboxylic group analysis

Colorimetric analysis was used to determine the amount of carboxylic groups present on the grafted PP films. The amounts of carboxylic groups on the grafted films were quantified using methylene blue dye. The amount of carboxylic groups present on the different degree of grafted films is shown in Figure 4.8. The analysis of carboxylic group on the grafted PP films shows that the maximum amount of carboxylic groups was present on the film with 34.6% degree of grafting. Further increase in degree of grafting did not increase the amount of accessible carboxylic groups. Table 4.5 shows 35% degree of grafting corresponding to the run order 18 with higher monomer concentration and lower dose (16 wt% and 8 kGy) in comparison to run order 12 and 16 where degree of grafting were 52 % and 60 %, respectively, with lower monomer concentration and higher dose (12 wt% and 12 kGy). Therefore, at higher dose &

lower monomer concentration higher degree of grafting can be achieved. But at the same time, due to higher dose, increase in thickness of grafted layer and increase in crosslinking prevent the amount of accessible carboxylic acid.

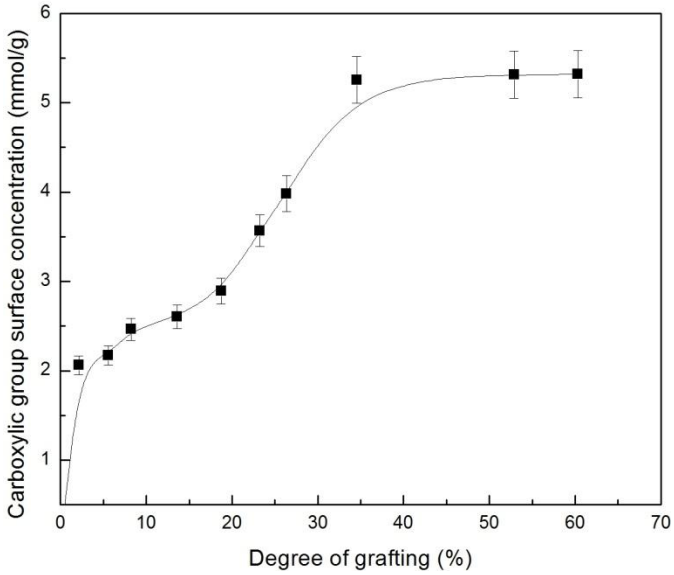

Figure 4.8 Carboxylic group surface concentration of grafted films with different degree of grafting

4.4.5 X-ray diffraction (XRD)

Figure 4.9 shows the X-ray diffraction peaks of PP and grafted PP films. The diffractogram of pure PP showed the diffraction peaks at 2θ =14.5° and 16° which correspond to crystallographic planes of 110 and 010, respectively. The intensity of the crystalline peak is lower in the grafting PP indicating the presence of grafting on PP films. It may be stated that acrylic acid chain decreases the crystallinity of the PP.

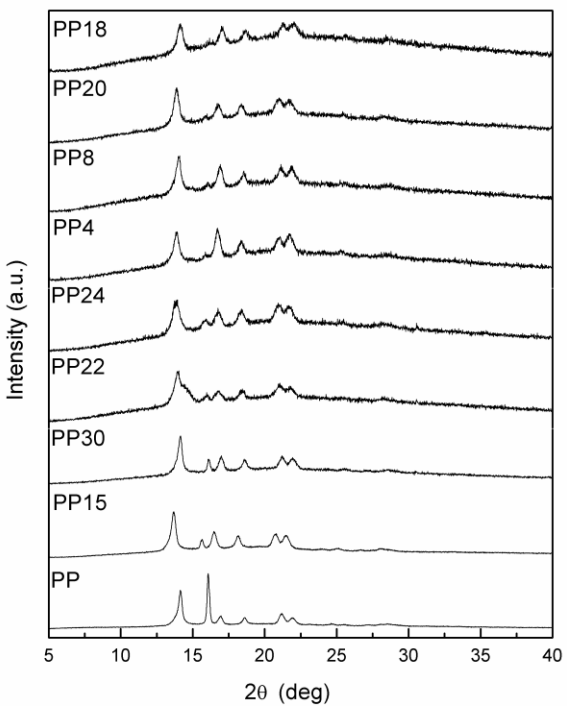

Figure 4.9 XRD patterns of PP and grafted PP films

4.4.6 Differential scanning calorimetry (DSC)

DSC studies were performed on PP and grafted PP films. The melting and crystallization behaviors of the films are shown in Figure 4.10 and Figure 4.11, respectively. The melting temperature (T_m), corresponding to the maxima of the peaks in the heating DSC curves, crystallization temperature (T_c), corresponding to the maxima of peaks in the cooling DSC diagrams, and enthalpy of melting (ΔH_m), estimated from the area under the melting peak, are listed in Table 4.10 for different films. The crystallinity of films were calculated from equation 3.2 and shown in Table 4.10. Increasing grafting percentage decreases enthalpy of melting. The crystallinity of the grafted PP films decreases with increase in grafting because of the presence of amorphous AAc. Amorphous AAc monomer inherently dilutes the crystallinity of the grafted PP films [150]. T_m of the grafted film decreases with increase in degree of grafting due to destruction of the ordered structure of the PP crystals on grafting [151]. Grafted PP films needed

more energy for the recrystallization as shown by increase in T_c with increase in degree of grafting. Furthermore, no significant changes in T_c were observed for degree of grafting from 8% to 24%. However, considerable change in %crystallinity was observed. On the otherhand, T_c was found to increase with degree of grafting (from 24% to 35%) with considerable change in decrease in %crystallinity. The observed increased T_c with decrease in crystallinity can be attributed due to the nucleation behavior of carboxylic group of acrylic acid into PP [152]. This might improve the crystallization capability of PP and crystallize it at higher temperatures. Similar results were also found by other authors [153-155].

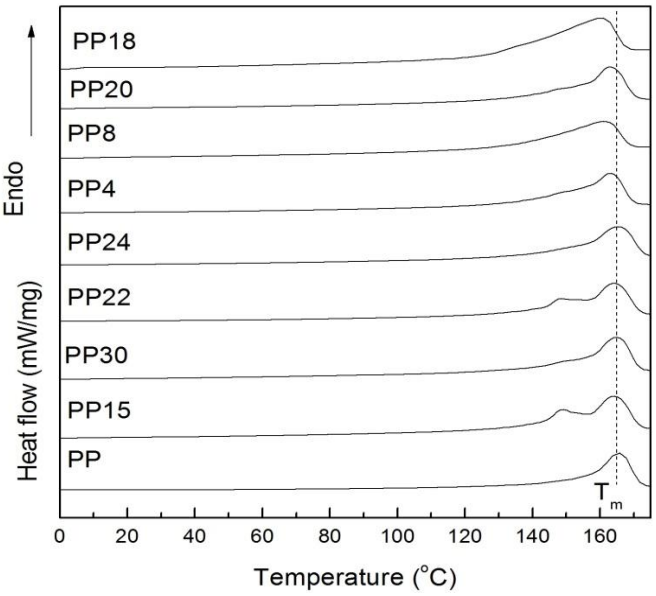

Figure 4.10 DSC melting thermographs of sample films

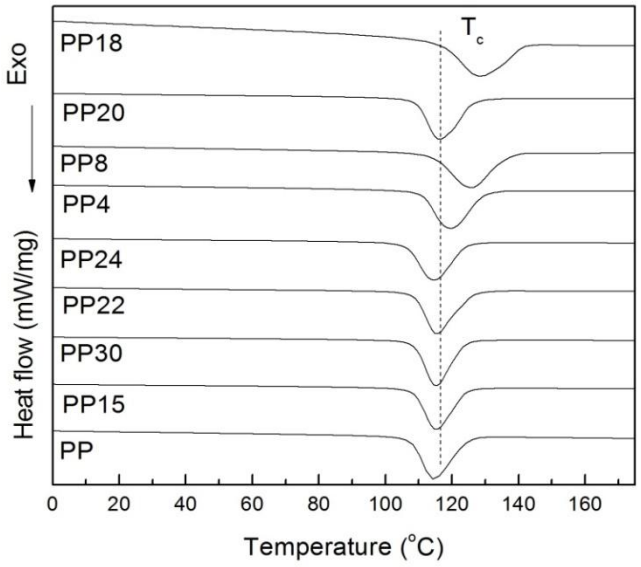

Figure 4.11 DSC crystallization thermographs of sample films

Table 4.10 DSC results of PP and grafted PP films

Polymer films	Degree of grafting (wt%)	T_m (°C)	T_c (°C)	ΔH_m (J/g)	Crystallinity (%)
PP	0	166	115	104	59
PP15	8	164	116	88	54
PP30	14	165	115	85	51
PP22	18	164	115	82	50
PP24	23	164	115	78	48
PP4	24	163	116	72	45
PP8	26	163	119	72	44
PP20	32	161	126	60	36
PP18	35	160	128	44	27

4.4.7 Thermogravimetric analysis (TGA)

Figure 4.12 shows the TGA curves of PP and grafted PP films and results are summarized in Table 4.11. Initial decomposition temperature (T_i) and final temperature (T_f) are the 5% loss of weight and 5% residue left of the films, respectively. Thermal stability of the grafted PP films

decreased with increase in grafting percentage. The T_i of the grafted PP films is lower than PP confirmed by the early degradation of the grafted PP films. The thermogram of PP film shows single stage decomposition and thermal stability up to 350°C, beyond which there was a smooth decrease in weight. The complete degradation of PP film occurs at near 530 °C. Whereas grafted films show three distinct steps of weight loss; first step starts from 30 to 200°C, this may be attributed to the elimination of moisture via dehydration process from the hydrophilic matrix. Such characteristic has been confirmed by various grafting systems [124]. Second step in between 200 to 400 °C, corresponds to the decomposition of carboxylic groups on the PP films [156] due to the decarboxylation process [124]. The third step in between 400 to 700°C was due to the weight loss because of degradation of PP backbone chain. Increasing grafting percentage increased weight loss as confirmed by the quantitative comparison of weight loss in second step. Thus, TGA studies confirmed that the thermal stability of grafted films is lower than that of PP film.

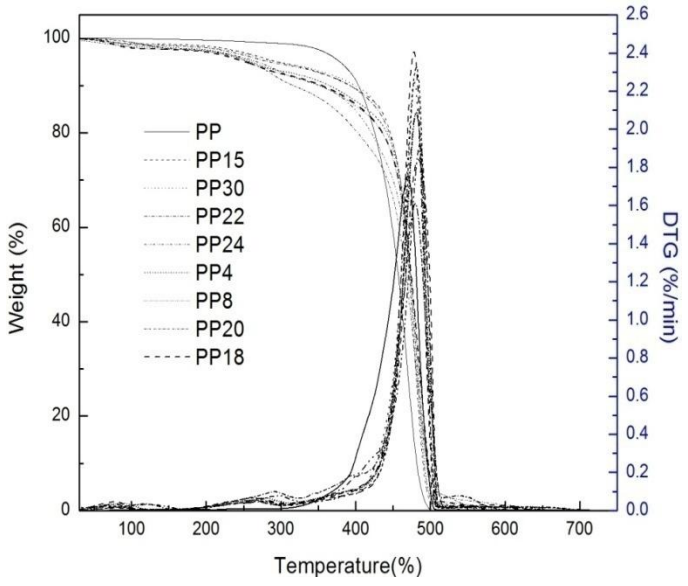

Figure 4.12 TGA profiles of PP and grafted PP films

Table 4.11 TGA results of PP and grafted PP films

Polymer films	T_i (°C)	T_f (°C)	% loss of weight	% residue left
PP	379	487	100	0
PP15	297	494	100	0
PP30	295	496	100	0
PP22	285	499	100	0
PP24	269	503	100	0
PP4	261	496	100	0
PP8	259	500	100	0
PP20	257	505	100	0
PP18	253	501	100	0

4.4.8 Scanning electron microscopy (SEM)

The SEM images of the original and grafted PP films are shown in Figure 4.13. The surface of grafted PP films was totally different from the original PP film. Scanning electron microscopy (SEM) analyses indicated that PP film surface was smooth but grafted films surface becomes heterogeneous due to the considerable deposition of carboxylic groups on the PP surface. It was observed that the presence of carboxylic groups on the surface of the PP film increased the roughness on the surface. Roughness is mostly related to the site of graft initiation, which would occur most frequently in the amorphous as opposed to crystalline surface regions of the film [120].

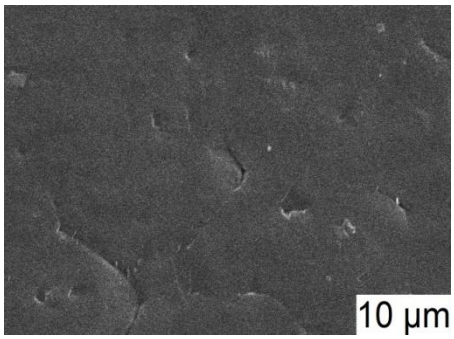

(a)

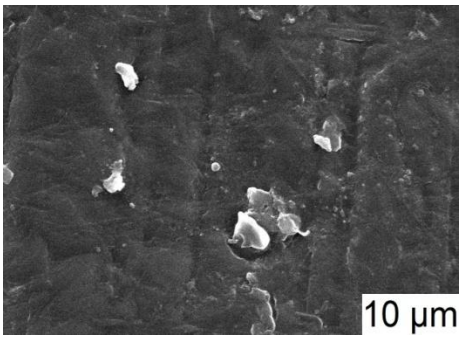

(b)

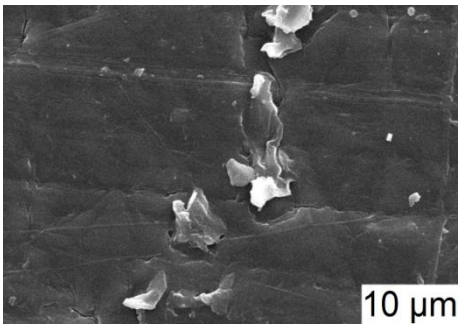

(c)

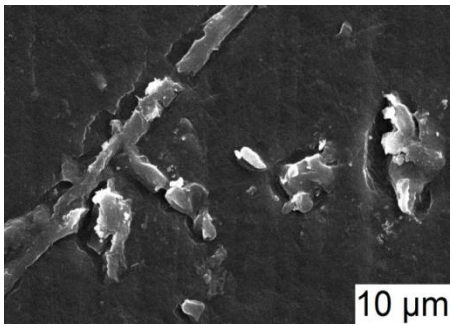

(d)

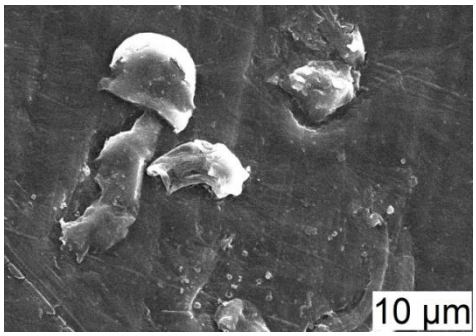

(e)

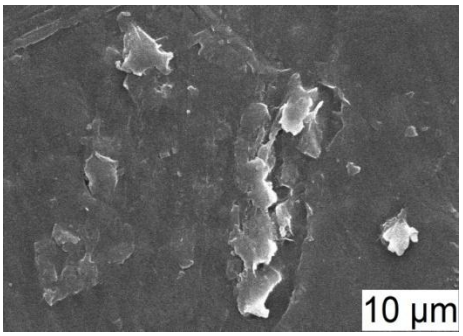

(f)

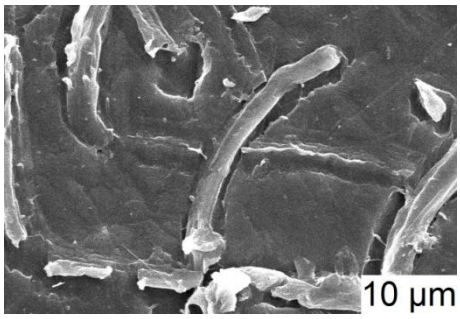

(g)

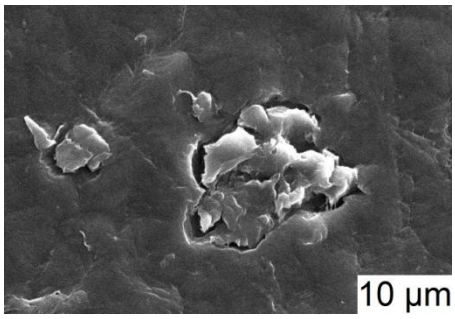

(h)

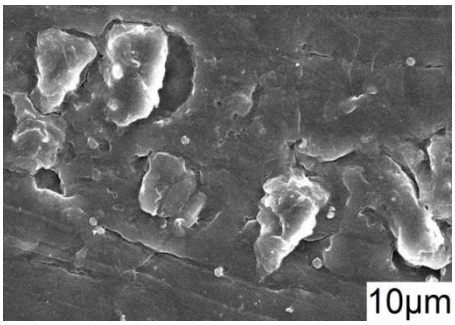

(i)

Figure 4.13 SEM of (a) PP, (b) PP15, (c) PP30, (d) PP22, (e) PP24, (f) PP4, (g) PP8, (h) PP20 and (i) PP18

4.5 Thermal degradation kinetics

PP and three desired grafted (18%, 22% and 35%) sample were taken for the thermal degradation study.

4.5.1 Thermal stability

To know the thermal stability of the grafted PP samples at different degrees of grafting, TGA analysis was performed, as the thermal stability requirements are different for different applications. The TG and DTG thermograms of neat PP and grafted PP films at four heating rates are shown in Figure 4.14. The expected thermal degradation of PP has been reported to occur via random scission followed by a radical transfer process. The scheme (a) accounts for the formation of the most abundant degradation products. Pathway A proceeds via a secondary radical and produces the major products such as pentane (24.3%), 2-methyl-1-pentene (15.4%), and 2,4-dimethyl 1-heptene (18.9%). The primary radical of pathway B forms only minor products with 1.9% propane being the most abundant. The TG thermogram of PP shows single step thermal degradation, whereas thermograms of grafted PP films show three stage degradation: first stage is between 30-200°C due to the dehydration process where

moisture is eliminated from the grafted PP surface due to the AAc content [121]. In the second stage, grafted chains of acrylic acid were degraded due to the decarboxylation and carbonization process in between 200-400 °C [157] and the third stage is the region for the maximum weight loss due to extensive degradation of the polymer backbone chain in between 400 to 700°C. The expected degradation mechanism of the PP-g-AAc is shown in scheme (b) [158]. In the first step, water is removed from the PP-g-AAc due to the dehydration process. In the second step, film is degraded into (C) PP substitute and (D) into acrylic substitute. In the third step, PP is further degraded into other smaller substitutes in the forms of E and F. The initial degradation temperature (T_i) corresponding to 5% weight loss and final degradation temperature (T_f) corresponding to 5% residual left, calculated at different heating rates, are summarized in Table 4.12 within the standard uncertainty of ± 2 °C. T_{max} shows the third stage degradation, where maximum weight loss occurs due to degradation of polymer backbone chain and used for the calculation of active energy E_a. At the heating rate of 5 °C/min, PP starts to decompose at 337 °C, whereas 35% degree of grafted PP starts to degrade at lower temperature (215 °C). The degradation temperatures at the heating rate of 5 °C/min for the grafted PP are 227 °C for PP22, 226 °C for PP8 and 215 °C for PP18. This shows that initial degradation temperature decreases with increase in degree of grafting. This is favorable for their environmental degradation. Similar results were also obtained at higher heating rates. The degradation temperatures of PP and grafted PP samples at different conversion levels are shown in Table 4.13. The results show that the thermograms are shifting to higher temperature with increasing heating rate due to the slow heat diffusion and late attainment of equilibrium [159].

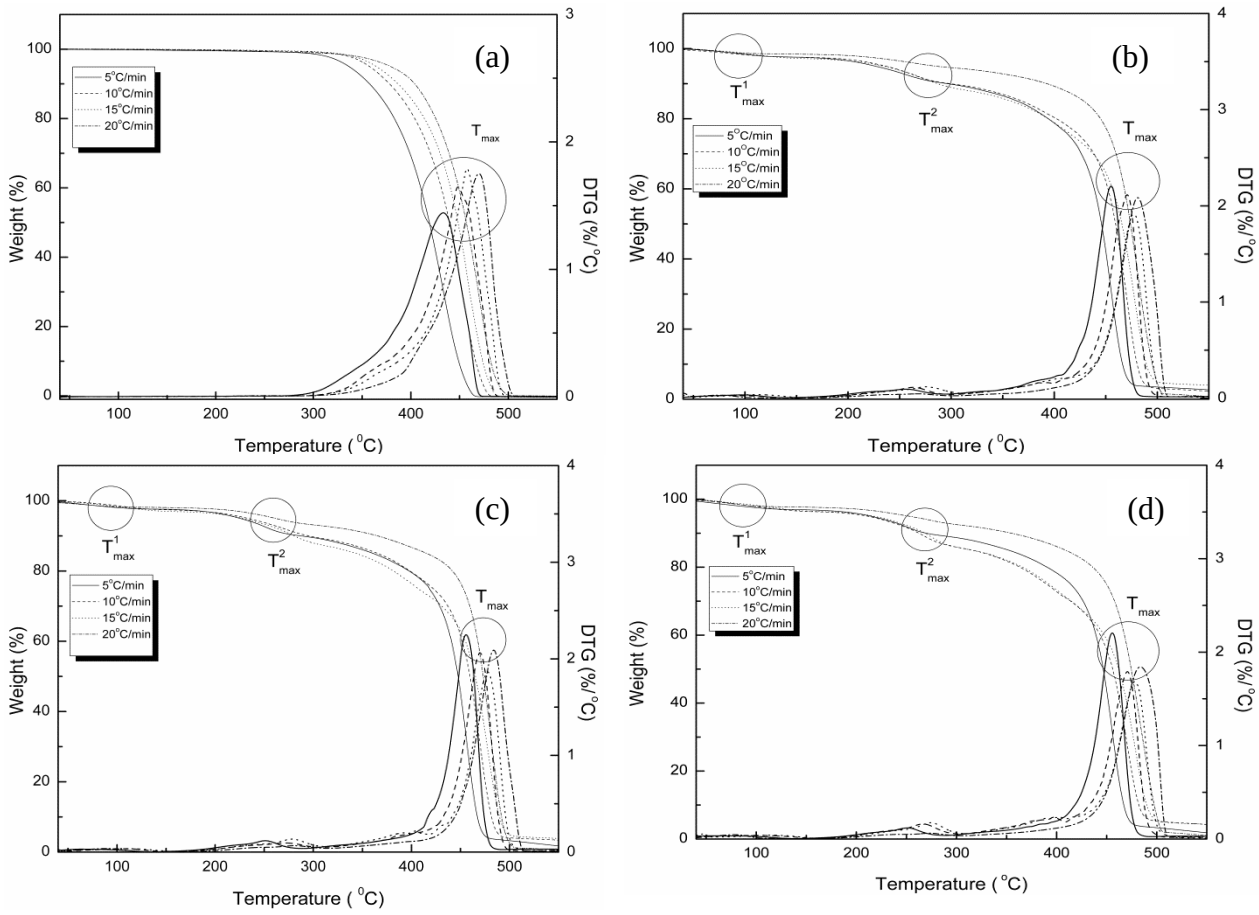

Figure 4.14 TG and DTG curves of (a) PP, (b) PP22, (c) PP8, and (d) PP18

Table 4.12 TGA data for PP and grafted PP films

Polymer sample	(%) Grafting	T_i (°C)	T^1max (°C)	T^2max (°C)	T_{max} (°C)	T_f (°C)
β = 5°C/min						
PP	0	337	-	-	436	454
PP22	18	227	102	256	456	498
PP8	26	226	101	252	456	496
PP18	35	215	103	251	457	505
β = 10°C/min						
PP	0	357	-	-	451	471
PP22	18	236	110	263	473	495
PP8	26	233	107	271	467	490
PP18	35	215	101	266	473	498
β = 15°C/min						
PP	0	364	-	-	456	478
PP22	18	238	110	275	478	503
PP8	26	236	106	278	477	494
PP18	35	217	112	274	478	499
β = 20°C/min						
PP	0	379	-	-	462	487
PP22	18	285	105	268	484	499
PP8	26	261	103	262	485	496
PP18	35	252	102	273	490	501

Table 4.13 Degradation temperatures for different percentage conversions at different heating rates

Conversion (%)	Degradation Temperature (°C)			
	PP	PP22	PP8	PP18
β = 5°C/min				
10	357	296	287	269
20	383	394	397	390
30	399	426	428	426
40	410	438	440	439
50	419	445	447	446
60	426	451	452	451
70	433	455	456	456
80	440	460	461	460
90	449	466	467	467
β = 10°C/min				
10	378	299	295	270
20	404	402	398	393
30	420	438	437	427
40	431	452	451	447
50	439	459	459	456
60	446	464	465	463
70	452	469	470	469
80	458	474	475	474
90	466	480	481	482
β = 15°C/min				
10	386	300	297	278
20	413	404	399	396
30	430	438	438	434
40	440	456	455	447
50	448	465	465	462
60	454	471	471	470
70	460	477	477	476
80	466	482	482	482
90	473	489	489	490
β = 20°C/min				
10	404	392	365	354
20	425	445	441	436
30	439	459	459	457
40	449	468	467	467
50	456	474	473	474
60	463	479	478	480
70	469	483	482	485
80	475	488	486	491
90	482	495	491	497

Suggested degradation schemes

(a)

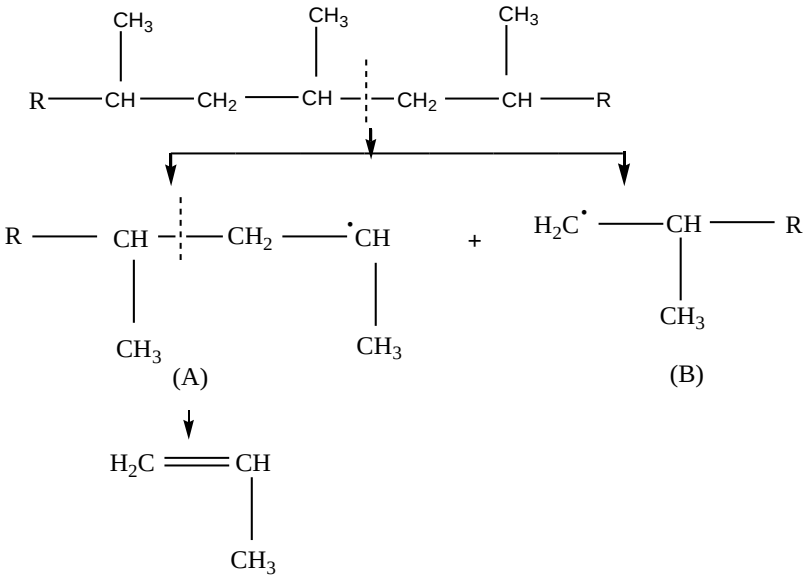

(b)

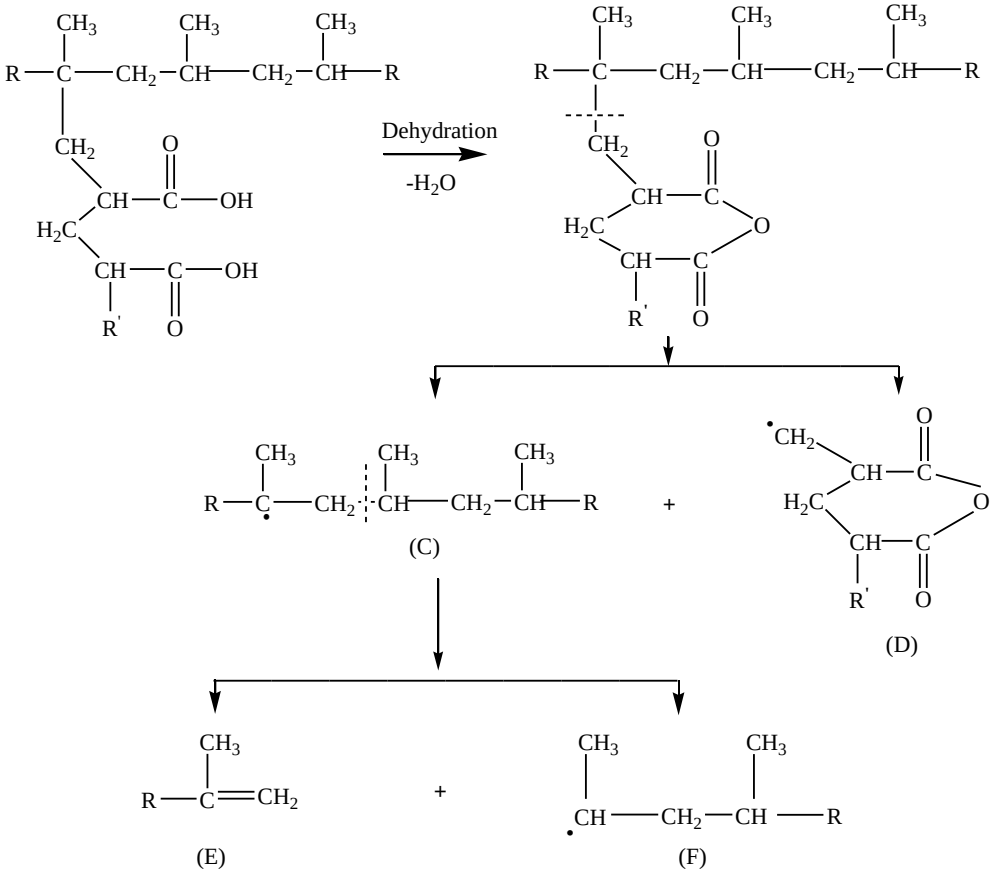

4.5.2 Kinetics of thermal degradation

4.5.2.1 Kissinger method

Figure 4.15 shows the plots between $\ln(\beta/T_{\max}^2)$ and $(1/T_{max})$ at different heating rates of 5, 10, 15, and 20°C/min. The calculated kinetic parameters for all the films are given in Table 4.14. The values of E_a for PP and grafted PP are 219, 194, 192 and 182 kJ/mol, respectively. It shows that the E_a value of PP decreases with increase in degree of grafting and PP18 has minimum activation energy E_a of 182 kJ/mol. This decrease in activation energy confirms the decreasing thermal stability of PP with increase in degree of grafting. There is almost similar reaction order for all the grafted samples, but frequency factor decreases with increase in degree of grafting.

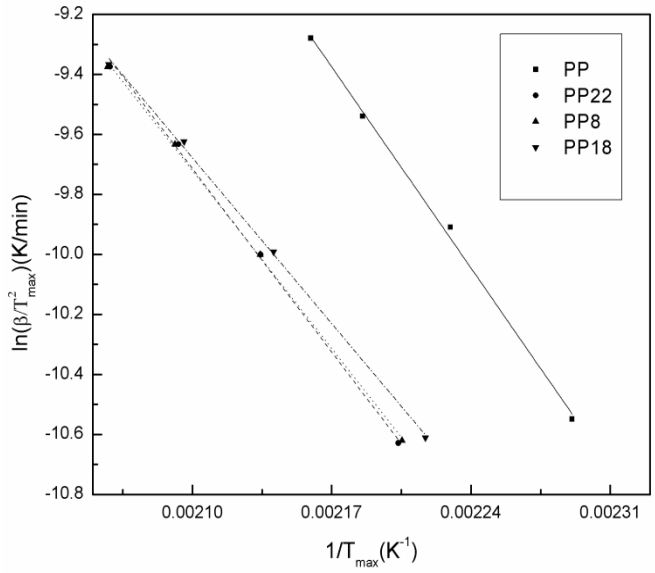

Figure 4.15 Kissinger plots for investigation of all samples

Table 4.14 Degradation kinetic parameters for PP and grafted PP, determined by Kissinger method

Sample code	Kinetic parameters		
	E_a (kJ/mol)	n	ln(Z)
PP	219	1.2	24.4
PP22	194	1.1	22.6
PP8	192	1.1	20.0
PP18	182	1.0	18.8

4.5.2.2 Kim-Park method

The Kim-Park plots for PP and grafted PP samples at maximum degradation are shown in Figure 4.16. The kinetic parameter values E_a, n and ln(Z) were determined by the slope of the plot between [ln(q)/(T_{max})] versus [$1/T$]. The calculated values of E_a, n and ln(Z) are summarized in Table 4.15. The linear-fitted straight line from the points is obtained from equations 4.15 and 4.16. The E_a values are almost similar to the previous method. The value of E_a is highest for the PP sample (223 kJ/mol) and lowest for the PP18 (183 kJ/mol). This also confirms that the grafting of acrylic acid on the PP decreases the thermal stability. There is small change in the reaction order but the frequency factor decreases with increase in degree of grafting.

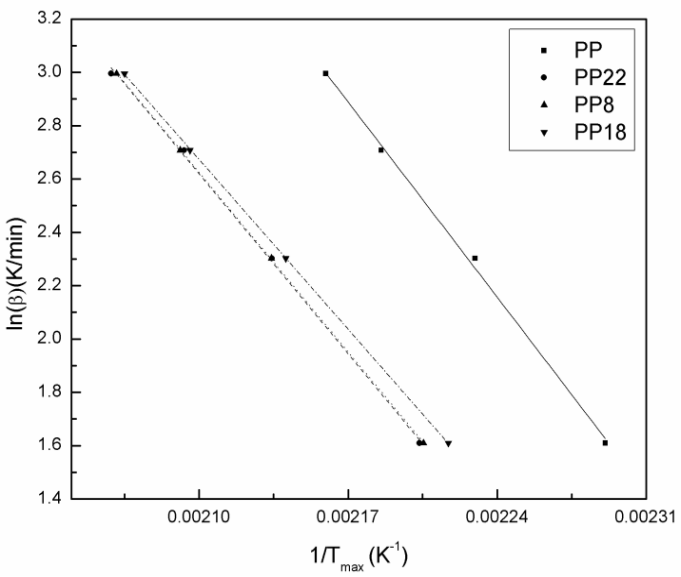

Figure 4.16 Kim-Park plots for PP and grafted PP films

Table 4.15 Degradation kinetic parameters for PP and grafted PP, determine by Kim–Park method

Sample code	Kinetic parameters		
	E_a (kJ/mol)	n	ln(Z)
PP	223	0.5	43.5
PP22	194	0.5	38.8
PP8	192	0.3	36.8
PP18	183	0.2	35.7

4.5.2.3 Flynn-Wall method

The Flynn-Wall plots obtained between ln(β) and *1/T* for PP and grafted PP samples at the heating rates of 5, 10, 15 and 20 °C/min are shown in Figure 4.17. The kinetic parameters are given in Table 4.16. The value of E_a for PP at 5% conversion is 188 kJ/mol and it increases to 258 kJ/mol for 15% conversion. Whereas for PP18, value of E_a is 111 kJ/mol and it increases up to 177 kJ/mol for 15% conversion. The value of E_a is highest for the PP sample and lowest for

the PP18 at all conversion levels confirming that the grafting of acrylic acid monomer on the PP decreases the thermal stability, whereas E_a increases with increase in percentage conversion for all the samples.

The degradation kinetic parameters are different due to different mechanisms at the initial and final stages; at the initial stage, the degradation occurs at comparatively weaker bonds. Therefore, low activation energies are associated with the initial decomposition stage. However, PP is a linear polymer; hence, the rate-limiting step of the thermal degradation of PP is caused by random scission, which requires higher activation energy [129]. Further, the polymeric structure of PP decomposes during the carbonization process, generating smaller intermediate products, which can further react and produce low molecular weight hydrocarbon molecules, liquids, and gases [160, 161]. However, this process is not followed by each bond broken in the polymer chain. Only small fragments could be evaporated at that particular temperature, and then weight loss happens, which is recorded and shown by the balance. Hence, the rate of weight change of the polymer and degradation kinetics is influenced by both physical and chemical processes [162].

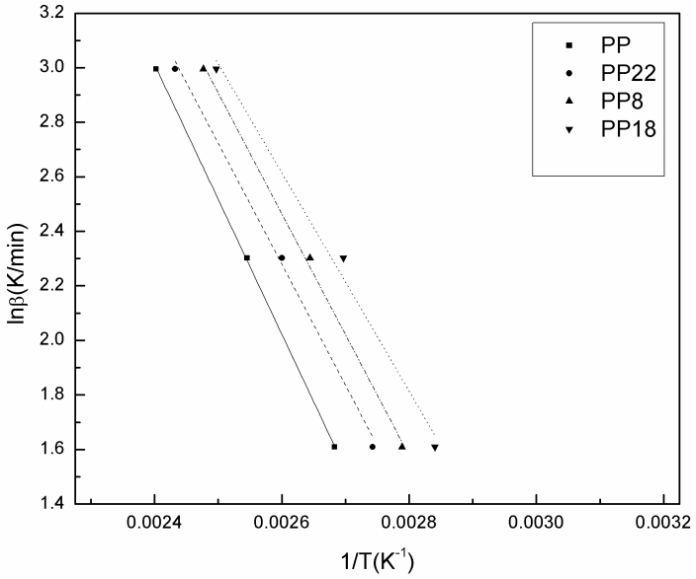

Figure 4.17 Flynn-Wall plots for all films at 15% conversion

Table 4.16 Thermal degradation kinetic parameters of the samples calculated by using Flynn-Wall method

Conversion	PP		PP22		PP8		PP18	
(%)	E_a *(kJ/mol)*	ln(*Z*)	E_a *(kJ/mol)*	ln(*Z*)	E_a *(kJ/mol)*	ln(*Z*)	E_a *(kJ/mol)*	ln(*Z*)
5	188	19.2	156	17.5	131	15.9	111	14.3
10	233	21.4	175	18.9	154	17.3	142	15.9
15	258	24.8	203	21.9	187	19.5	177	17.0

4.5.3 Rate constant versus temperature

The changes in the rate constant with temperature for all the films are plotted. The rate constant changes with temperature and the values obtained at conversion levels of 5% are shown in Figure 4.18. The rate constant value slowly increases with the temperature in the lower temperature range, but increases exponentially at higher temperatures. The rate constant of PP is lowest, but increases with increase in degree of grafting. The trend of grafted PP is also same as PP throughout the degradation region, although the threshold value of the rate constant is

different for the grafted PP as compared to neat PP sample. The rate constant value for the grafted PP is higher than that of PP sample.

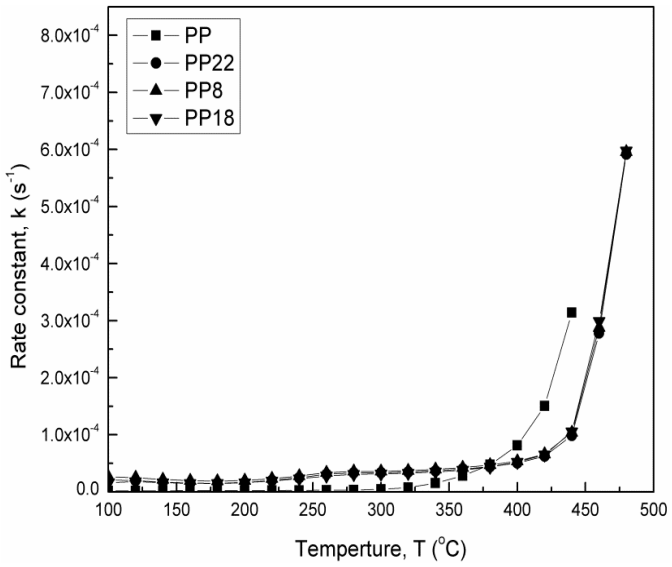

Figure 4.18 Rate constant versus temperature plots for PP and grafted PP samples at 5% conversion

4.5.4 Lifetime estimation

The lifetime of all the samples at different temperatures is calculated using equation 3.18 with the value of E_a from Kissinger, Kim-Park and Flynn-Wall (at conversion = 15%) methods and heating rate (β) of 5 °C/min. The results of lifetime estimation are shown in Figure 4.19. It is very clear that the lifetime of all the samples decreases with increase in temperature irrespective of the method used for estimation. For example, the lifetime of neat PP by thermal degradation at 50 °C estimated by three methods namely Kissinger, Kim-Park and Flynn-Wall method is 2.6×10^5, 6.04×10^5 and 18.6×10^7 years, respectively. Whereas, these values are much lower at 70 °C - 2.25×10^3, 4.69×10^3 and 6.9×10^5 years, respectively. Similarly, in case of PP18 the estimated lifetime is 492.9, 584.3 and 210.7 years at 50 °C and 9.5, 11.2 and 4.53 years at 70°C,

respectively. The lifetime of acrylic acid grafted films is lower than that of PP due to the low thermal stability caused by the formation of radicals during the degradation process due to the presence of carboxylic group on the surface of grafted PP.

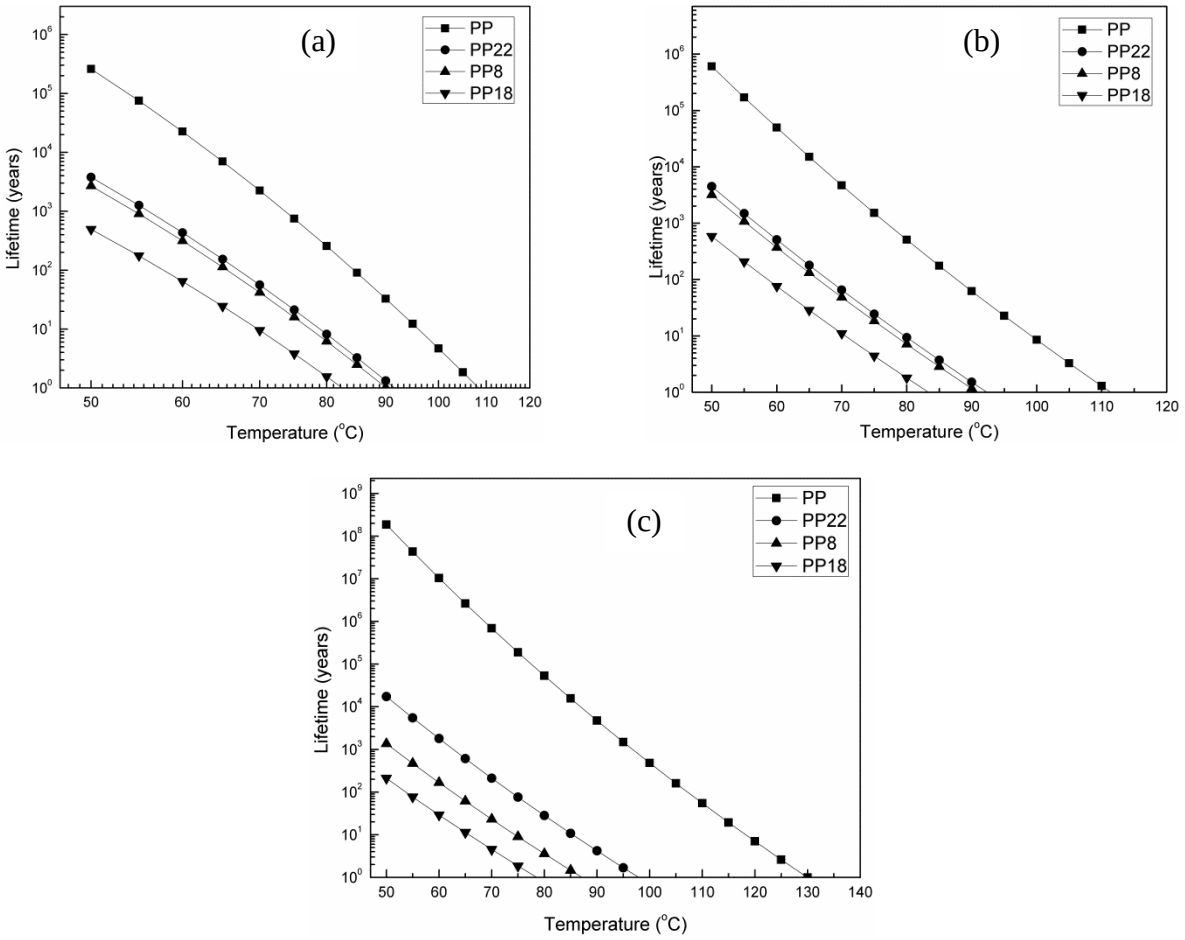

Figure 4.19 Lifetime of PP and grafted PP by (a) Kissinger (b) Kim-Park and (c) Flynn-Wall methods

4.6 Biodegradability studies

The total organic carbon (TOC) of different samples were measured to calculate the theoretical carbon dioxide [CO_2(th)], and shown in Table 4.17.

Table 4.17 Total organic carbon (%) and theoretical CO_2 (g) evolution from the samples

Sample	TOC (%)	Wt. of carbon in 1 g of sample (g)	Th. CO_2 evolution (g)
Microcrystalline cellulose (MCC)	42	0.42	1.54
PP	94	0.94	3.44
PP15	87	0.87	3.18
PP30	86	0.86	3.14
PP22	85	0.85	3.11
PP24	85	0.85	3.11
PP4	84	0.84	3.07
PP8	84	0.84	3.07
PP20	83	0.83	3.03
PP18	82	0.82	3.00

Example calculation for theoretical CO_2

CO_2 (*Th*) for PP18 sample = $1 \times 0.82 \times \frac{44}{12} = 3.00$

The values of CO_2 produced (in grams) and the percent biodegradation of each sample were calculated using equation 3.20., which are shown in Table 4.17.

Example calculation for percent biodegradation

Vol. of $Ba(OH)_2$ taken = 30 ml

Normality of $Ba(OH)_2$ = 0.024

Therefore, molarity of $Ba(OH)_2$ = $\frac{0.024}{2} = 0.012$ [as the acidity of $Ba(OH)_2$ is 2]

Hence, mmols of $Ba(OH)_2$ taken = 30 x 0.012 = 0.36 mmols

And,

Vol. of HCl used = 9.7 ml

Normality of HCl = 0.05

Molarity of HCl = 0.05 [as the basicity of HCl is 1]

Hence, mmols of HCl used = 9.7 x 0.05 = 0.485 mmols

Now,

mmols of CO_2 produced = $\text{mmoles of } Ba(OH)_2 \text{ at start} - \frac{\text{mmoles of HCl}}{2}$

$$= 0.36 - \frac{0.485}{2} = 0.118 \text{ mmols}$$

We know that,

1 mol of CO_2 = 44 g/l

Therefore, 1 mmol of CO_2 = 44 x 10^{-3} = 0.044 g/l

Hence, grams of CO_2 produced = 0.118 x 0.044 = 0.005 g

In this way, the readings were taken in interval of 5 days for 45 days and the cumulative sum of CO_2 produced for PP18 sample was 9.660 grams.

Finally, using equation 3.21, we get

Biodegradation (%) = $\frac{9.66 - 9.49}{3} \times 100$ = 5.5%

PP film was taken as negative reference and cellulose was taken as positive reference. The biodegradable component of the grafted PP films should eventually be mineralized into H_2O and CO_2 by activity of the microorganisms present in the compost. Biodegradation of all the films are shown in Figure 4.20. The resultant sequence of percent biodegradation was: cellulose (76%) > PP18 (5.5%) > PP20 (4.9%) > PP8 (4.5%) > PP4 (3.59%) > PP24 (2.6%) > PP22 (2.2%) > PP30 (1.78%) > PP15 (1.5%). Long carbon chain, hydrophobic nature and high molecular weight makes PP film difficult to degrade. Swelling of hydrophilic AAc before the chain scission accelerated biodegradation of grafted PP films. AAc enhances the hydrophilic nature of the grafted PP films by attaching the functional group on the surface of the PP. Hydrophilicity increases the chain scission and reduces the molecular weight of the grafted PP films. Microorganisms easily assimilated the small constituents of the grafted PP films and converted them into carbon dioxide and water [163]. Increasing grafting percentage increases biodegradation as confirmed by the results. All the grafted PP films show almost same type of curves. Biodegradation 5.5% at 35% grafting was the maximum biodegradation achieved.

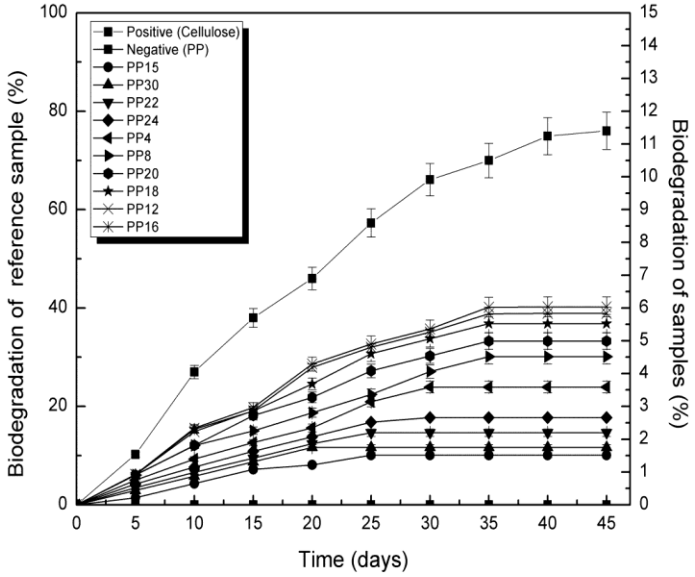

Figure 4.20 Biodegradation of PP (negative reference), cellulose (positive reference) and different grafted PP films

4.7 Ecotoxicological studies

4.7.1 Microbial toxicity test

Table 4.18 shows the number of bacterial colony in the compost extracts. The CFU count in the blank (control) sample was 0.2×10^4 and highest for the cellulose (bacterial lawn). High CFU count confirms the normal growth of the bacteria in all the compost samples containing biodegradable intermediates of grafted films.

Example calculation for colony forming unit (CFUs)

Total Dilution Factor used $=10^{-3}$

Colonies per ml plated for PP18, which are shown in Table 4.18 = 11

Using equation 3.22, we get

$$\text{CFU/ml for PP18} = \frac{11\,\text{colonies/ml plated}}{10^{-3}} = 1.1\times10^4$$

Table 4.18 Bacterial colonies (CFUs) from water extract of compost samples, blank, cellulose, PP and grafted PP films

Sample	Degree of grafting (wt%)	Number of colonies/ml	CFU/ml count * 10^4
Control	Not applicable	2	0.2
Cellulose	Not applicable	Bacterial lawn	Bacterial lawn
PP	0	4	0.4
PP15	8	5	0.5
PP30	14	5	0.5
PP22	18	6	0.6
PP24	23	8	0.8
PP4	24	8	0.8
PP8	26	9	0.9
PP20	32	11	1.1
PP18	35	11	1.1

4.7.2 Plant growth test

The growth of plants (corn and tomato) confirmed the non-toxic nature of biodegradable intermediates [64]. The visual observation of growth of plants (corn and tomato) after 21 days and 100% emergence of plants confirmed non-toxic nature of biodegradable intermediates. The growth of both the plants and the control are similar (Figure 4.21 and Figure 4.22). After 21 days of growth, plants were harvested, dried and weighed. Growth in terms of percentage of dry weight against the control is almost 100% as shown in Figure 4.23.

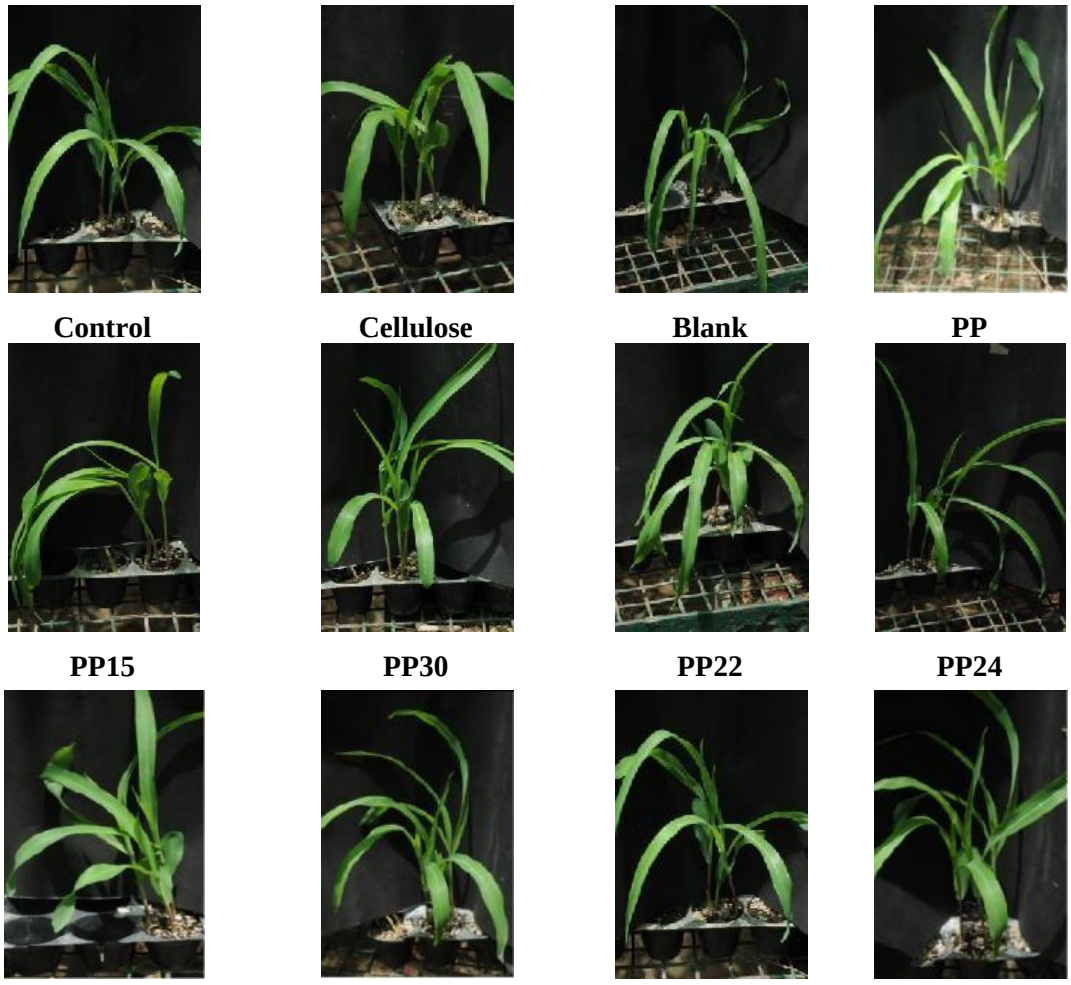

Figure 4.21 Growth of corn plants in compost medium (after 45 days biodegradation)

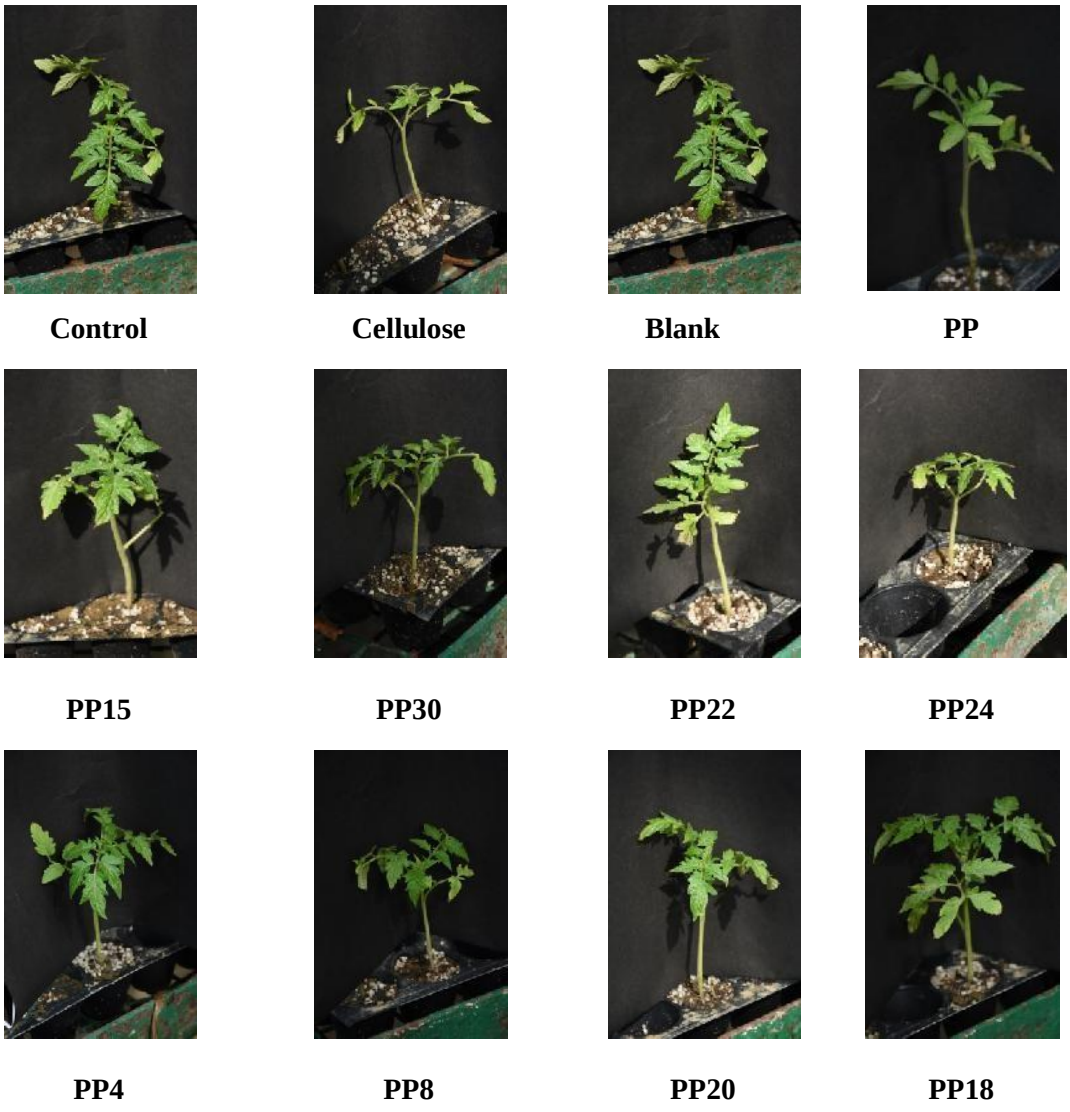

Figure 4.22 Growth of tomato plants in compost medium (after 45 days biodegradation)

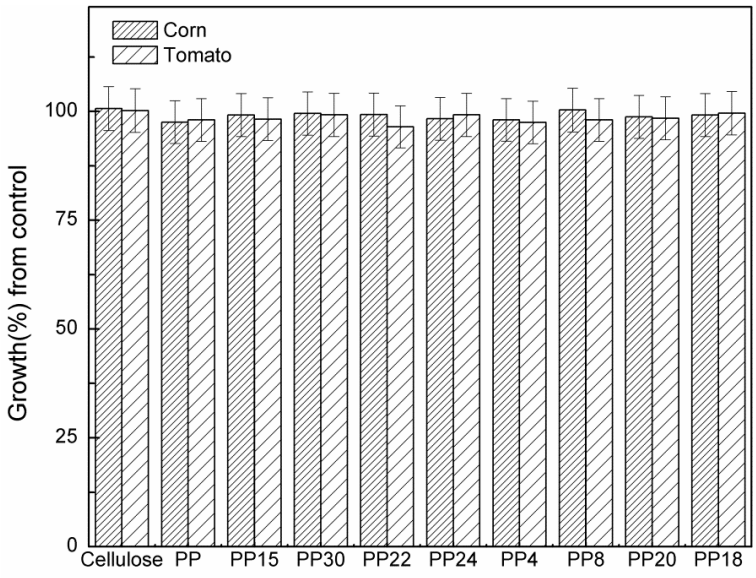

Figure 4.23 Dry weights of plants after 21 days of growth

Chapter 5-PP Blends and Composites

5.1 PP/PLA blends with compatibilizer

5.1.1 Preparation

The blends of PP and PLA with and without compatibilizer prepared by melt blending using Internal Mixer (Haake Poly Lab, Germany) are detailed in Table 5.1. The ingredients (weighed at prescribed ratio) were manually mixed and transfered to the mixer for melt blending. The composition of PP/PLA in blends varied from 100/0 to 75/25. PP/PLA (85/15) was our optimum blend and compatibilized by varying the compatibilizer ratio from 2-8 phr. The melt mixing was done for 4 min, during the mixing rotor speed kept 60 rpm and the temperature maintained at 190°C. The blend was passed through a two-roll mill having 2 mm nip gap.

Table 5.1 Blend compositions

S.No.	Polymer blends	Composition		
		PP (wt%)	PLA (wt%)	PP-*g*-MA (phr)
1	PP	100	0	0
2	PP95PL5	95	5	0
3	PP90PL10	90	10	0
4	PP85PL15	85	15	0
5	PP80PL20	80	20	0
6	PP75PL25	75	25	0
7	PP85PL15MA2	85	15	2
8	PP85PL15MA4	85	15	4
9	PP85PL15MA6	85	15	6
10	PP85PL15MA8	85	15	8

5.1.2 Film preparation

The films of 80-85 μm thickness were prepared from PP/PLA blends and compatibilized PP/PLA blends. Teflon sheets were used to restrict the sticking of melt with plates. The temperature and pressure maintained during the compression molding were 180 °C and 400 kN/m^2. Cooling was performed by water.

5.1.3 Tensile properties

Tensile strength and elongation at break of PP and PP/PLA blends with different compositions are shown in Table 5.2. In an ideal and highly compatible polymer blend, the strength is expected to be higher than or at least between that of the pure polymers [25]. The tensile strength of PP/PLA (85/15) blend was 28 MPa where it was 39 MPa for pure PP. This lower tensile strength of blend is mainly due to immiscibility between the two polymers. Addition of PLA more than 15 wt% reduced the tensile strength drastically to 13 MPa. On the basis of above observation, PP85PL15 is considered optimum composition having sufficiently good tensile strength and requiring relatively low concentration of expensive material. Percentage elongation at break of PP/PLA (85/15) blend was 1.7 where it was 3.6 for pure PP, which may be due to the change from ductile to brittle deformation. The PLA has a lower percentage elongation compared to PP and there is incompatibility between PP and PLA. On the basis of tensile strength, which is in the practical range (ASTM D 4635) we considered PP85PL15 as our optimum blend for further studies.

Table 5.2 shows the effect of variation of compatibilizer (2-8 phr), on the tensile strength. The tensile strength of PP/PLA/MA (85/15/4) blend was 30 MPa as against 28 MPa of PP/PLA (85/15). The improvement in tensile strength of compatibilized blend was mainly due to the

strong bonding and better interaction between the two polymers. The PP85PL15MA4 was chosen as an optimum blend having relatively good tensile strength and low proportion of expensive compatibilizer, for further studies.

Table 5.2 Tensile properties of film samples

S.No.	Polymer blends	Tensile strength (MPa)	Elongation at break (%)
1	PP	39±2	3.6±0.2
2	PP95PL5	37±2	3.1±0.2
3	PP90PL10	35±2	2.1±0.1
4	PP85PL15	28±2	2.0±0.1
5	PP80PL20	13±1	1.9±0.1
6	PP75PL25	11±1	1.7±0.1
7	PP85PL15MA2	28±2	1.7±0.1
8	PP85PL15MA4	30±2	1.7±0.1
9	PP85PL15MA6	31±2	1.8±0.1
10	PP85PL15MA8	18±1	1.5±0.1

5.1.4 Moisture content

The moisture content of PP85PL15 is 2.88% in comparison to PP (0%). The moisture content increased due to increase in incompatibility (void formation and phase separation) between the blend, whereas addition of compatibilizer decreased the moisture content due to increase in compatibility. The moisture content in compatibilized PP/PLA blend was 1.59%.

5.1.5 Fourier transform infrared (FTIR) spectroscopy

The FTIR spectra of all the samples are shown in Figure 5.1, in which peaks between 2949-2866, 1454 and 1375 cm^{-1} were assigned to C-H stretching, CH_3 bending, and C-H bending, respectively for PP [164]. In the spectrum of PLA, the peaks at 1746, 1178, and 1084 cm^{-1} , are associated with C=O stretching, symmetric C-O-C stretching, and asymmetric CH_3, respectively [25]. The peaks in PP/PLA blend (PP85PL15) were observed around 2949-2866, 1454, 1375, 1178, and 1086-1184 cm^{-1}. Addition of compatibilizer in blend PP85PL15MA4 is confirmed by the emergence of new peak at 1757 cm^{-1} representing the carbonyl of ester linkage stretching [25].

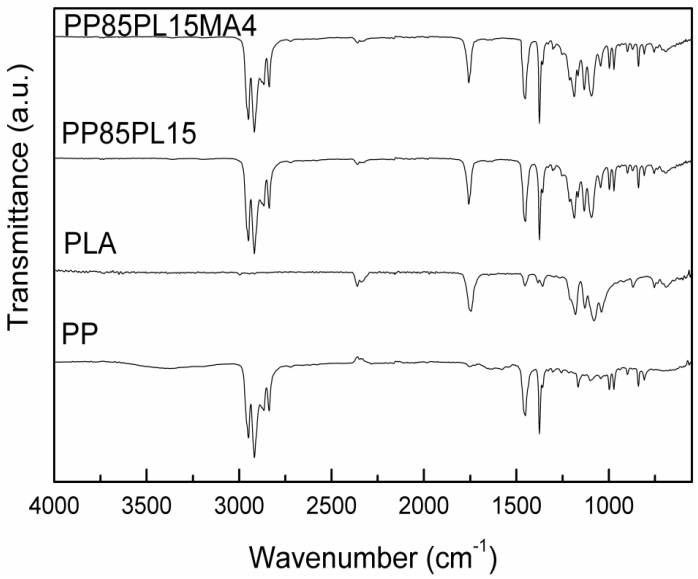

Figure 5.1 FTIR spectra of PP/PLA blends

5.1.6 X-ray diffraction (XRD)

Figure 5.2 shows the XRD patterns of blended films. The peaks of the PP corresponding to the α-monoclinic form are at 2θ = 14.1°, 16.9°, 18.6°, 21.1° and 21.9° [25]. For the PP/PLA blends,

XRD patterns were almost identical to that of the neat PP film. It is confirmed that the peaks in the blend films are dominated by the PP. The diffraction peaks of the blends are similar to PP after addition of PLA.

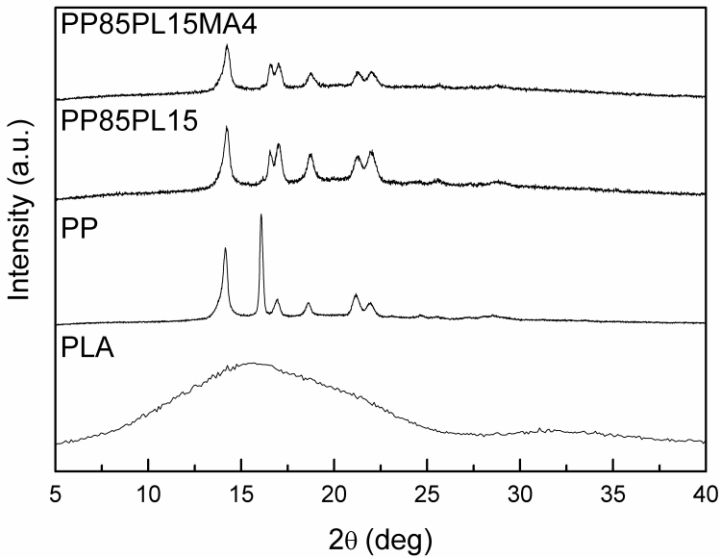

Figure 5.2 XRD patterns of PP/PLA blends

5.1.7 Differential scanning calorimetry (DSC)

The DSC curves of all the blended films are shown in Figure 5.3 and 5.4. The value of melting temperature (T_m), crystallization temperature (T_c) and enthalpy of melting (ΔH_m) of films are shown in Table 5.3. The equation 3.2 was used to determine the crystallinity of all the samples. The crystallinity and T_m of PP are 63% and 166 °C, respectively. The crystallinity and T_m of the PP/PLA (85/15) blend decrease upto 48% and 162°C, respectively. This decrease in crystallinity is mainly due to the incompatibility between two different phases of blend. The different phases of PLA (amorphous) in PP (crystalline) decrease the ordered structure [165]. Whereas addition

of PP-*g*-MA in PP/PLA (85/15) blend shows no further change in T_c [91]. Addition of compatibilizer increases the crystallinity of blend due to the improvement in compatibility.

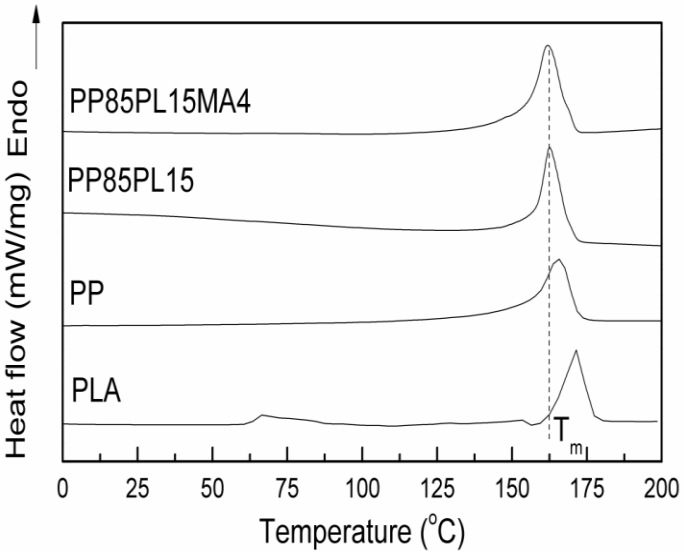

Figure 5.3 DSC melting thermographs of the blends

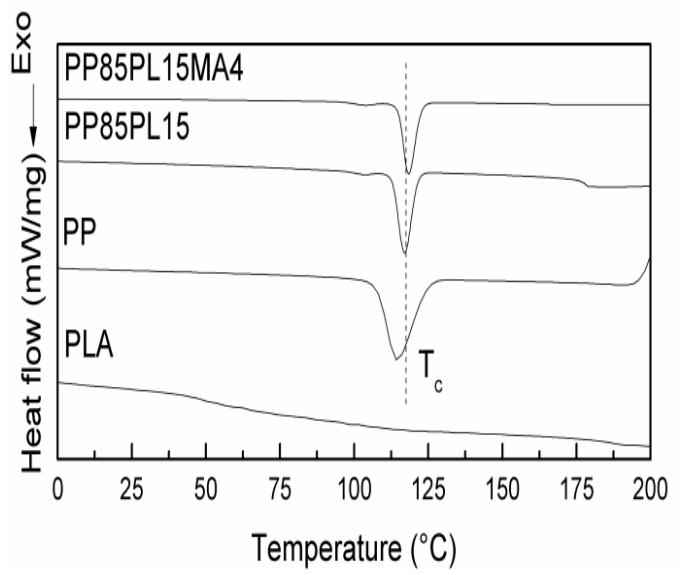

Figure 5.4 DSC crystallization thermographs of the blends

Table 5.3 DSC melting and crystallization parameters of blended films

Samples	T_g (°C)	T_m (°C)	T_c (°C)	ΔH_m (Jg^{-1})	X_c (%)
PP	--	166	117	104	63
PLA	66	171	--	34	Negligible (Amorphous)
PP85PL15	--	162	118	78	48
PP85PL15MA4	--	162	118	95	58

5.1.8 Thermogravimetric analysis (TGA)

Figure 5.5 shows the TG and DTG curves of PP, PLA and blended samples. Curves of neat PP and PLA show single stage degradation. Whereas the blend of PP/PLA shows two-stage degradation due to the immiscibility between the polymers [166]. The initiation (T_i) and final temperature (T_f) are shown in Table 5.4. The initial degradation temperature (T_i) corresponds to 5% weight loss of the polymer sample, and the final degradation temperature (T_f) corresponds to 5% residual left after which no appreciable loss is possible. The initiation and final temperature of thermal degradation of the polymers are essential for evaluating their thermal sensitivity [90]. PP is more thermally stable than PLA, the T_i of PP is 380 °C, higher than that of PLA (335 °C). The addition of PLA decreases the T_i of the blend PP85PL15 upto 345 °C, due to the partial compatibility between the polymers of blend. However, addition of compatibilizer improves the compatibility between the blend components due to which thermal stability of PP85PL15MA4 has improved upto 351 °C. The DTG curves showed single maxima for PP and PLA whereas two maxima for blended films, confirming the phase separation between the two polymers of blend.

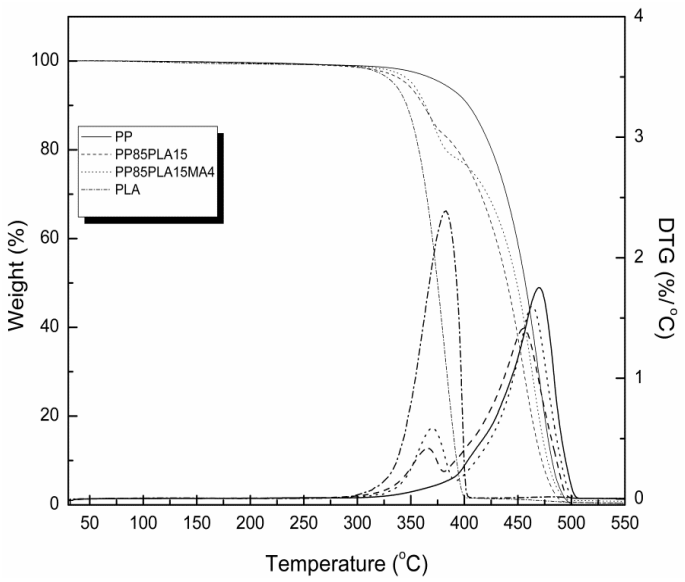

Figure 5.5 TGA profiles of the blends

Table 5.4 TG and DTG analysis of PP/PLA blended samples

Blend/Composite samples	T_i (°C)	T_f (°C)
PP	380	487
PLA	335	396
PP85PL15	345	479
PP85PL15MA4	351	484

5.1.9 Scanning electron microscopy (SEM)

Figure 5.6 shows the SEM micrographs of PP, PLA, PP85PL15, PP85PL15MA4 blends. The SEM observation confirmed the smother surfaces of PP and PLA. But, roughness and voids are present in PP85PL15 blend due to immiscibility between two different polymers. There was immiscibility in the blends as the PLA is brittle in nature and phase separation between two

polymers. The compatibilized blend PP85PL15MA4 is showing much smoother surface and continuous phase compared to PP85PL15 due to compatibility and improved facial adhesion.

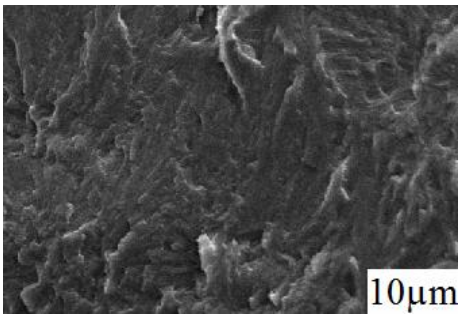

PP

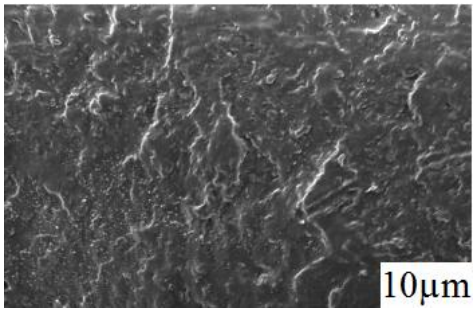

PLA

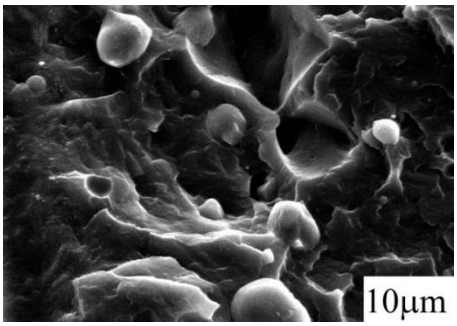

PP85PL15

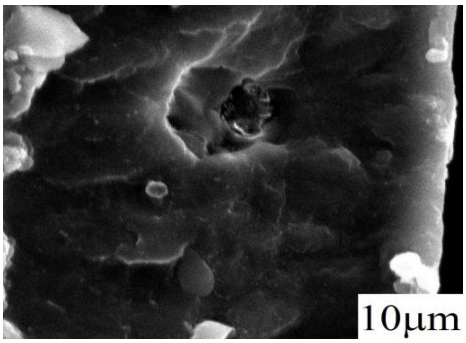

PP85PL15MA4

Figure 5.6 SEM image of PP, PLA, PP85PL15 and PP85PL15MA4

5.1.10 Rheological properties

The rheological study is important to understand structure–property relationship of materials, during the processing especially in the melt state. Dynamic shear strain sweep test was applied to characterize the viscoelastic region (VLE). The storage modulus (G') is used to know the elastic behavior of the materials. On the other hand, the loss modulus (G") is used to characterize the viscous behavior. Figure 5.7 shows the rheological behavior of PP, PLA and blended samples.

Figures 5.7(a) and (b) show the dependence of storage modulus (G') and loss modulus (G") on the shear strain for all the blended samples.

The complex viscosity (η*) was used to measure the resistance to flow. Figure 5.7 (c) shows the complex viscosity (η*) as a function of angular frequency (ω) curves for the PP/PLA blended films. The monotonically decrease in η* with increase in ω confirmed the pseudo-plastic behavior of all the blends. The decrease in viscosity, due to addition of PLA in PP/PLA (85/15) blend, confirmed reduced entanglement and weak interactions between the two different polymers. The increase in complex viscosity due to the addition of compatibilizer PP-g-MA (4 phr) in PP85PL15MA4 blend confirmed an improvement in the interaction and compatibility between the two different polymers. The increase in compatibility due to increase in chain mobility at the interface caused by a chemical reaction between the end group of PLA and MA group of PP-*g*-MA.

Figures 5.7(d) and 5.7(e) show the storage modulus and loss modulus as a function of angular frequency. The dependency of G' and G" on ω, decides the relative motion of all molecules in the bulk and provides important information on the flow behavior of the melts. Storage modulus of PLA at low frequency is extremely small but sharply increases with increase in frequency. The elasticity of the blends is higher than that of PLA due to the strong interactions and chain entanglement. Compatibilizer in the PP85PLA15MA4 blend enhances the storage modulus at all frequencies. The loss modulus trends are quite similar to that of storage modulus.

Figure 5.7(f) shows the dependency of loss angle (tan δ) on frequency. The loss angle, represented as the ratio of the loss to the storage modulus, exhibits the viscoelastic damping behavior of a polymer system. The tan δ of blends decreases with increase in frequency. A

positive slope of tan δ curve shows the elastic response of the viscoelastic samples. It can be seen from Figure 5.7(f) that the slope of the tan δ curve is negative for all the samples, showing that all the blends behave as viscoelastic.

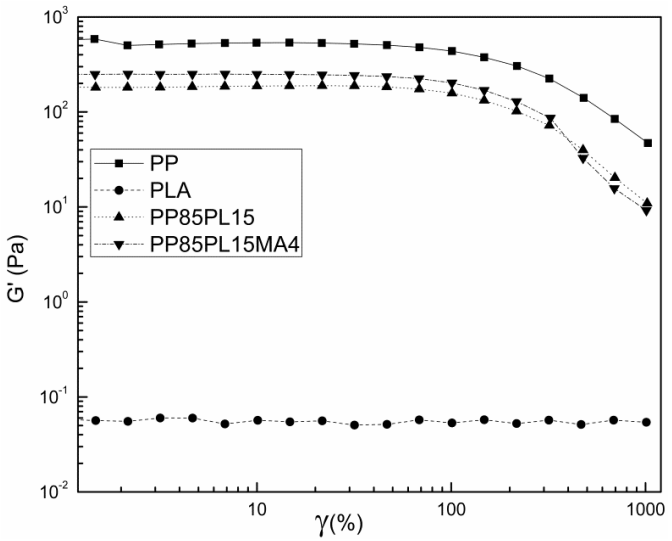

Figure 5.7(a) Storage modulus (G') as a function of shear strain (γ) of PP and blended PP films

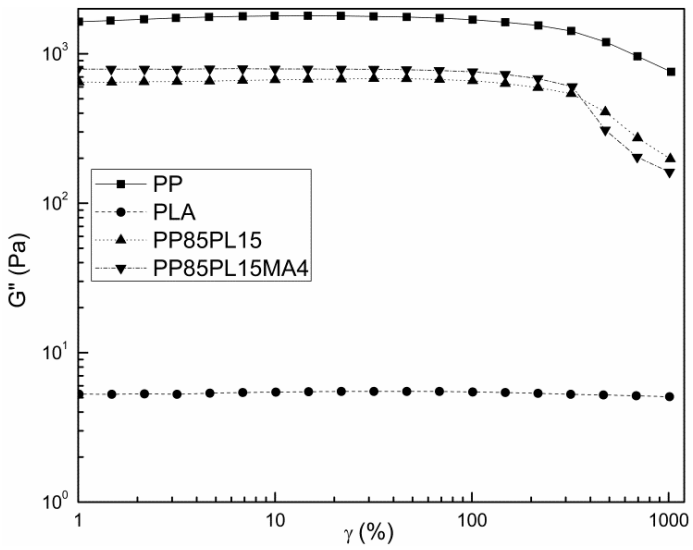

Figure 5.7(b) Loss modulus (G") as a function of shear strain (γ) of PP and blended PP films

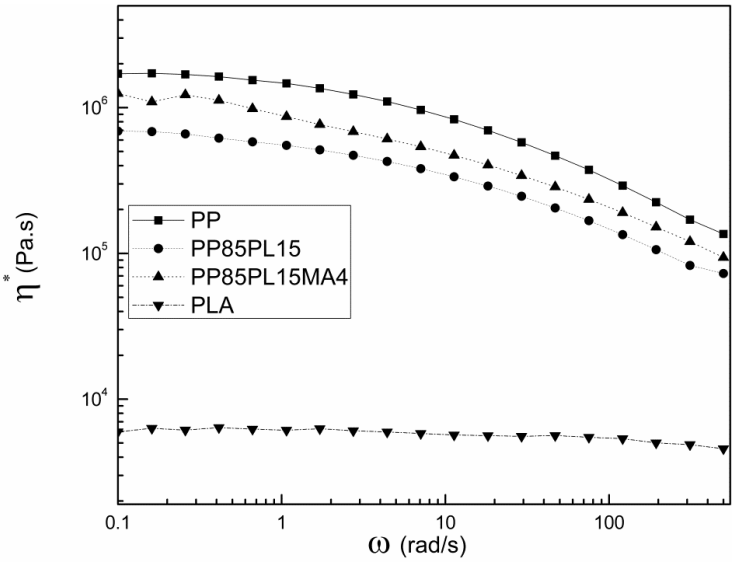

Figure 5.7(c) Complex viscosity (η*) as a function of angular frequency (ω) of PP and blended PP films

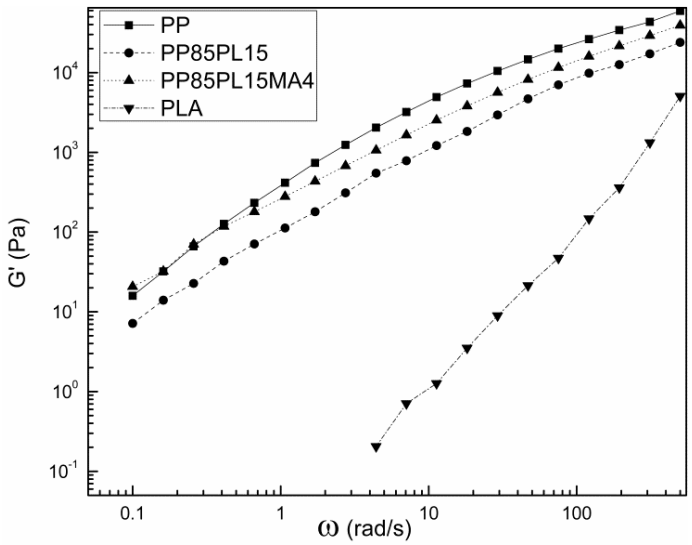

Figure 5.7(d) Storage Modulus (G') as a function of angular frequency (ω) of PP and blended PP films

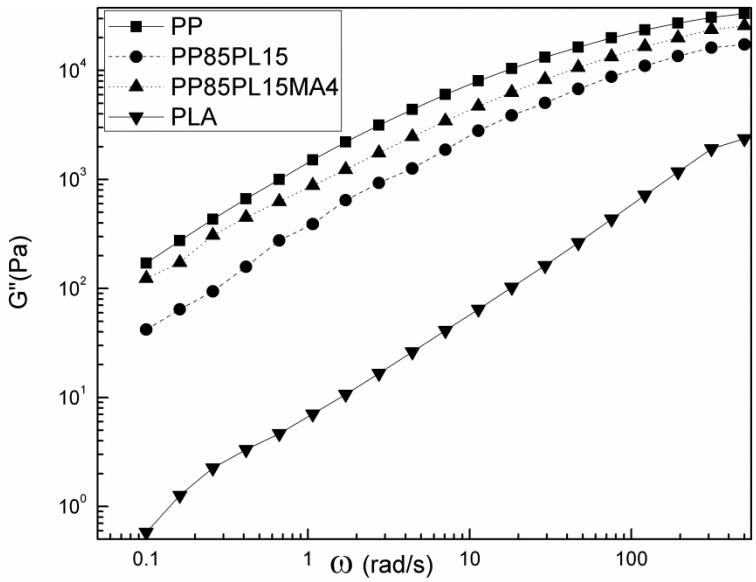

Figure 5.7(e) Loss Modulus (G") as a function of angular frequency (ω) of PP and blended PP films

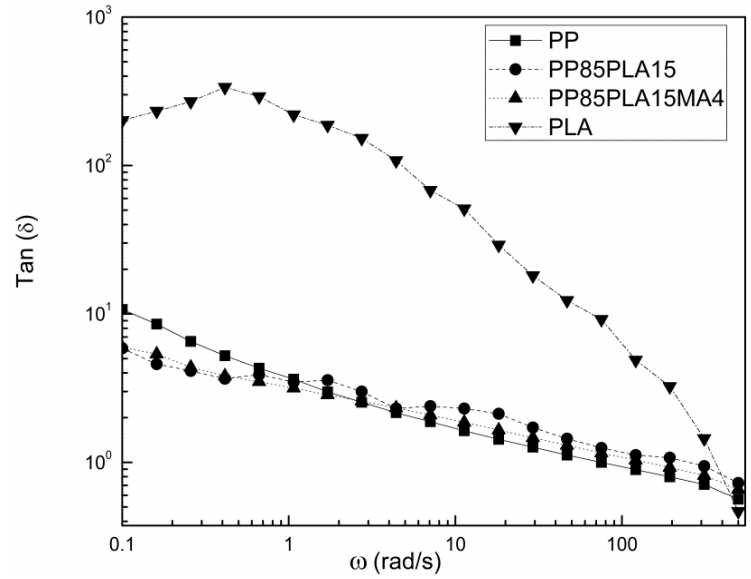

Figure 5.7(f) Tan (δ) as a function of angular frequency (ω) of PP and blended PP films

5.2 PP and PP/PLA blends with compatibilizer and pro-oxidant

5.2.1 Preparation

Pro-oxidant (0.2-2 wt%) filled PP and PP/PLA/MA (85/15/4) blend having 0.2 wt% calcium or cobalt stearate were prepared in an internal mixer (Haake Poly Lab, Germany). The melt mixing was performed at 180 °C for 4 min, at rotor speed of 60 rpm. The details of the prepared pro-oxidant filled PP are given in Table 5.5.

Table 5.5 Compositions of sample films

Sr. No.	Polymer samples	Composition				
		PP (wt%)	CoSt (wt%)	CaSt (wt%)	PLA (wt%)	PP-g-MA (phr)
1	PP	100	0	0	0	0
2	PP100CoSt0.2	100	0.2	0	0	0
3	PP100CoSt0.4	100	0.4	0	0	0
4	PP100CoSt0.6	100	0.6	0	0	0
5	PP100CoSt0.8	100	0.8	0	0	0
6	PP100CoSt1.0	100	1.0	0	0	0
7	PP100CoSt1.5	100	1.5	0	0	0
8	PP100CoSt2.0	100	2.0	0	0	0
9	PP100CaSt0.2	100	0	0.2	0	0
10	PP100CaSt0.4	100	0	0.4	0	0
11	PP100CaSt0.6	100	0	0.6	0	0
12	PP100CaSt0.8	100	0	0.8	0	0
13	PP100CaSt1.0	100	0	1.0	0	0
14	PP100CaSt1.5	100	0	1.5	0	0
15	PP100CaSt2.0	100	0	2.0	0	0
16	PP85PL15MA4CaSt0.2	85	0	0.2	15	4
17	PP85PL15MA4CoSt0.2	85	0.2	0	15	4

5.2.2 Film preparation

The films of 80-85 μm thickness were prepared from all the blend samples. Teflon sheets were used to restrict the sticking of melt with plates. The temperature and pressure maintained during the compression molding were 180 °C and 400 kN/m^2. Cooling was performed by water.

5.2.3 Tensile properties

Tensile strength and elongation of the PP, blends and pro-oxidant filled films are shown in Table 5.6. The pure PP had tensile strength of 39 MPa and elongation 3.6% and decreased on the addition of pro-oxidant due to melt blending at high temperature of 180°C. Pro-oxidant might have oxidized the PP to some extent resulting in low tensile strength. With increase in the proportion of pro-oxidant, tensile strength of PP100CaSt2.0 and PP100CoSt2.0 resulted in the lowest values. With addition of 0.2 phr calcium stearate/cobalt stearate, the tensile strength reduced to 35 MPa. However, on further increase in the proportion of calcium stearate/cobalt stearate (0.4 phr) the tensile strength drastically decreased to 24 and 25 MPa, respectively. The blend was optimized for pro-oxidant concentration (0.2 phr) to get the desired strength properties (above 30 MPa). The films of PP100CaSt0.2 and PP100CoSt0.2 have lower values of E_b and all other composition have also shown lower values of E_b in comparisons to PP. The tensile strength of most of the compositions is lower than that of PP but PP100CaSt0.2 and PP100CoSt0.2 showed strength quite close to PP. Therefore, PP100CaSt0.2, PP100CoSt0.2, PP85PL15MA4CaSt0.2 and PP85PL15MA4CoSt0.2 were chosen for further studies.

Table 5.6 Tensile properties of sample films

S.No.	Polymer samples	Tensile strength (MPa)	Elongation at break, E_b (%)
1	PP	39±2	3.6±0.2
2	PP100CoSt0.2	35±2	3.4±0.1
3	PP100CoSt0.4	25±1	2.7±0.1
4	PP100CoSt0.6	19±1	2.5±0.1
5	PP100CoSt0.8	18±1	2.1±0.1
6	PP100CoSt1.0	17±1	1.5±0.1
7	PP100CoSt1.5	17±1	1.2±0.1
8	PP100CoSt2.0	17±1	1.1±0.1
9	PP100CaSt0.2	35±2	3.3±0.1
10	PP100CaSt0.4	24±1	2.7±0.2
11	PP100CaSt0.6	23±1	2.6±0.1
12	PP100CaSt0.8	22±1	2.4±0.1
13	PP100CaSt1.0	17±1	2.1±0.1
14	PP100CaSt1.5	16±1	1.9±0.1
15	PP100CaSt2.0	15±1	1.8±0.1
16	PP85PL15MA4CaSt0.2	29±1	1.6±0.1
17	PP85PL15MA4CoSt0.2	28±1	2.2±0.1

5.2.4 Moisture content

The moisture content of PP85PL15MA4CaSt0.2 and PP100CaSt0.2 is 3.02% and 0.73% in comparison to PP (0%). The moisture content increased due to the increase in incompatibility (void formation and phase separation) between the blend due to pro-oxidant addition.

5.2.5 Fourier transform infrared (FTIR) spectroscopy

The FTIR spectra of all the samples are shown in Figure 5.8, in which peaks between 2949-2866, 1454 and 1375 cm^{-1} were assigned to C-H stretching, CH_3 bending, and C-H bending,

respectively for PP [164]. In the spectrum of PLA, the peaks at 1746, 1178, and 1084 cm^{-1} are associated with C=O stretching, symmetric C-O-C stretching, and asymmetric CH_3, respectively [25]. Peak at 1560 cm^{-1} confirms the presence of metal stearate, which can be attributed to asymmetric vibration stretching of the carbonyl group coordinated to the metal ion [106]. This confirms the presence of pro-oxidant filled samples.

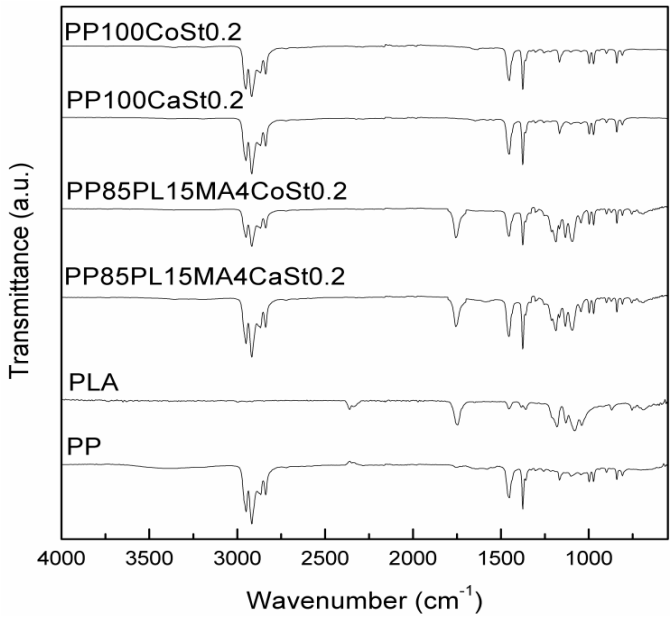

Figure 5.8 FTIR of pro-oxidant filled PP/PLA blend samples

5.2.6 X-ray diffraction (XRD)

Figure 5.9 shows the XRD patterns of blended films. The peaks of the PP corresponding to the α-monoclinic form are at 2θ = 14.1°, 16.9°, 18.6°, 21.1° and 21.9° [25]. Addition of pro-oxidant in PP decreased the intensity of these peaks, indicating reduced crystallinity. For the pro-oxidant filled PP/PLA blends, XRD patterns were almost identical to that of the neat PP film. It is confirmed that the peaks in the blend films are dominated by the PP. The addition of calcium and cobalt stearate did not result in any changes in the diffraction angles of blended PP [167],

though there is a decrease in the peak intensity, which clearly indicates that the addition of calcium and cobalt stearate affects the crystallinity of the PP films.

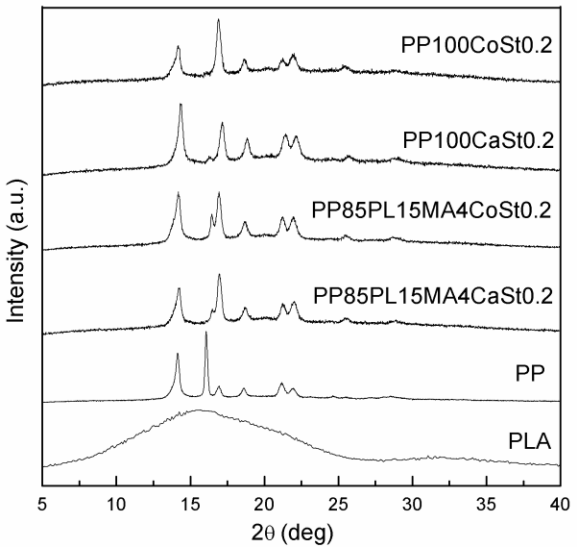

Figure 5.9 XRD patterns of pro-oxidant filled PP/PLA blend samples

5.2.7 Differential scanning calorimetry (DSC)

The DSC curves of all the blended films are shown in Figure 5.10 and 5.11. The melting temperature (T_m), crystallization temperature (T_c) and melting enthalpy (ΔH_m) values (obtained from DSC curves) are listed in Table 5.7. The crystallinity of the samples is calculated by using equation 3.2. The crystallinity and T_m of PP are 63% and 166 °C, respectively. The crystallinity of pro-oxidant filled PP and PP/PLA blends are lower than that of pure PP due to insertion of the side and/or functional groups [168]. Pro-oxidant reduces the crystallinity, and therefore, makes pro-oxidant filled PP more susceptible to microbial attacks [72].

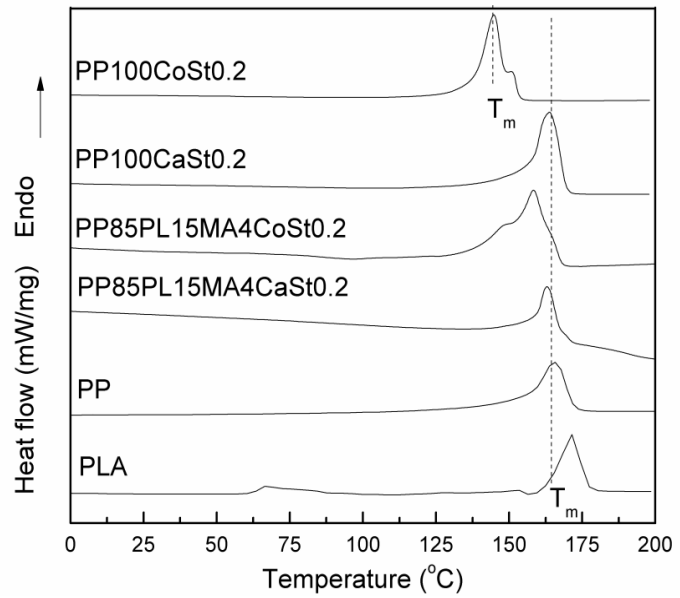

Figure 5.10 DSC melting thermographs of pro-oxidant filled blend samples

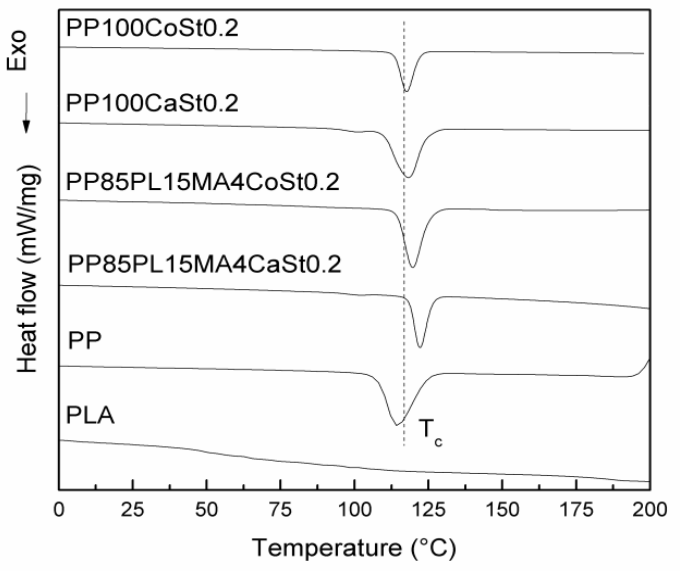

Figure 5.11 DSC crystallization thermographs of pro-oxidant filled blend samples

Table 5.7 DSC melting and crystallization parameters of pro-oxidant filled blended films

Blended/Composite samples	T_g (°C)	T_m (°C)	T_c (°C)	ΔH_m (Jg^{-1})	X_c (%)
PP	--	166	117	104	63
PLA	66	171	--	34	Negligible (Amorphous)
PP85PL15MA4CaSt0.2	--	162	123	90	55
PP85PL15MA4CoSt0.2	--	158	119	77	47
PP100CaSt0.2	--	164	122	78	48
PP100CoSt0.2	--	145	114	78	48

5.2.8 Thermogravimetric analysis (TGA)

Figure 5.12 shows the thermogravimetric and differential themogravimetric analysis curves of the pro-oxidant filled PP samples. Curves of neat PP and PLA show single stage degradation. Whereas the blend of pro-oxidant filled PP/PLA shows two-stage degradation due to the immiscibility between the polymers [166]. The initiation (T_i) and final temperature (T_f) are shown in Table 5.8. The initial degradation temperature (T_i) corresponds to 5% weight loss of the polymer sample, and the final degradation temperature (T_f) corresponds to 5% residual left after which no appreciable loss is possible. The initiation and final temperature of thermal degradation of the polymers are essential for evaluating their thermal sensitivity [90]. PP is more thermally stable than PLA, the T_i of PP is 380 °C, higher than that of PLA (335 °C). Degradation of PP films increased on addition of pro-oxidant because of initiation of degradation due to presence of metal ions in the pro-oxidant filled PP films [169]. T_f of the pro-oxidant filled films was also lower than that of the PP film. Thermal stability of PP, PP100CaSt0.2 and PP100CoSt0.2 was 380, 376 and 356°C as shown in Figure 5.12.

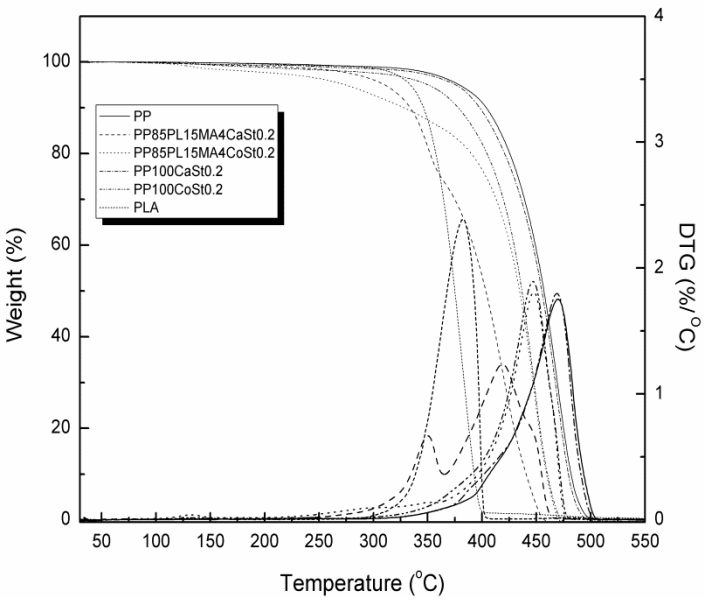

Figure 5.12 TGA profiles of pro-oxidant filled blend samples

Table 5.8 TG and DTG analysis of pro-oxidant filled blended samples

Samples	T_i (°C)	T_f (°C)
PP	380	487
PLA	335	396
PP85PL15MA4CaSt0.2	310	460
PP85PL15MA4CoSt0.2	278	436
PP100CaSt0.2	376	451
PP100CoSt0.2	356	446

5.2.9 Scanning electron microscopy (SEM)

The morphology of PP, PLA, PP100CaSt0.2, PP100CoSt0.2, PP85PL15MA4CaSt0.2, and PP85PL15MA4CoSt0.2 obtained by SEM are shown in Figure 5.13. These SEM images were taken of the cryofractured surfaces of PP, PLA and blended samples. The surfaces of PP and PLA looks smoother than other samples. Addition of pro-oxidant in blends of has reduced the

interfacial interaction, and several holes and pits were also observed. Addition of calcium stearate or cobalt stearate did not significantly change the morphology of the PP.

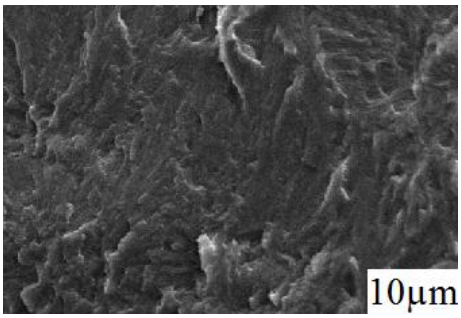

PP

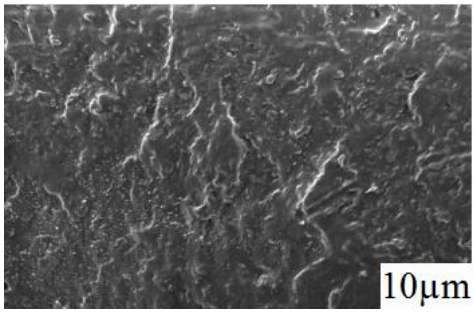

PLA

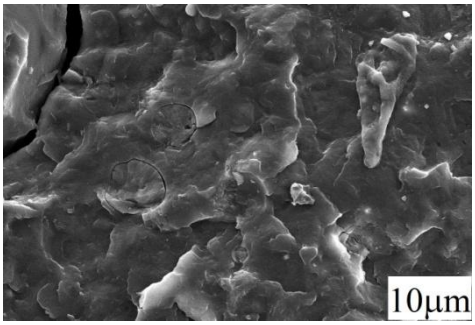

PP85PL15MA4CaSt0.2

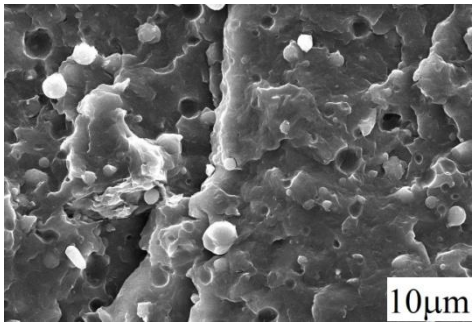

PP85PL15MA4CoSt0.2

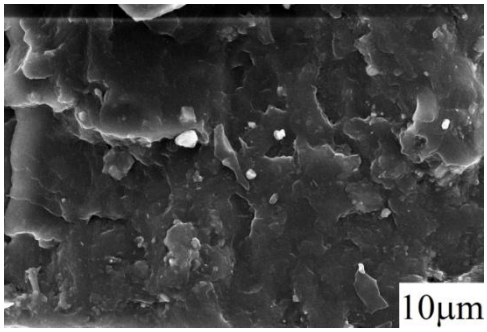

PP100CaSt0.2

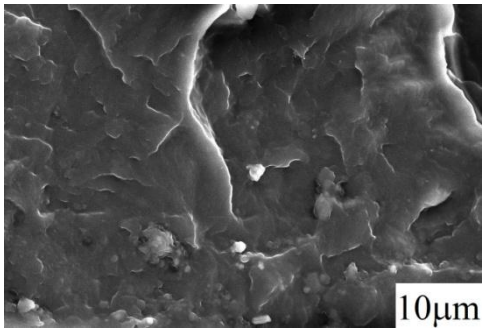

PP100CoSt0.2

Figure 5.13 SEM image of PP, PLA, PP85PL15MA4CaSt0.2, PP85PL15MA4CoSt0.2, PP100CaSt0.2 and PP100CoSt0.2

5.2.10 Rheological properties

The result of rheological studies with pro-oxidant filled PP, PLA blended samples are shown in Figure 5.14. The dependency of storage modulus (G') and loss modulus (G") on the shear strain for all modified PP samples are shown in Figures. 5.14(a) and (b). All blended samples have shown a linear behavior (Newtonian plateau) at lower shear strain and a non linear behavior at higher shear strain.

The complex viscosity (η*) as a function of angular frequency (ω) curves for the modified PP blends are given in Figure 5.14 (c). The η* decreases monotonically with increase in angular frequency (shear thinning) for all the samples. The decrease in η* with increase in ω indicates the pseudo-plastic behavior of all the blended samples. With increase in shear rate, the viscosity has decreased for all the blends as expected. Addition of pro-oxidant in PP blends (PP100CoSt0.2, PP100CaSt0.2, PP85PL15MA4CoSt0.2 and PP85PL15MA4CaSt0.2) also decreases the complex viscosity but less significantly due to better mixing.

The elastic and viscous characteristics of the polymer blends are presented in Figures 5.14(d) and 5.14(e) depicting the storage modulus and loss modulus as a function of angular frequency. The dependency of G' and G" on ω, indicates the relative motion of all molecules in the bulk and can provide important information about the flow behavior of the melts. Storage modulus of PLA at low frequency is extremely smaller than that of PP, but it sharply increases with the increase in frequency. Storage modulus of all blends increases monotonically with increase in frequency. The elasticity of the blends is higher than that of PLA due to strong interaction and chain entanglement. The loss modulus trends are quite similar to that of storage modulus.

Dependence of loss angle (tan δ) on frequency of two different polymers' blends with pro-oxidant is shown in Figure 5.14(f). The loss angle, expressed as the ratio of the loss to the storage modulus, exhibits the viscoelastic damping behavior. As seen in the figure, the tan δ decreases with increase in frequency. A positive slope of tan δ curve shows the elastic response of the viscoelastic samples. It is seen from Figure 5.14(f) that the slope of the tan δ curve is negative for all the samples, showing that the blends behave as viscoelastic.

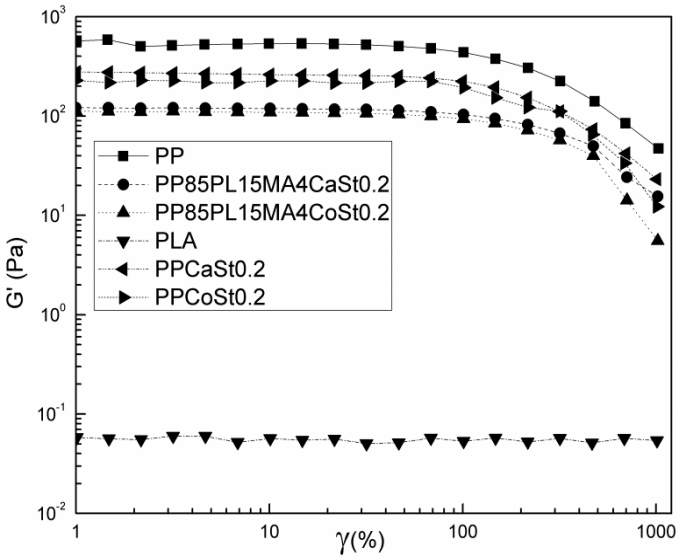

Figure 5.14(a) Storage modulus (G') as a function of shear strain (γ) of pro-oxidant filled blended films

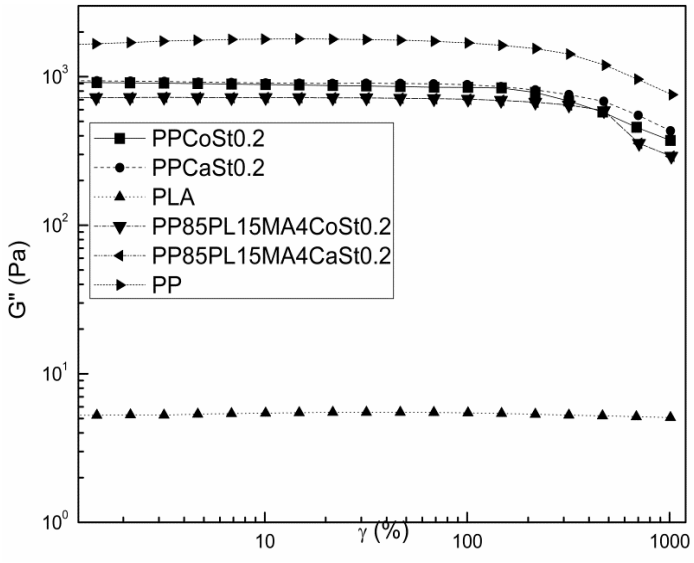

Figure 5.14(b) Loss modulus (G") as a function of shear strain (γ) of pro-oxidant filled blended films

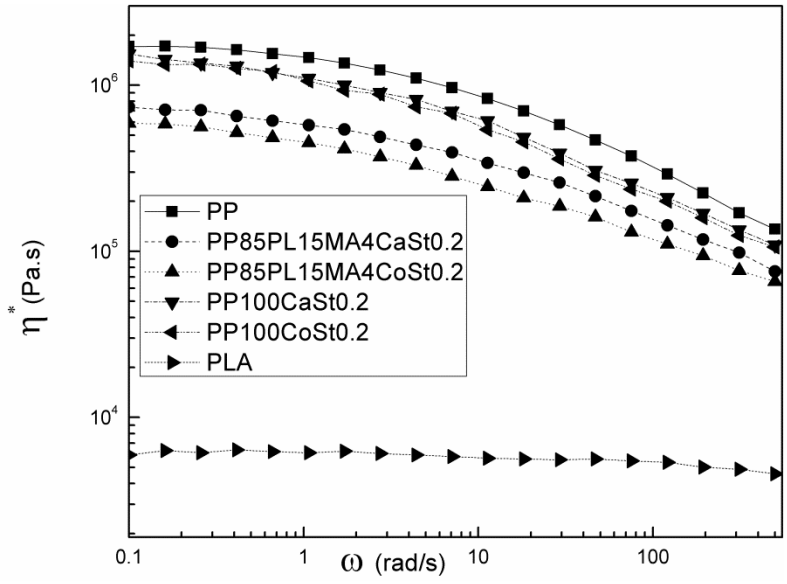

Figure 5.14(c) Complex viscosity (η*) as a function of angular frequency (ω) of pro-oxidant filled blended films

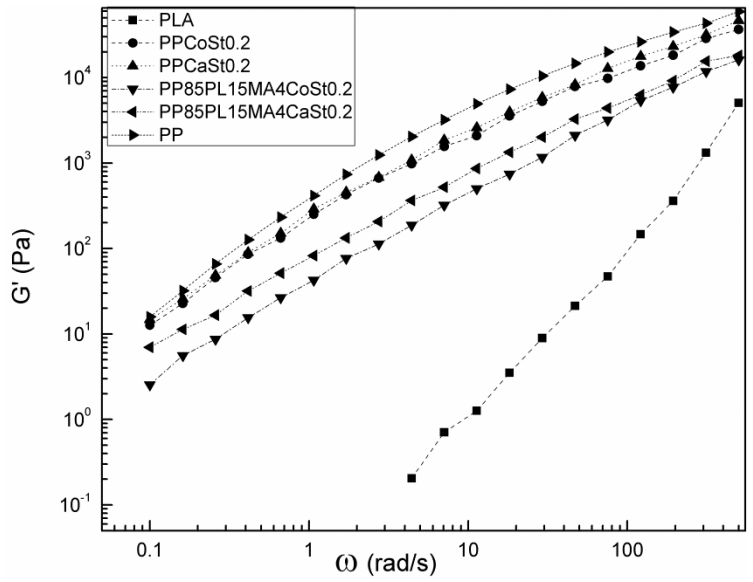

Figure 5.14(d) Storage Modulus (G') as a function of angular frequency (ω) of pro-oxidant filled blended films

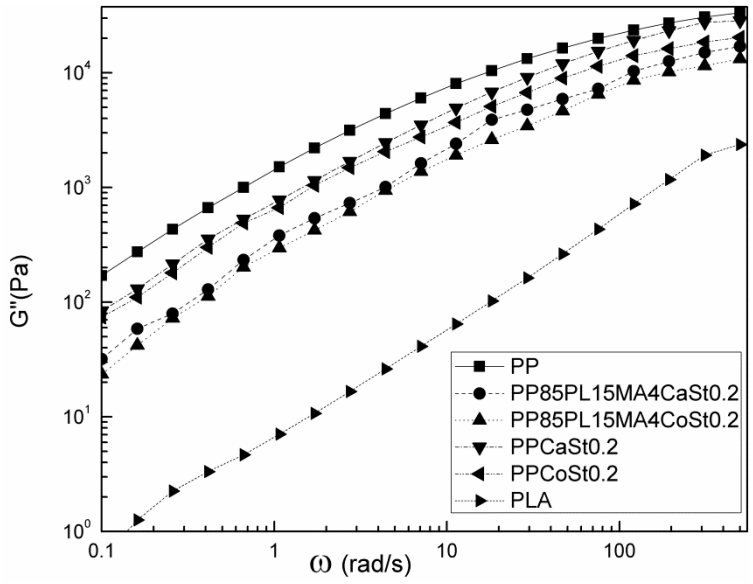

Figure 5.14 (e) Loss Modulus (G") as a function of angular frequency (ω) of pro-oxidant filled blended films

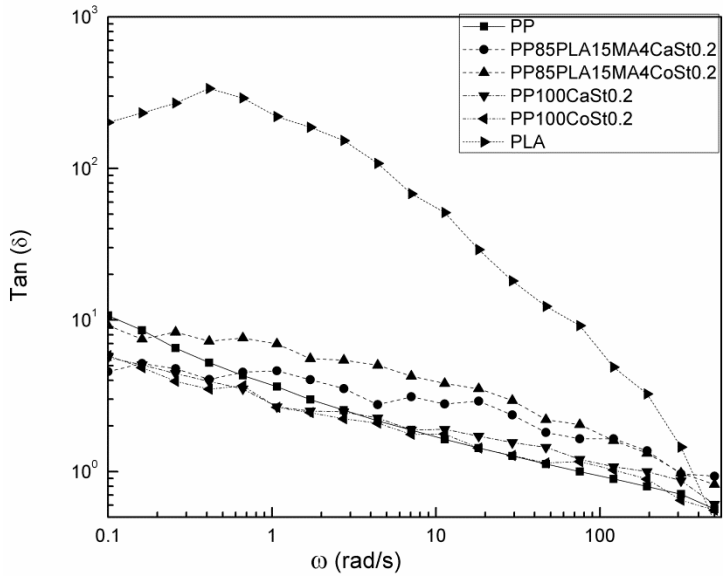

Figure 5.14(f) Tan (δ) as a function of angular frequency (ω) of pro-oxidant filled blended films

5.3 PP and PP/PLA blend with compatibilizer and nanoclay

5.3.1 Preparation

The different compositions of PP with nanoclay and compatibilized PP/PLA blends with nanoclay are shown in Table 5.9. Mixer supplied by Haake Poly Lab, Germany was used for melt blending. Materials were weighed and manually mixed and loaded in the mixer. The concentration of nanoclay with PP varied from 0 to 5 wt%. The mixing chamber temperature was 180 °C and rotor speed of 60 rpm were maintained during the mixing for 4 min.

Table 5.9 PP /PLA blends with different compositions and nanoclay filled PP composites

S.No	Samples	Composition			
		PP (wt%)	PLA (wt%)	PP-*g*-MA (phr)	Nanoclay (wt%)
1	PP	100	0	0	0
2	PP100NC1	100	0	0	1
3	PP100NC2	100	0	0	2
4	PP100NC3	100	0	0	3
5	PP100NC4	100	0	0	4
6	PP100NC5	100	0	0	5
7	PP85PL15MA4NC2	85	15	4	2

5.3.2 Preparation of film

The films of 80-85 μm thickness from prepared blends were prepared by compression molding at 180 °C and 400 kN/m^2 pressure. Teflon sheets kept in between the mold restricted the sticking of molten material with the plates and were cooled by water.

5.3.3 Tensile properties

The effect of addition of nanoclay on the strength of PP/nanoclay composite is shown in Table 5.10. Tensile strength of PP is 39 MPa which increased upto 42 MPa with addition of nanoclay (2 wt%) beyond which there was not much change. The increase in tensile strength is due to strong interaction between the PP matrix and nanoclay [170]. PP100NC2 was taken as optimum composition and tensile strength of PP85PL15MA4NC2 was 32 MPa. On the basis of tensile strength, we considered PP85PL15MA4NC2 and PP100NC2 as our optimum composites for further studies.

Table 5.10 Tensile strength of blended and composite films

S.No.	Samples	Tensile strength (MPa)	Elongation (%)
1	PP	39±2	3.6±0.2
2	PP100NC1	40±1	3.8±0.1
3	PP100NC2	42±2	4.0±0.1
4	PP100NC3	41±2	3.8±0.1
5	PP100NC4	41±2	3.6±0.1
6	PP100NC5	41±2	3.5±0.1
7	PP85PL15MA4NC2	32±1	1.9±0.1

5.3.4 Moisture content

The moisture content of PP85PL15NC2 and PP100NC2 is 1% and 1.27% in comparison to PP (0%). The moisture content increased due to hydrophilic nature of nanoclay.

5.3.5 Fourier transform infrared (FTIR) spectroscopy

The FTIR spectra of the samples are shown in Figure 5.15, in which peaks between 2949-2866, 1454 and 1375 cm^{-1} were assigned to C-H stretching, CH_3 bending, and C-H bending, respectively for PP [164]. In the spectrum of PLA, the peaks at 1746, 1178, and 1084 cm^{-1} are associated with C=O stretching, symmetric C-O-C stretching, and asymmetric CH_3, respectively [25]. The peaks in composite PP100NC2 and PP85PL15MA4NC2 at between 900-1100 cm^{-1} confirmed the presence of nanoclay in the composite samples [171].

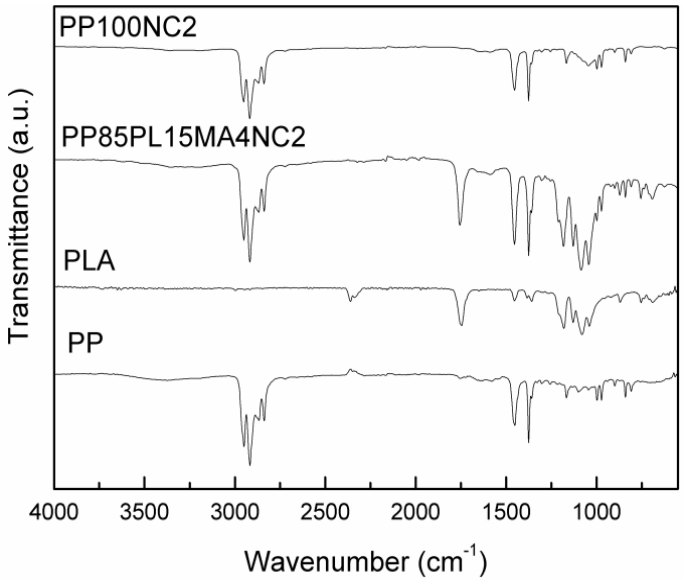

Figure 5.15 FTIR spectra of nanoclay filled composite samples

5.3.6 X-ray diffraction (XRD)

Figure 5.16 shows the XRD patterns of composite films. The peaks of the PP corresponding to the α-monoclinic form are at 2θ = 14.1°, 16.9°, 18.6°, 21.1° and 21.9° [25]. There were no significant shifts in the diffraction peaks in the composites. This shows that the nature of the crystalline lattices did not undergo a large change. For some nanocomposites, a small peak is observed around 2θ = 20°. Some authors interpreted this peak as a (130) γ-reflection as a result of the confined PP crystallization in the presence of well dispersed clay [172]. In our case, this peak in composite PP100NC2 and PP85PL15MA4NC2, is associated to the presence of clay in the samples.

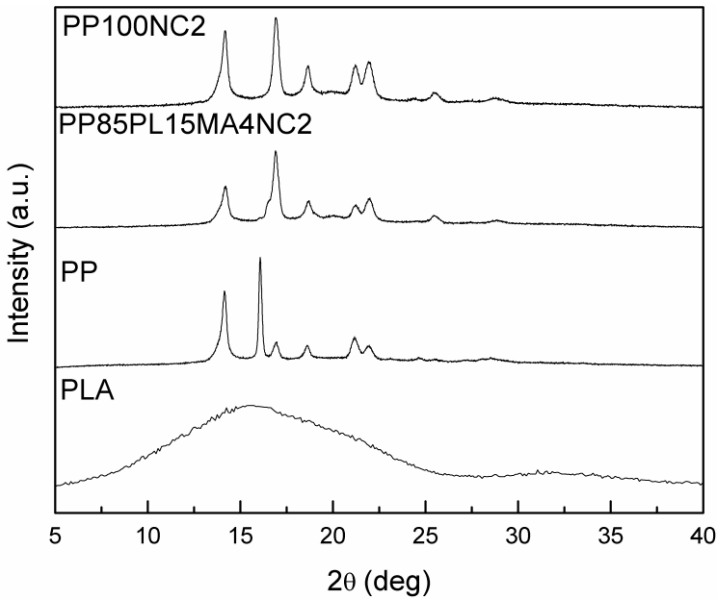

Figure 5.16 XRD patterns of PP, PLA and nanoclay filled composite samples

5.3.7 Differential scanning calorimetry (DSC)

The DSC curves of the composite films are shown in Figure 5.17 and 5.18. The melting temperature (T_m), crystallization temperature (T_c) and melting enthalpy (ΔH_m) of the samples, (obtained from DSC curves) are listed in Table 5.11. The crystallinity of the samples is calculated (from heat of melting) by using equation 3.2. The crystallinity and T_m of PP are 63% and 166 °C, respectively. The decrease in crystallinity of PP and compatibilized PP/PLA blend on the addition of nanoclay is due to the nanoclay platelets which could hinder the motion of the polymer chain segments and retards the crystal growth. Increase in amorphous nature is helpful for biodegradation of blended and composite films.

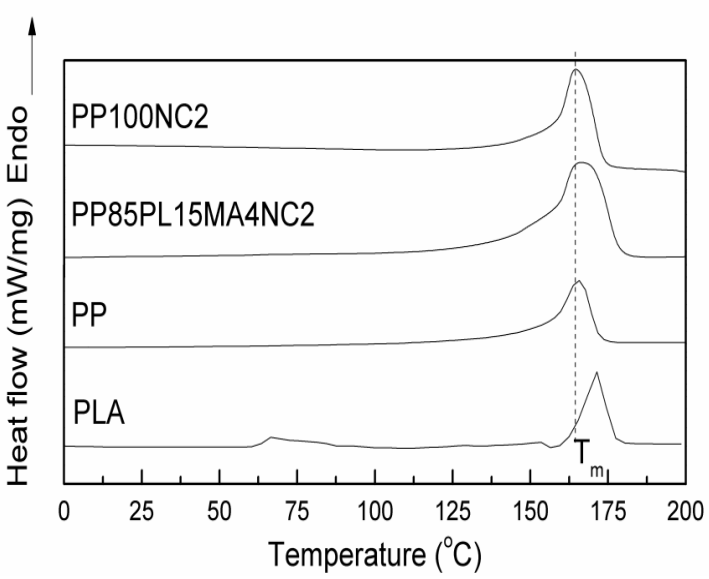

Figure 5.17 DSC melting thermographs of composite films

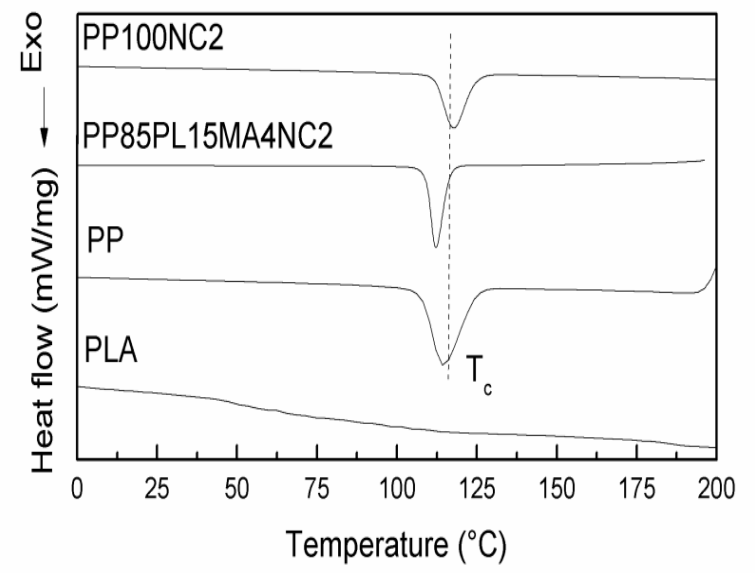

Figure 5.18 DSC crystallization thermographs of composite films

Table 5.11 DSC melting and crystallization parameters of blended and composite films

Samples	T_g (°C)	T_m (°C)	T_c (°C)	ΔH_m (Jg^{-1})	X_c (%)
PP	--	166	117	104	63
PLA	66	171	--	34	Negligible (Amorphous)
PP85PL15MA4NC2	--	155	120	78	48
PP100NC2	--	157	120	82	50

5.3.8 Thermogravimetric analysis (TGA)

Figure 5.19 shows the TG and DTG curves of the samples. Curves of neat PP and PLA show single stage degradation. The initiation (T_i) and final temperature (T_f) are shown in Table 5.12. The initial degradation temperature (T_i) corresponds to 5% weight loss of the polymer sample, and the final degradation temperature (T_f) corresponds to 5% residual left after which no appreciable loss is possible. The initiation and final temperature of thermal degradation of the polymers are essential for evaluating their thermal sensitivity [90]. PP is more thermally stable than PLA, the T_i of PP is 380 °C, higher than that of PLA (335 °C). In the thermal degradation of PP and PP/clay nanocomposite, the initiation temperature of PP and PP100NC2 was 380 °C and 378 °C, respectively. This shows that addition of nanoclay decreases the initiation degradation temperature due to the catalytic effect of nanoclay towards the degradation of polymer matrix under nitrogen atmosphere [112]. Whereas the nanocomposite PP85PL15MA4NC2 shows the lowest initiation degradation temperature (300 °C) due to the lowest thermal stability. The decrease in thermal stability of the composite samples is helpful for their biodegradation.

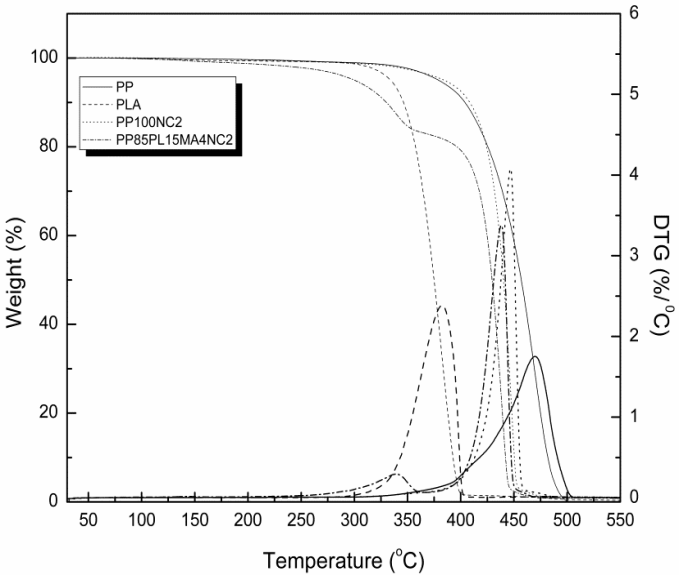

Figure 5.19 TGA profiles of the composite films

Table 5.12 TG and DTG analysis of nanoclay filled composite samples

Samples	T_i (°C)	T_f (°C)
PP	380	487
PLA	335	396
PP85PL15MA4NC2	300	443
PP100NC2	384	452

5.3.9 Scanning electron microscopy (SEM)

The morphology of PP, PLA, PP100NC2 and PP85PL15MA4NC2 composites have been studied by SEM and shown in Figure 5.20. These SEM images were taken on the cryofractured surfaces of nanocomposite samples. The surfaces of PP and PLA look smoother than that of other samples. In the case of PP85PL15MA4NC2 and PP100NC2 nanocomposite, nanoclay was

dispersed into the compatibilized PP/PLA and PP matrix in the form of large and small aggregates.

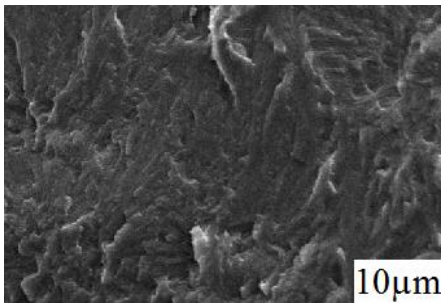

PP

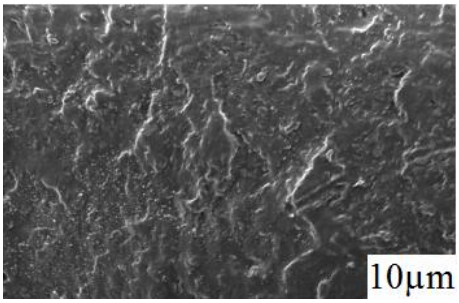

PLA

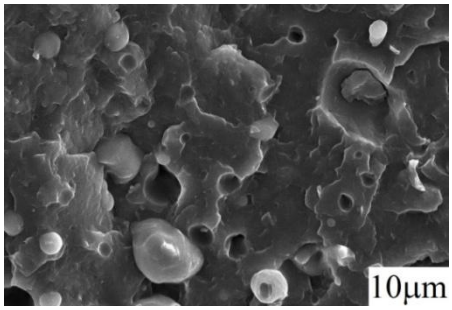

PP85PL15MA4NC2

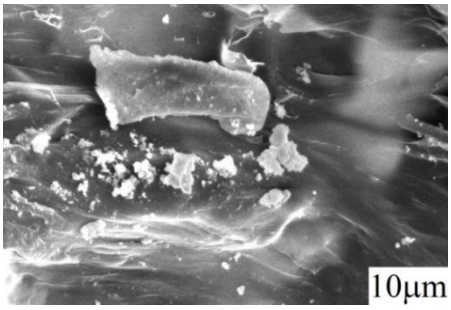

PP100NC2

Figure 5.20 SEM of PP, PLA, PP85PL15MA4NC2 and PP100NC2

5.3.10 Rheological properties

The result of rheological study of PP, PLA and nanocomposite samples are shown in Figure 5.21. The dependency of storage modulus (G') and loss modulus (G") on the shear strain all of the modified PP samples is shown in Figures 5.21(a) and (b). All nanocomposite samples have shown a linear behavior (Newtonian plateau) at lower shear strain and a non linear behavior at higher shear strain. The storage modulus and loss modulus of the nanoclay composite samples are lower than those of PP and PP100NC2.

The viscosity is a measure of the resistance to how, specially the complex viscosity (η*). The complex viscosity (η*) as a function of angular frequency (ω) curves for the modified PP blends and composites are given in Figure 5.21(c). The complex viscosity decreases monotonically with increase in angular frequency (shear thinning) for all the samples. The decrease in η* with increase in ω indicates the pseudo-plastic behavior. Addition of nanoclay in PP (PP100NC2 and PP85PL15MA4NC2) also increases the complex viscosity, due to better interaction between nanoclay particles and PP, which reduces the flow during the molten state.

The elastic and viscous behavior of the nanocomposites are well rejected in Figures 5.21(d) and 5.21(e) depicting the storage modulus and loss modulus as a function of angular frequency. The dependency of G' and G" on the ω, indicates the relative motion of all molecules in the bulk and can provide important information about the flow behavior of the melts. Storage modulus of PLA at low frequencies is smaller than that of PP, but it sharply increases with the increase in frequency. The elasticity of the composites is higher than that of PLA due to the strong interaction and chain entanglement. The loss modulus results are quite similar to the storage modulus.

The dependency of the loss angle (tan δ) on frequency of nanoclay filled PP/PLA blend is shown in Figure 5.21(f). The loss angle, expressed as the ratio of the loss to the storage modulus, exhibits the viscoelastic damping behavior. As seen for the blends, tan δ decreases with increase in frequency. A positive slope of tan δ curve shows the elastic response of the viscoelastic samples. It can be observed from Figure 5.21(f) that the slope of the tan δ curve is negative for all the samples, which indicates that the blend/composite behave as viscoelastic material.

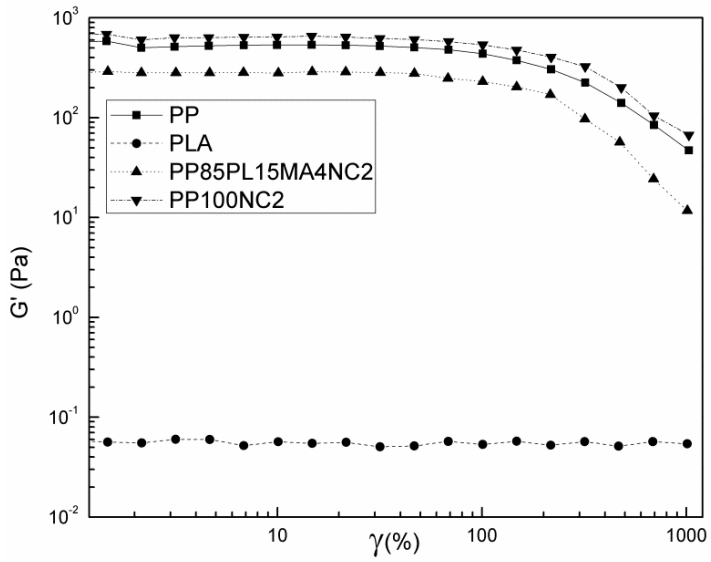

Figure 5.21(a) Storage modulus (G') as a function of shear strain (γ) of composite films

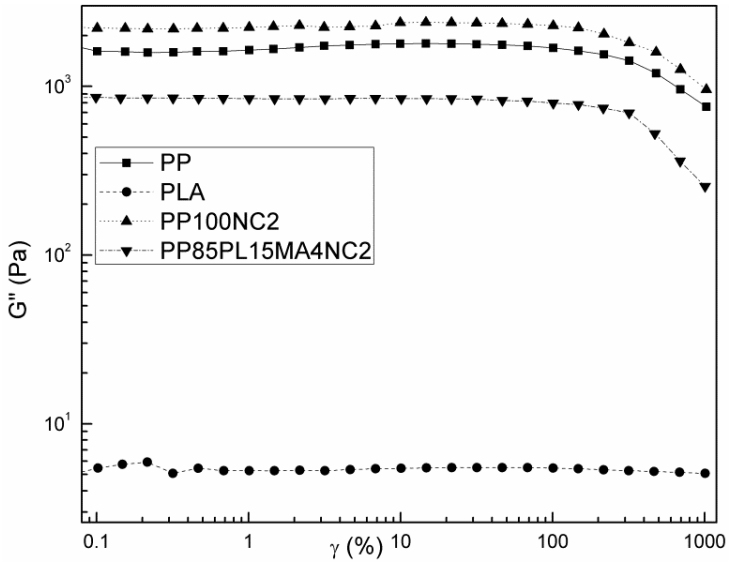

Figure 5.21(b) Loss modulus (G'') as a function of shear strain (γ) of composite films

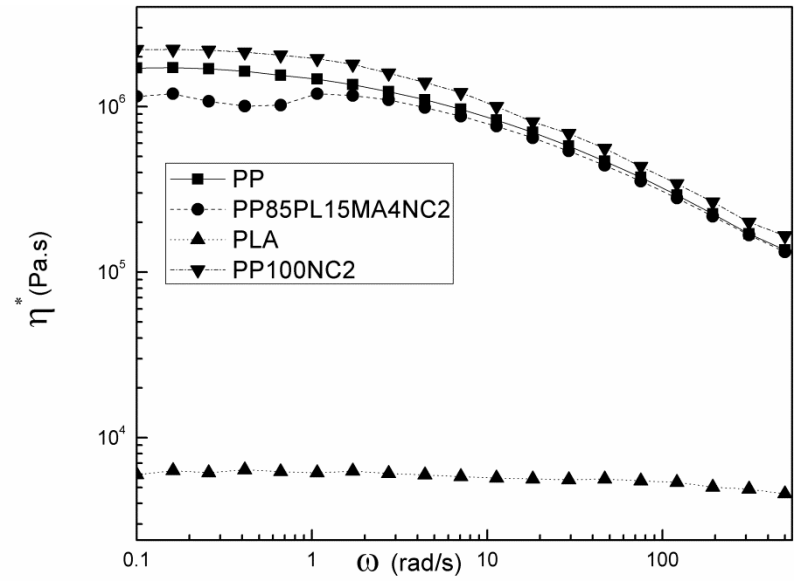

Figure 5.21(c) Complex viscosity (η*) as a function of angular frequency (ω) of composite films

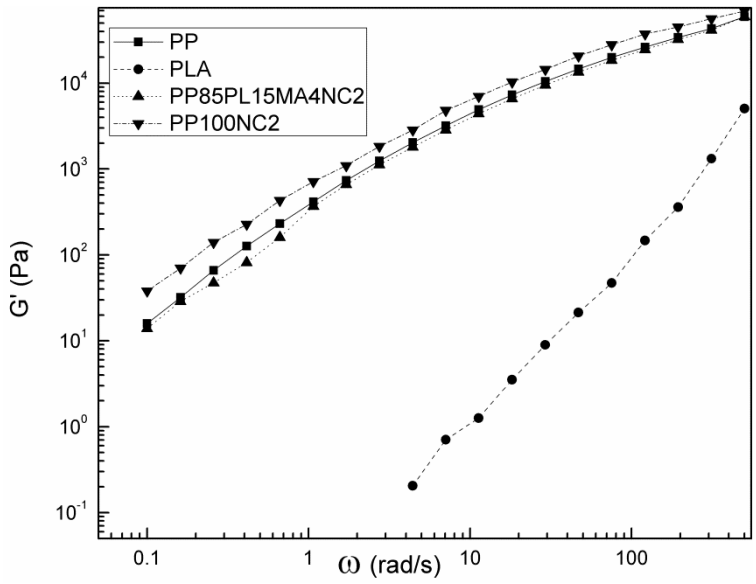

Figure 5.21(d) Storage Modulus (G') as a function of angular frequency (ω) of composite films

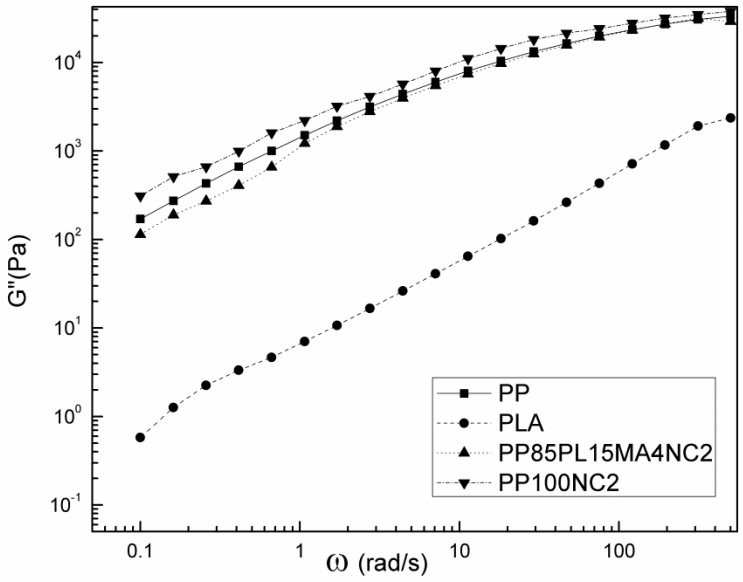

Figure 5.21(e) Loss Modulus (G") as a function of angular frequency (ω) of composite films

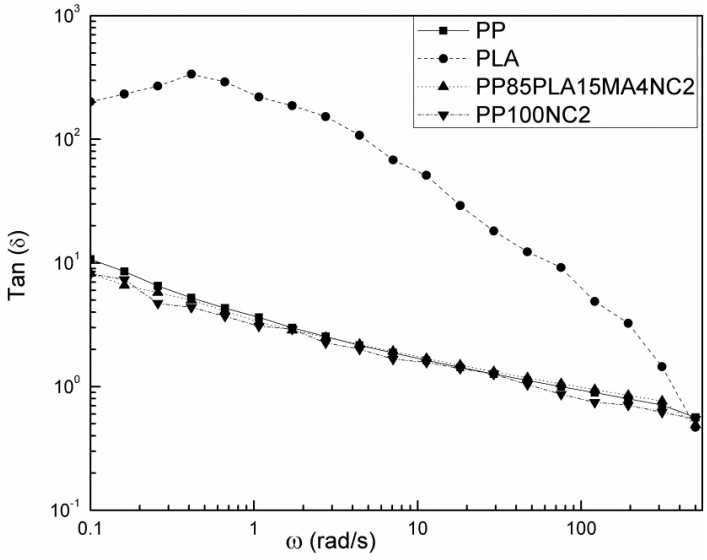

Figure 5.21(f) Tan (δ) as a function of angular frequency (ω) of composite films

5.4 Thermal degradation kinetics of PP/PLA blends and nanocomposites

5.4.1 Thermal stability

Different thermal stabilities are required for different applications. Figure 5.22 shows the TG and DTG thermograms of all the blend and nanocomposite samples. The TG thermograms of PP, PLA, PP100CaSt0.2, PP100CoSt0.2 and PP100NC2 samples show single stage decomposition. In the nitrogen atmosphere, thermal decomposition of PP via random scission is a primary pathway followed by a radical transfer process [173]. The decomposition temperature shifted towards the higher temperature with increase in heating rate. This could be due to the principal of time-temperature superimposition. The TG thermograms of all the blend samples (i.e. PP85PL15, PP85PL15MA4, PP85PL15MA4CaSt0.2, PP85PL15MA4CoSt0.2 and PP85PL15MA4NC2) show two step thermal decomposition, which confirmed the presence of two components PP and PLA in blends. The initial degradation temperature (T_i) corresponds to 5% weight loss of the samples, and the final degradation temperature (T_f) corresponds to 5% residual left after which no appreciable loss is possible and T_{max} is the temperature for the maximum weight loss calculated at different heating rates; the results are summarized in Table 5.13. The degradation temperatures of PP, PP/PLA, pro-oxidant filled blends and its nanocomposite samples at different conversion levels are shown in Table 5.14. At the heating rate of 5 °C/min, initial degradation temperature of PP was 337 °C, However, addition of PLA decreased the initial degradation temperature to 291 °C due to the incompatibility between the two polymers. However, addition of compatibilizer in PP85PL15 blend increased the initial degradation temperature upto 304 °C mainly due to increase in interaction between two polymers, resulting in increased thermal stability of the blend [90]. In the case of pro-oxidant filled PP, T_i of PP100CaSt0.2 and PP100CoSt0.2 was 335 °C and 323 °C, respectively. Addition of pro-oxidant in compatibilized

PP/PLA blend also decreased T_i of PP85PL15MA4CaSt0.2 and PP85PL15MA4CoSt0.2 to 292 °C and 261°C, respectively.

PP100NC2 composite has initial degradation temperature of 291°C, which is lower than PP. The decrease in initial degradation temperature may be due to the catalytic effect of nanoclay towards the degradation of polymer matrix under nitrogen atmosphere [174]. Addition of nanoclay in compatibilized blend decreases the thermal stability of nanocomposite sample.

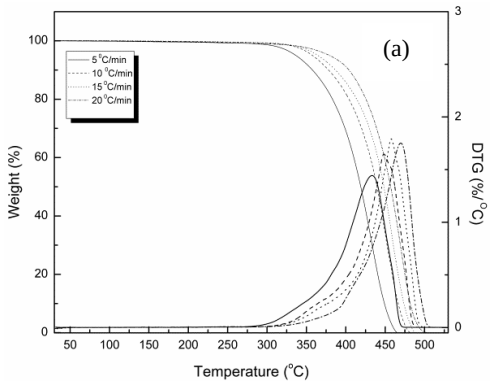

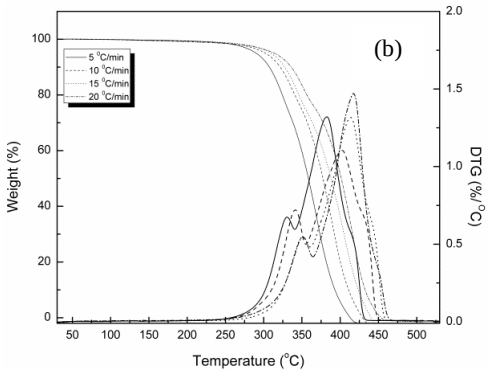

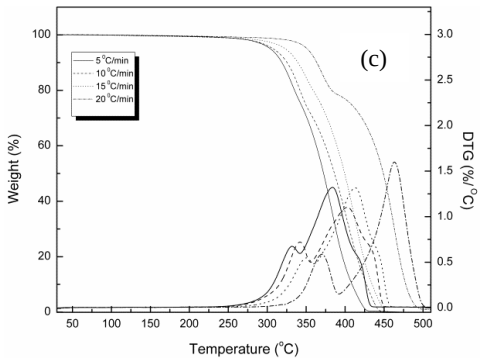

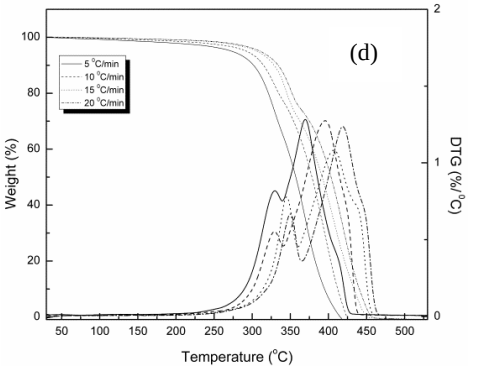

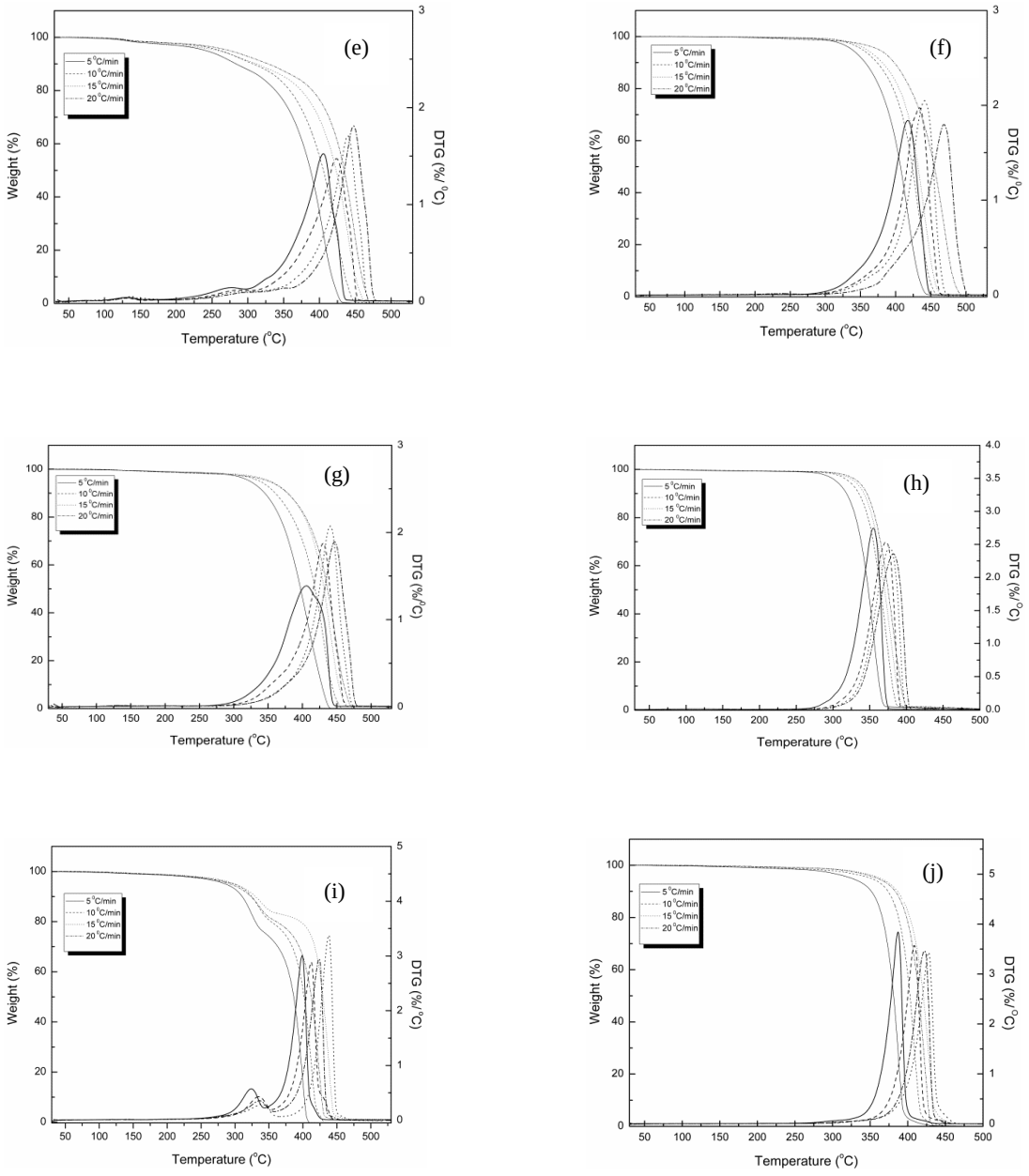

Figure 5.22 TG and DTG curves of (a) PP, (b) PP85PL15, (c) PP85PL15MA4, (d)PP85PL15MA4CaSt0.2, (e) PP85PL15MA4CoSt0.2, (f) PP100CaSt0.2, (g) P100CoSt0.2, (h) PP100NC2 (i) PP85PL15MA4NC2 and (j) PLA

Table 5.13 TGA data of PP, PP/ PLA blends and its nanocomposites of different compositions at different heating rates

Samples	PP/PLA/MA-g-PP /CaSt/CoSt/Nanoclay	T_i (°C)	T_{max} (°C)	T_f (°C)
β = 5°C/min				
PP	100:0:0:0:0:0	337	436	454
PP85PL15	85:15:0:0:0:0	291	385	384
PP85PL15MA4	85:15:4:0:0:0	303	394	417
PP85PL15MA4 CaSt0.2	85:15:4:2:0:0	277	407	418
PP85PL15MA4 CoSt0.2	85:15:4:0:2:0	241	402	420
PP100CaSt0.2	100:0:0:2:0:0	335	421	435
PP100CoSt0.2	100:0:0:0:2:0	323	416	432
PP85PL15MA4 NC2	85:15:4:0:0:2	286	403	404
PP100NC2	100:0:0:0:0:2	327	403	395
PLA	0:100:0:0:0:0	305	356	366
β = 10°C/min				
PP	100:0:0:0:0:0	357	451	471
PP85PL15	85:15:0:0:0:0	328	398	419
PP85PL15MA4	85:15:4:0:0:0	307	407	435
PP85PL15MA4 CaSt0.2	85:15:4:2:0:0	292	426	420
PP85PL15MA4 CoSt0.2	85:15:4:0:2:0	261	421	437
PP100CaSt0.2	100:0:0:2:0:0	352	436	450
PP100CoSt0.2	100:0:0:0:2:0	337	431	447
PP85PL15MA4 NC2	85:15:4:0:0:2	294	417	421
PP100NC2	100:0:0:0:0:2	350	412	417
PLA	0:100:0:0:0:0	322	372	384
β = 15°C/min				
PP	100:0:0:0:0:0	365	457	478
PP85PL15	85:15:0:0:0:0	310	407	431
PP85PL15MA4	85:15:4:0:0:0	324	412	442
PP85PL15MA4 CaSt0.2	85:15:4:2:0:0	306	436	440
PP85PL15MA4 CoSt0.2	85:15:4:0:2:0	270	426	447
PP100CaSt0.2	100:0:0:2:0:0	358	441	457
PP100CoSt0.2	100:0:0:0:2:0	350	441	456
PP85PL15MA4 NC2	85:15:4:0:0:2	298	426	436
PP100NC2	100:0:0:0:0:2	359	421	430
PLA	0:100:0:0:0:0	329	380	391
β = 20°C/min				
PP	100:0:0:0:0:0	380	462	487
PP85PL15	85:15:0:0:0:0	315	412	441
PP85PL15MA4	85:15:4:0:0:0	351	421	484
PP85PL15MA4 CaSt0.2	85:15:4:2:0:0	310	441	460
PP85PL15MA4 CoSt0.2	85:15:4:0:2:0	278	436	467
PP100CaSt0.2	100:0:0:2:0:0	376	451	484
PP100CoSt0.2	100:0:0:0:2:0	356	446	464
PP85PL15MA4 NC2	85:15:4:0:0:2	300	436	444
PP100NC2	100:0:0:0:0:2	364	426	439
PLA	0:100:0:0:0:0	335	385	396

Table 5.14 Thermal degradation of films as percentage conversion at different heating rates

Conversion (%)	Degradation Temperature (°C)									
	PP	PP85PL15	PP85PL15MA4	PP85PL15MA4CaSt 0.2	PP85PL15MA4CoSt 0.2	PP100CaSt0.2	PP100CoSt0.2	PP85PL15MA4NC2	PP100NC2	PLA
β =5°C/min										
10	357	307	319	301	283	356	345	311	351	318
20	383	324	335	321	333	378	366	330	366	331
30	399	338	351	333	360	390	379	363	373	338
40	410	350	363	346	377	399	389	379	378	344
50	419	358	372	357	387	407	397	387	381	348
60	426	366	380	365	395	412	404	392	384	352
70	433	374	388	373	402	418	411	395	387	355
80	440	382	397	382	409	423	419	399	389	359
90	449	393	408	394	417	430	428	402	392	364
β = 10°C/min										
10	378	322	325	314	307	373	360	325	374	335
20	404	341	342	334	358	396	385	353	388	347
30	420	357	359	354	376	409	400	384	394	355
40	431	369	375	368	392	417	410	395	399	360
50	439	378	386	378	403	423	418	402	403	365
60	446	385	396	387	410	429	424	406	406	369
70	452	392	405	395	420	434	430	410	409	373
80	458	400	415	403	425	439	435	413	411	377
90	466	411	427	412	432	445	442	417	414	381
β = 15°C/min										
10	386	328	340	328	326	380	378	333	383	342
20	413	346	359	345	370	405	403	361	398	354
30	430	364	377	362	392	417	415	394	405	361
40	440	378	389	379	409	425	423	406	410	365
50	448	388	399	391	420	432	430	412	414	370
60	454	397	408	401	428	437	435	417	417	374
70	460	405	415	411	434	442	440	420	423	378
80	466	413	423	421	441	447	445	425	420	383
90	473	424	440	433	448	453	451	428	426	387
β = 20°C/min										
10	404	336	364	334	328	403	378	330	486	346
20	425	356	383	352	390	424	404	396	402	358
30	439	377	422	375	413	436	419	417	410	364
40	449	391	438	391	425	446	429	425	416	369
50	456	401	449	403	434	452	436	430	421	375
60	463	409	457	412	441	460	442	433	424	380
70	469	416	463	420	446	466	445	436	427	383
80	475	423	469	429	452	471	447	439	429	388
90	482	432	478	440	459	455	450	442	433	393

5.4.2 Kinetic analysis

The degradation study of PP, PP/PLA, pro-oxidant filled PP/PLA blends and its nanocomposites was performed with the help of three multiple heating rate techniques viz. Kissinger [126], Kim-Park [135] and Flynn-Wall [127]. These multiple heating rate methods were used to calculate the parameters of degradation kinetics viz. activation energy (E_a), reaction order (n) and frequency factor (Z).

5.4.2.1 Kissinger method

Figure 5.23 shows the plot of $\ln(\beta/T_{\max}^2)$ vs. ($1/T_{max}$) at different heating rates (5, 10, 15, and 20°C/min). The plots for PP, PP/PLA, pro-oxidant filled blends and its nanocomposites show straight lines and the calculated parameter values are presented in Table 5.15. The values of E_a for PP and PLA are 219 kJ/mol and 154 kJ/mol, respectively. Whereas, the E_a of PP100CaSt0.2 and PP100CoSto.2 are 206 kJ/mol and 185 kJ/mol, respectively. Addition of PLA in PP decreased the activation energy due to the incompatibility between two polymers. Whereas addition of compatibilizer increases the compatibility between two polymers and enhances the activation energy. Filling of pro-oxidant in PP and PP/PLA blend decreased the activation energy due to presence of metal ions, which decreases the thermal stability of the modified sample [169].

Filling of PLA and nanoclay in PP decreases the value of E_a to 177 kJ/mol and 198 kJ/mol, respectively. The activation energy of PP100NC2 decreased due to the catalytic action of nanoclay on the polymer matrix in the composite system [174]. Whereas activation energy of the PP85PL15 blend decreased due to the incompatibility between the two polymers. Addition of compatibilizer increases the compatibility of the PP85PL15 blend and enhances the activation

energy to 182 kJ/mol. Further addition of nanoclay in PP85PL15MA4 blend decreases the activation energy to 165 kJ/mol.

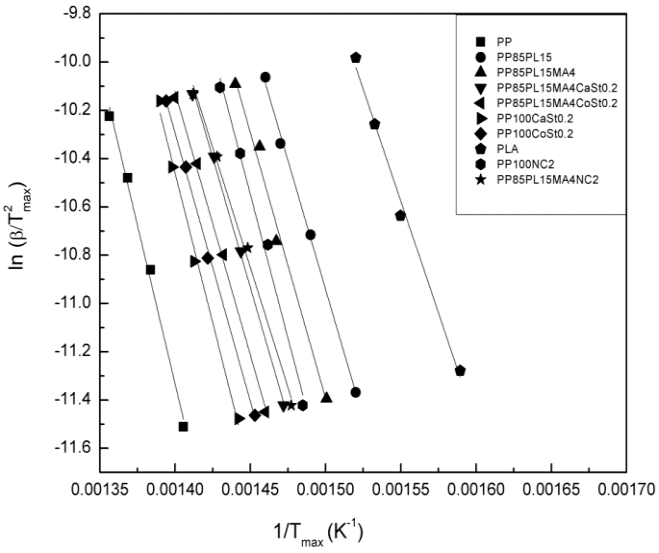

Figure 5.23 Kissinger plots for the samples under nitrogen at different heating rates

Table 5.15 Degradation kinetic parameters for the samples by Kissinger method

Sample	Kinetic parameters		
	E_a (kJ/mol)	n	ln(Z)
PP	219	1.2	24
PP85PL15	177	0.6	17
PP85PL15MA4	182	0.5	20
PP85PL15MA4 CaSt0.2	178	0.4	18
PP85PL15MA4 CoSt0.2	181	0.4	19
PP100CaSt0.2	206	0.8	22
PP100CoSt0.2	185	0.7	21
PP85PL15MA4 NC2	165	0.4	14
PP100NC2	198	0.2	20
PLA	154	0.2	16

5.4.2.2 Kim-Park method

The kinetic parameters of degradation such as E_a, n and Z are determined using the Kim-park method [135]. Figure 5.24 shows the plot of ln(β) vs. ($1/T_{max}$) at different heating rates. The plot for PP, PP/PLA, pro-oxidant filled PP/PLA blends and its nanocomposites show straight line and their values are presented in Table 5.16. The values of E_a calculated for PP and PLA are 223 kJ/mol and 156 kJ/mol, respectively. Whereas, the E_a of PP100CaSt0.2 and PP100CoSto.2 was 203 kJ/mol and 190 kJ/mol, respectively. Addition of PLA in PP decreased the activation energy due to the incompatibility between two polymers. Whereas addition of compatibilizer increases the compatibility between two polymers and enhances the activation energy. Filling of pro-oxidant in PP and PP/PLA blend decreased activation energy due to the presence of metal ions, which decreases the thermal stability of the modified sample [169].

Filling of PLA and nanoclay in PP decreases the value of E_a to 176 kJ/mol and 199 kJ/mol, respectively. The activation energy of PP100NC2 decreases due to the catalytic action of nanoclay on the polymer matrix in composite system [174]. Whereas activation energy of the PP85PL15 blend decreases due to the incompatibility between two polymers. Addition of compatibilizer increases the compatibility of the PP85PL15 blend and therefore, enhances the activation energy to 184 kJ/mol. Further addition of nanoclay in PP85PL15MA4 blend decreases the activation energy to 168 kJ/mol.

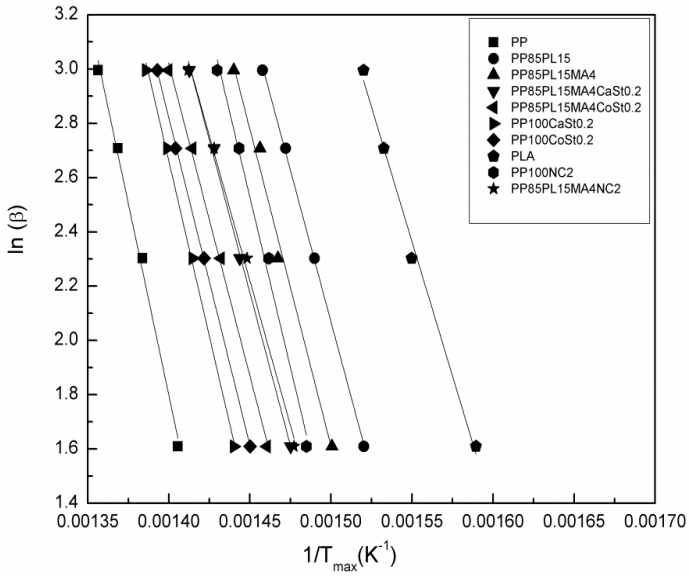

Figure 5.24 Kim-Park plots for the samples under nitrogen at different heating rates

Table 5.16 Degradation kinetic parameters for the samples by Kim-Park method

Samples	Kinetic parameters		
	E_a (kJ/mol)	n	ln(Z)
PP	223	0.5	44
PP85PL15	176	0.4	38
PP85PL15MA4	184	0.5	41
PP85PL15MA4 CaSt0.2	178	0.2	39
PP85PL15MA4 CoSt0.2	181	0.1	37
PP100CaSt0.2	203	0.4	42
PP100CoSt0.2	190	0.3	41
PP85PL15MA4 NC2	168	0.2	35
PP100NC2	199	0.2	42
PLA	156	0.2	26

5.4.2.3 Flynn-Wall method

The kinetic parameters of degradation was estimated by Flynn-Wall method [127]. The plot of ln(β) vs. ($1/T$) produced a straight line with the slope of -0.4567 (E_a/R). E_a of thermal decomposition is calculated from the slope. The Flynn-Wall model can also be used to calculate the activation energy of solid-phase reaction. Figure 5.25 shows the plot of ln(β) vs. ($1/T$) at different heating rates. The plot of PP, PP/PLA, pro-oxidant filled PP/PLA blends and its nanocomposites show straight line and their calculated kinetic parameter values are presented in Table 5.17. The values of E_a at 15% conversion for PP and PLA are 259 kJ/mol and 156 kJ/mol, respectively.

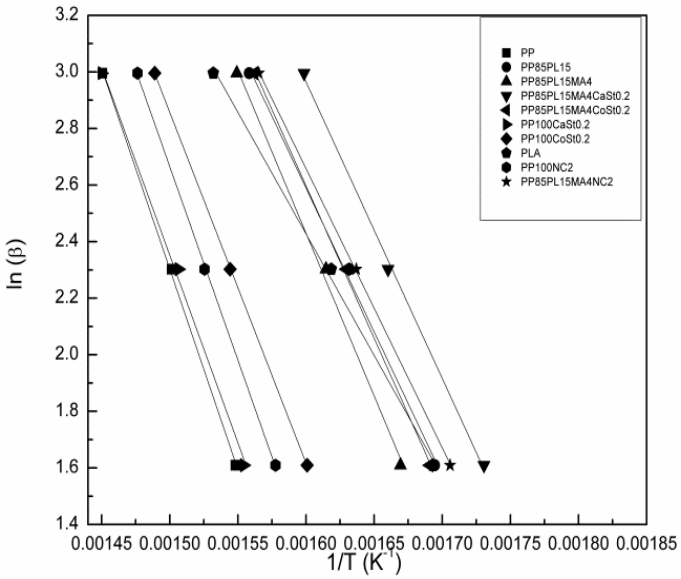

Figure 5. 25 Flynn-Wall plots for samples under nitrogen at different heating rates for 15% conversion

Table 5.17 Degradation kinetic parameters of samples using Flynn-Wall method

Samples	Conversion (%)	Kinetic parameters	
		E_a (kJ mol^{-1})	ln(Z)
PP	5	188	19
	10	233	21
	15	259	25
PP85PL15	5	165	17
	10	175	19
	15	185	22
PP85PL15MA4	5	171	18
	10	183	20
	15	209	23
PP85PL15MA4CaSt0.2	5	172	17
	10	181	19
	15	190	21
PP85PL15MA4CoSt0.2	5	180	17
	10	187	18
	15	196	21
PP100CaSt0.2	5	170	18
	10	218	19
	15	241	23
PP100CoSt0.2	5	173	17
	10	190	18
	15	225	22
PP85PL15MA4NC2	5	162	14
	10	170	16
	15	180	18
PP100NC2	5	175	15
	10	220	17
	15	249	21
PLA	5	148	13
	10	151	14
	15	156	16

The E_a of PP100CaSt0.2 and PP100CoSto.2 is 241 kJ/mol and 225 kJ/mol, respectively. Addition of PLA in PP decreased the activation energy due to the incompatibility between two polymers. Whereas addition of compatibilizer increases the compatibility between two polymers and enhances the activation energy. Filling of pro-oxidant in PP and PP/PLA blend decreased the

activation energy due to the presence of metal ions, which decreases the thermal stability of the modified sample [169].

Filling of PLA and nanoclay in PP decreases the value of E_a to 185 kJ/mol and 249 kJ/mol, respectively. The activation energy for PP100NC2 decreases due to the catalytic action of nanoclay on the polymer matrix in composite system [174]. Whereas activation energy of PP85PL15 decreases due to the incompatibility between two polymers. Addition of compatibilizer increases the compatibility of the PP85PL15 blend and enhances the activation energy to 209 kJ/mol. Further addition of nanoclay in PP85PL15MA4 blend decreases the activation energy to 180 kJ/mol.

The decomposition kinetic parameters are affected by different degradation mechanisms at both stages; initial and final. In the initial stage, weaker bonds are the main cause of polymer degradation, which is confirmed by the low activation energy at the initial stage. Whereas, degradation of PP is a complex radical chain mechanism initiated by random chain scission and followed by radical transfer process [175]. The presence of methyl side groups in PP favors intermolecular hydrogen transfer during thermal degradation of PP [176]. The decomposition of PP generates smaller intermediate products after which further reaction produces low molecular weight products in the form of liquids and gases [161]. In this process, small fragments from the polymers could be evaporated and weight loss is recorded. Hence, the weight change rate of the polymer is influenced by both chemical and physical processes.

5.4.2.4 Rate constant versus temperature

Figure 5.26 shows plots of rate constant versus temperature for PP, PP/PLA, pro-oxidant filled blends and its nanocomposites. The rate constant changes with the temperature. All samples show slow increase of rate constant at lower temperature and exponential increase of rate constant at higher temperature. The values of rate constant of all the blend and nanocomposite samples are lower than that of PP but the trend of all the samples are almost similar throughout the region. The threshold value of the rate constant is different for all the samples.

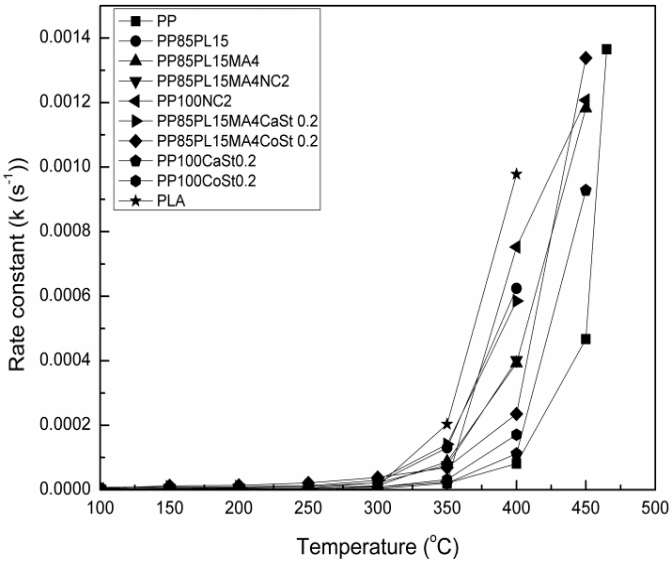

Figure 5.26 Rate constant versus temperature plots for film samples at 5% conversion

5.4.2.5 Lifetime estimation

The life cycle of PP, PP/PLA, pro-oxidant blends and nanocomposites is calculated using Toop equation [136]. Where, X_f is E_a/RT_c and T_c (K) is the temperature at 5% weight loss [137]. t_f is estimated as the time of failure (min). T_f is the failure temperature (K) and log $p(X_f)$ is a function of X_f. The activation energy (E_a) is calculated from Kissinger, Kim-Park and Flynn-Wall (at 15% conversion) methods at β of 5°C/min. Lifetime values of PP, PP/PLA blends and its

composites were calculated using equation 3.19. Estimated lifetimes of PP, PP/PLA blends and nanocomposites are shown in Figure 5.27. It is very clear that the lifetime of all the samples decreases with increase in temperature irrespective of the method used for estimation. For example, the lifetime of neat PP by thermal degradation at 30 °C estimated by three methods namely Kissinger, Kim-Park and Flynn-Wall method is 4.6×107, 1.2×10^{8} and 1.05×10^{11} years, respectively. Whereas, these values are much lower at 50 °C (2.6×10^{5}, 6.04×10^{5} and 18.6×10^{7} years, respectively). Similarly, in case of PP85PL15 the estimated lifetime is 4.6×10^{5}, 3.7×10^{5} and 1.5×10^{6} years at 30 °C and 6.1×10^{3}, 4.9×10^{3} and 1.6×10^{4} years at 50°C, respectively. In the case of PP100CoSt0.2, the estimated lifetime is 1.5×10^{6}, 7.5×10^{5} and 1.7×10^{8} years at 30 °C and 1.6×10^{4}, 7.1×10^{3} and 7.1×10^{5} years at 50°C, respectively. In the case of PP100NC2, the estimated lifetime is 7.0×10^{6}, 2.8×10^{7} and 1.8×10^{10} years at 30 °C and 1.7×10^{4}, 1.7×10^{5} and 4.09×10^{7} years at 50°C, respectively. The lifetime of PP85PL15 blend is lower than PP due to the incompatibility of two polymers, which decreases the thermal stability and lifetime of the blended sample [90]. The lifetime of PP100CoSt0.2 is lower than PP due to the presence of metal ions in the polymer matrix, which decreases the thermal stability and lifetime of the samples. The lifetime of PP100NC2 composite is lower than PP due to the catalytic effect of nanoclay in the polymer matrix, which decreases the thermal stability and lifetime of the composite materials.

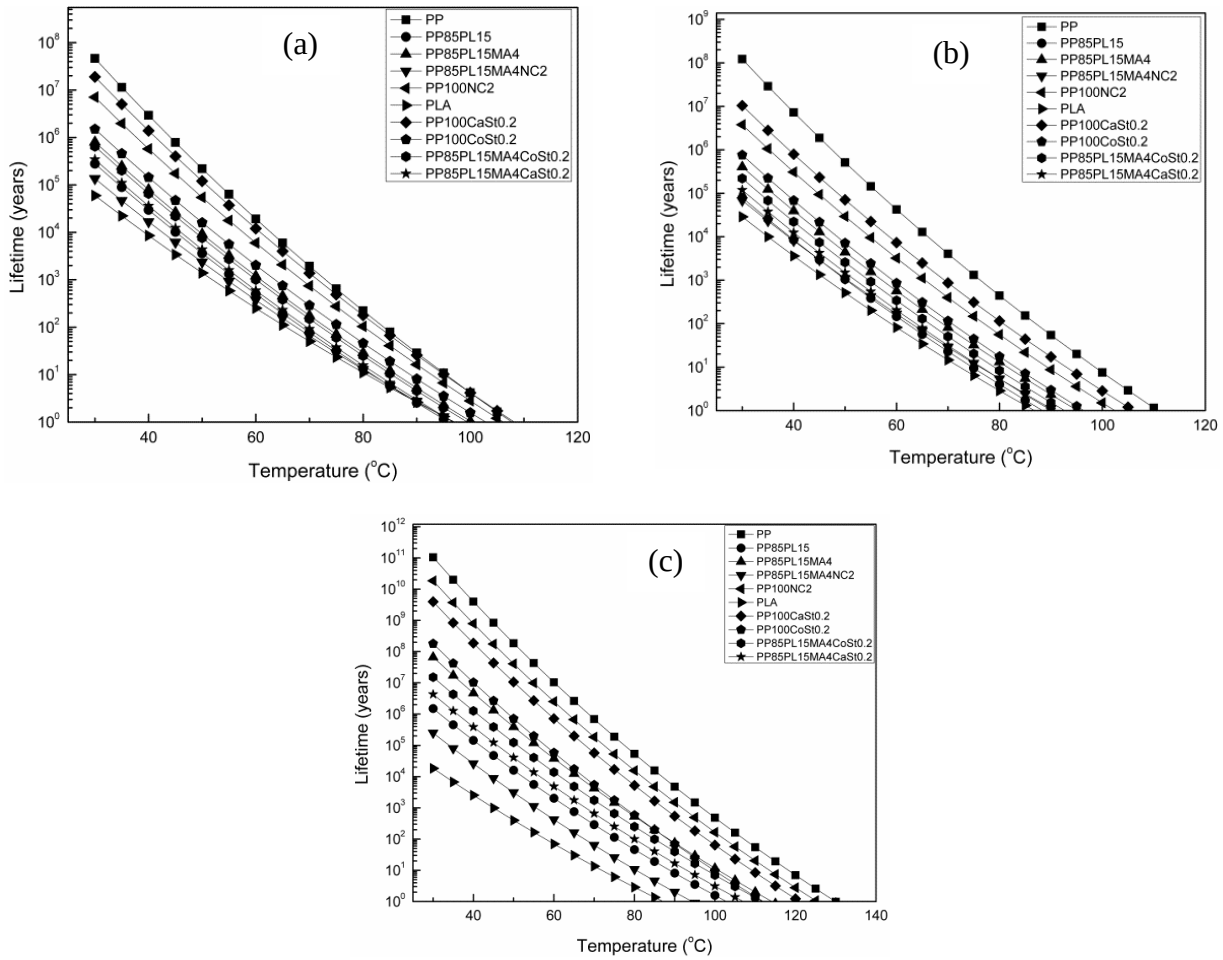

Figure 5.27 Lifetime of films samples by (a) Kissinger (b) Kim-Park and (c) Flynn-Wall methods

5.5 Biodegradability studies

The total organic carbon (TOC) of different samples were measured to make it possible to calculate the theoretical carbon dioxide [CO_2(th)] and shown in Table 5.18.

Table 5.18 Total organic carbon (%) and theoretical CO_2 (g) evolution from the samples

Sample	TOC (%)	Wt. of carbon in 1 g of sample (g)	Th. CO_2 evolution (g)
Microcrystalline cellulose (MCC)	43	0.43	1.56
PP	94	0.94	3.45
PP85PL15	87	0.87	3.18
PP85PL15MA4	82	0.82	2.99
PP85PL15MA4CaSt0.2	84	0.84	3.19
PP85PL15MA4CoSt0.2	87	0.87	3.07
PP85PL15MA4NC2	80	0.80	2.94
PP100CaSt0.2	92	0.92	3.39
PP100CoSt0.2	90	0.90	3.29
PP100NC2	89	0.91	3.40

Example calculation for theoretical CO_2

CO_2 (th) for PP85PL15 sample $= 1 \times 0.87 \times \frac{44}{12} = 3.18$

The values of CO_2 produced (in grams) and the percent biodegradation of each sample were calculated using equation 3.20, which are shown in Table 5.18.

Example calculation for percent biodegradation

Vol. of $Ba(OH)_2$ taken = 30 ml

Normality of $Ba(OH)_2$ = 0.024

Therefore, molarity of $Ba(OH)_2$ = $\frac{0.024}{2} = 0.012$ [as the acidity of $Ba(OH)_2$ is 2]

Hence, mmols of $Ba(OH)_2$ taken = 30 x 0.012 = 0.36 mmols

And,

Vol. of HCl used = 9.9 ml

Normality of HCl = 0.05

Molarity of HCl = 0.05 [as the basicity of HCl is 1]

Hence, mmols of HCl used = 9.9 x 0.05 = 0.495 mmols

Now,

mmols of CO_2 produced = $\text{mmoles of } Ba(OH)_2 \text{ at start} - \frac{\text{mmoles of HCl}}{2}$

$$= 0.36 - \frac{0.495}{2} = 0.113 \text{ mmols}$$

We know that,

1 mol of CO_2 = 44 g/L

Therefore, 1 mmol of CO_2 = 44 x 10^{-3} = 0.044 g/L

Hence, grams of CO_2 produced = 0.113 x 0.044 = 0.0049 g

In this way, the readings were taken at an interval of 5 days for 45 days and the cumulative sum of CO_2 produced for PP85PL15 sample was 9.59 grams.

Finally, using equation 3.21, we get

Biodegradation (%) = $\frac{9.59 - 9.49}{3.18} \times 100$ = 3.3%

The biodegradation of all the samples is shown in Figure 5.28. The test was conducted for 45 days and the biodegradability is calculated from the equation 3.21. PP confirmed its non biodegradable nature. Whereas, cellulose has shown 76% biodegradability due to easily assimilation by the microorganisms. The biodegradability of PP85PL15 and PP85PL15MA4 was 3.3% and 3.5%, respectively. Incorporation of polylactide in the PP/PLA (85/15) increases amorphous phase in the blend and enhances the biodegradability; the microbes can easily assimilate the amorphous part of the blends. Addition of compatibilizer in PP85PL15MA4 blend also enhances the biodegradation to a small extent.

Filling of pro-oxidant (cobalt stearate/ calcium stearate) enhances the biodegradability of PP and PP/PLA due to increase in the functional groups, amorphous nature and weak linkages. The amorphous nature of the pro-oxidant filled blends makes them susceptible to the microbial attack [72]. The biodegradation of PP100NC2 and PP85PL15MA4NC2 composite was enhanced to 1.2% and 4.6%, respectively due to nanoclay, as the nanoclay maintains the pH level of the environment at conducive levels, which is helpful for microbial growth [177]. It has been reported that exchange of cation and increase in surface area due to the presence of clay is the main reason for microbial growth [178, 179]. The microorganisms convert the low molecular weight product into CO_2, water and biomass, which is helpful in the biodegradation of the composites.

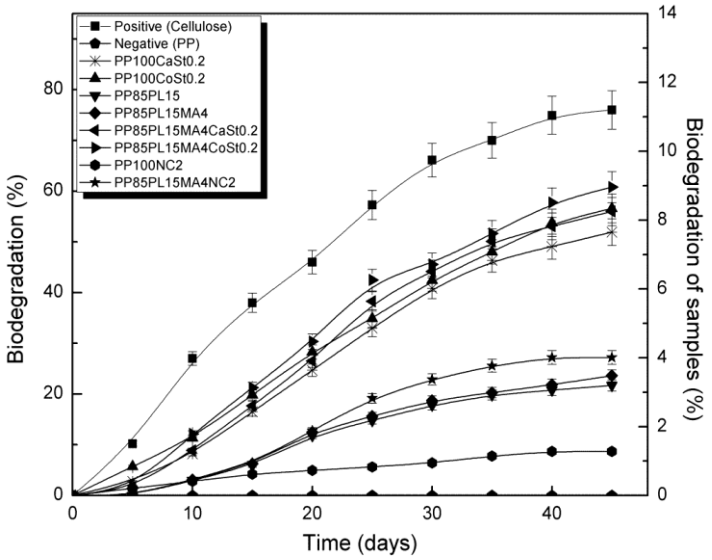

Figure 5.28 Biodegradability of all blended and composite samples

5.6 Ecotoxicological studies

5.6.1 Microbial toxicity test

Colony forming bacteria in the soil extracts is presented in Table 5.19. It is seen that the blank sample gave CFU count of 0.2×10^4 and the cellulose gave the highest number (bacterial lawn) of CFU. CFU count in the all the compost samples of blended and composites are closer to or higher than blank sample, indicating the normal growth of the bacteria in the soil samples. Therefore, it can be concluded that the biodegraded products from these blends and composites are non-toxic in nature.

Example calculation for colony forming unit (CFUs)

Total Dilution Factor used $=10^{-3}$

Number of colonies (per ml) for PP85PL15, shown in table 5.17 = 4

Using equation 3.22, we get

$$\text{CFU/ml for PP18} = \frac{4\ \text{colonies/ml plated}}{10^{-3}} = 1.1\times10^{4}$$

Table 5.19 The CFU count from the soil extracts of compost

Sr. No.	Samples	Number of colonies/ml	CFU/ml count * 10^4
1	Control	2	0.2
2	Cellulose	Bacterial lawn	Bacterial lawn
3	PP	3	0.3
4	PLA	7	0.7
5	PP85PL15	4	0.4
6	PP85PL15MA4	4	0.4
7	PP85PL15MA4NC2	6	0.6
8	PP100NC2	7	0.7
9	PP85PL15MA4CaSt0.2	6	0.6
10	PP85PL15MA4CoSt0.2	8	0.8
11	PP100CaSt0.2	5	0.5
12	PP100CoSt0.2	4	0.4

5.6.2 Plant growth test

The pH of the growth medium was measured to confirm the suitability of composted PP films as growth medium for the plant growth as the optimal pH range for the growth of most plants is about 5.5 [180]. Extremely low or high pH will affect solubility and availability of nutrients in the growth medium. In this study, pH of the medium was adjusted to 5.8 - 6.0, which is near to optimum value.

To know the toxic effects of biodegradation products of PP, PP/PLA, pro-oxidant filled PP/PLA and their nanocomposites on the quality of the medium, plant growth test have been carried out with tomato and corn [64]. After 21 days test, the visual evaluations of seedlings (corn and tomato) in the growing medium indicated that average amount of plant emergence is 100%. There was hardly any difference in growth of both the plants between control and test samples

(Figure 5.29 and Figure 5.30). After 21 days of growth, plants were harvested, dried and weighed. Dry weights of corn and tomato as percentage of dry weight of the control is almost 100% as shown in Figure 5.31.

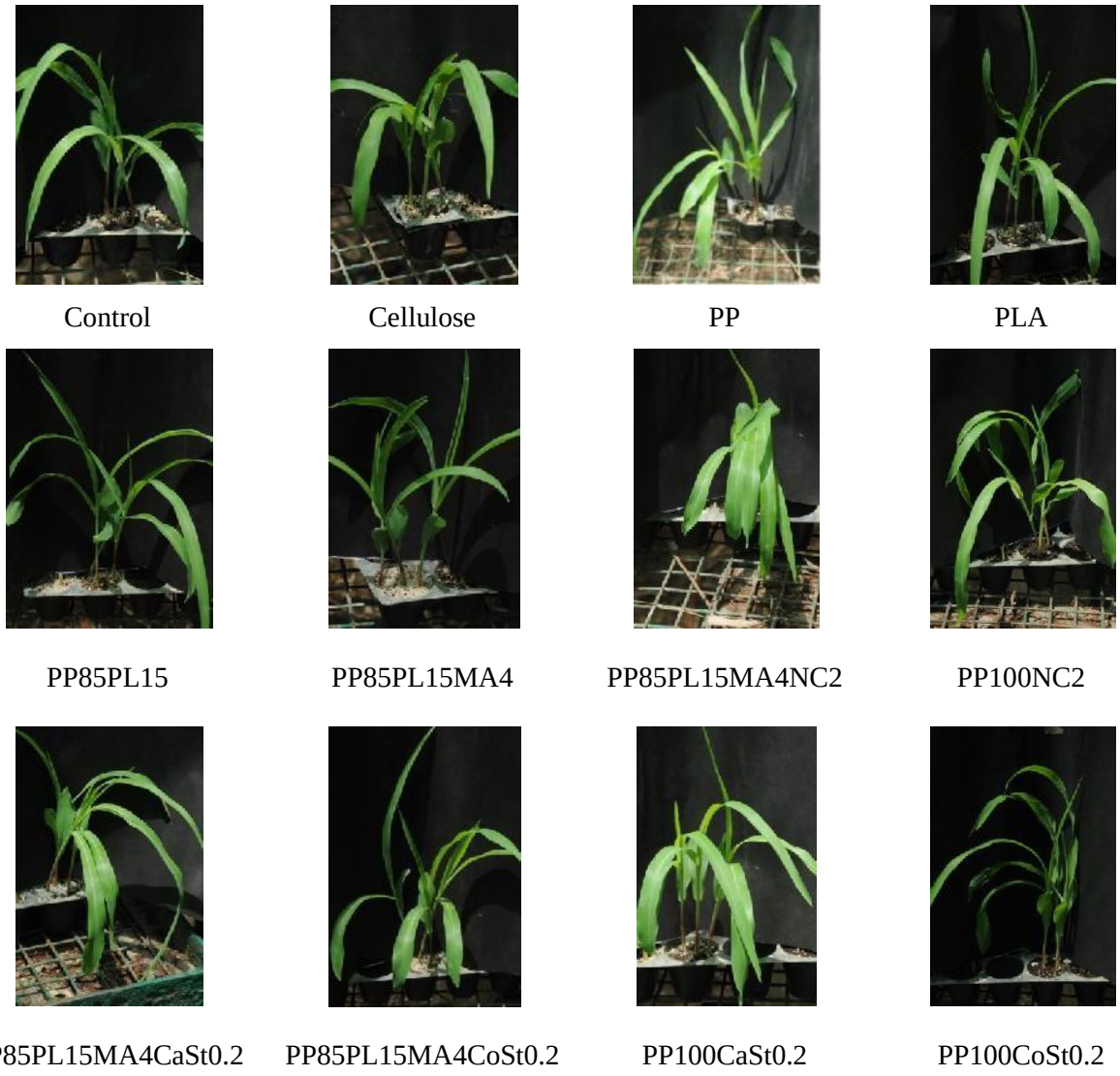

Figure 5.29 Corn plant growth in a composite medium (after biodegradation)

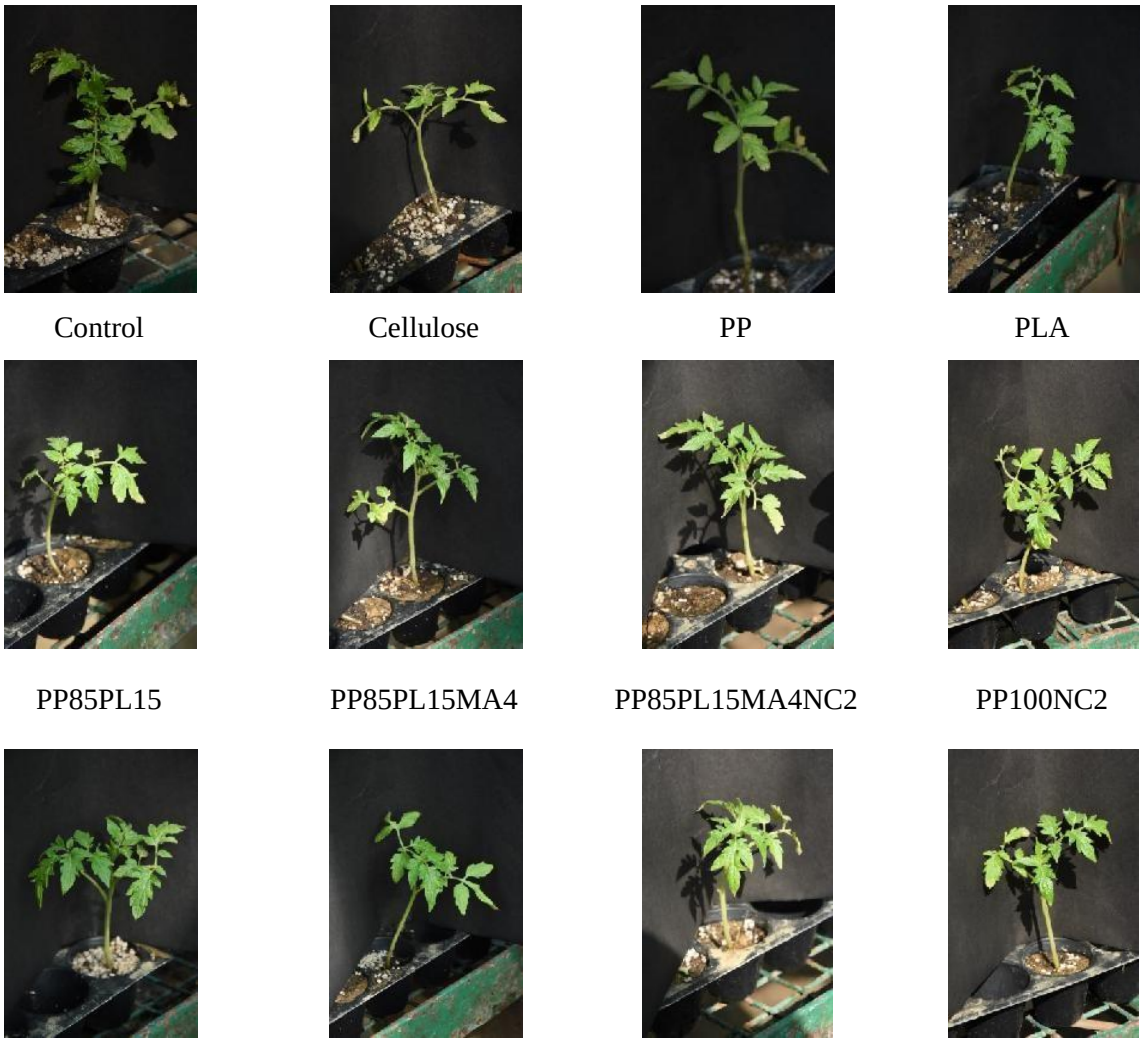

Figure 5.30 Tomato plant growth in composite medium (after biodegradation)

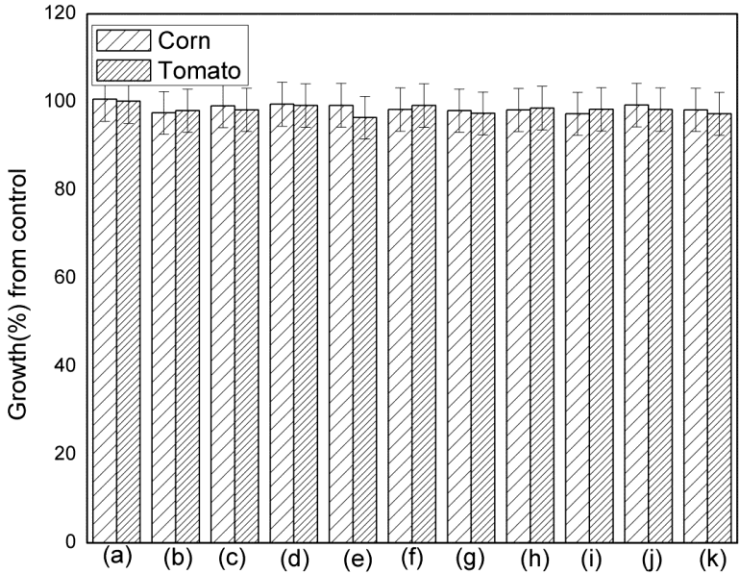

Figure 5.31 Dry weights of plant after 21 days of growth (a) Cellulose, (b) PP, (c) PLA, (d) PP85PL15, (e) PP85PL15MA4, (f) PP85PL15MA4CaSt0.2, (g) PP85PL15MA4CoSt0.2, (h) PP85PL15MA4NC2, (i) PP100CaSt0.2, (j) PP100CoSt0.2, and (k) PP100NC2

Chapter 6-Conclusions and Recommendations for Future Work

6.1 Conclusions

In this work, acrylic acid has been successfully grafted onto the PP by radiation grafting method. The grafting parameters viz. radiation dose, inhibitor concentration, sulfuric acid concentration and monomer concentration were optimized by RSM method. The optimized conditions to achieve 35% degree of grafting, viz. monomer concentration 12.09 wt%, radiation dose 12.40 kGy, inhibitor concentration 0.07 M and sulfuric acid concentration 0.12 M were suggested by the model, and further it was experimentally confirmed, where the degree of grafting 34% was achieved at this optimized condition. Results concluded that the grafting process has satisfactorily described by this predictive models and 35% targeted degree of grafting can be predicted under any given conditions within the experimental range. Swelling of PP18 was 12.82%, higher than PP (0%) confirmed that the grafting of AAc increases the hydrophilic nature of the grafted PP films. The presence of graft is qualitatively confirmed by carbonyl peak in between 1701 cm^{-1} to 1705 cm^{-1} and quantitatively by carboxylic group analysis on the surface of the PP. Tensile strength of PP18 (35% grafted) decreases to 21 MPa which is suitable for packaging applications (as against 38.8 MPa of PP). TGA studies have concluded that the grafting of acrylic acid on PP films significantly decreases the thermal stability of grafted PP. The crystallinity of grafted PP (PP18) reduced to 26%, from 59% of PP. PP film shows single stage degradation, but grafted PP shows three stage degradation. The increase in the degree of grafting decreases the thermal stability of PP-*g*-AAc films. The activation energy (E_a) for thermal degradation is calculated by three multiple heating rate methods, namely Kissinger, Flynn-Wall and Kim-Park methods. The values of the activation energy (E_a) depend on the degree of grafting, heating rate and the calculation methods. A detailed study on the lifetime and

stability of the PP and grafted PP has been undertaken. The lifetime depends on temperature and degree of grafting. The lifetime of PP and grafted PP films decreases with increase in temperature. The lifetime of grafted PP films is shorter than that of the pure PP film. Biodegradability increases with increase in degree of grafting and maximum biodegradation achieved is ~ 6% at 35% grafting. Eco-toxicological test confirmed that the biodegradation products are non-toxic in nature.

Pro-oxidant and nanoclay filled blends and composites have been successfully developed. Addition of PLA leads to decrease in the T_m and crystallinity of PP85PL15 blend. Filling of pro-oxidant also decreases the crystallinity of the bends. The linear viscoelastic results have confirmed the enhancement of the complex viscosity and storage modulus of PP85PL15MA4 blend. However, addition of pro-oxidant reduces the complex viscosity and storage modulus. The shear thinning behavior is observed in all the blends. Morphological study has confirmed the increase in the void and roughness on the addition of PLA in PP. The addition of compatibilizer reduces the void and roughness, but further addition of pro-oxidant (more than 0.2 wt%) increases the void and roughness in the blend. PP, PLA and nanoclay filled PP show a single-step thermal degradation thermogram. Whereas PP/PLA blends show two step thermal degradation thermogram. The thermal stability of PP decreases on the blending of PLA. Whereas addition of compatibilizer increases the thermal stability of PP/PLA blends mainly due to the increased interfacial adhesion and interaction between the polymer chains of the two polymers. Addition of nanoclay also decreases the thermal stability of PP films. The variation in the degradation trends shown by the data of different samples is due to the difference in degradation reaction mechanism, sample composition, and microstructural features of the polymers in the blends and nanocomposites. The activation energies of PP/PLA blends are lower than that PP

due to radical character of degraded PLA derivatives, which affects the initial thermal degradation reaction. The degradation kinetic parameters E_a, n, and ln(Z) of the blends and composites are constituent dependent. The lifetime of all the samples decreases drastically with the increase in temperature. The addition of nanoclay results in reduced lifetime of PP. FTIR studies have confirmed the compatibility between two polymers in the blend and the presence of nanoclay in composite samples. Biodegradability study has confirmed that the addition of pro-oxidant in the PP/PLA blend enhances the biodegradability of PP85PL15MA4CoSt0.2 blend up to ~ 9%.

6.2 Recommendations for future work

The development in science and technology is a never ended process. Each conclusion of the research opens up a new range of questions and avenues that can be further explored in multiple directions. However, some areas for future research are following:

1. The fate of non-biodegradable part of the grafted, blended and nanocomposite films be investigated. Non-toxicity of the resultant fragmented products(s) need to be verified by conducting earthworm test.
2. The relative biodegradability of novel grafted, blended and nanocomposite polymers can be studied under all possible circumstances of degradation, viz. synergistic effect of photo- and biodegradation, and characterization of effect of these degradations on the structure of the polymers.
3. Some other analytical techniques may also be applied to study the degradation behavior, e.g. chromatography, matrix-assisted laser desorption/ionization time of flight (MALDI-TOF), nuclear magnetic resonance (NMR), etc.

4. The positive outcomes of the research shall be tested firstly on pilot scale and then on commercial scale.

References

[1] Gowariker VR, Viswanathan N, Sreedhar J. Polymer Science: New Age International, 1986.

[2] Geyer R, Jambeck JR, Law KL. Production, use, and fate of all plastics ever made. Science Advances. 2017;3:1-5.

[3] Wire B. https://wwwbusinesswirecom/news/home/20170509006321/en/Trends-Opportunities -Indian-Packaging-Industry-2017-Analysis (accessed 01.02.2018)

[4] Selke SE, Culter JD. Plastics packaging: properties, processing, applications, and regulations: Carl Hanser Verlag 2016, p.448.

[5] Plastic Packaging - The sustainable choice. Tata strategic managment group. http://ficci.in/spdocument/20690/Plastic-packaging-report.pdf (accessed 28.08.2017)

[6] Sam S, Nuradibah MA, Ismail H, Noriman N, Ragunathan S. Recent advances in polyolefins/natural polymer blends used for packaging application. Polymer Plastics Technology and Engineering. 2014;53:631-644.

[7] Hoornweg D, Bhada-Tata P. What a waste: a global review of solid waste management.Urban Development Series Knowledge Papers. 2012;15:1-95.

[8] Gironi F, Piemonte V. Bioplastics and petroleum-based plastics: strengths and weaknesses. Energy Sources, Part A: Recovery, Utilization and Environmental Effects 2011;33:1949-1959.

[9] Sarker M, Rashid MM, Rahman MS. Conventional Naphtha Chemical Produced From Municipal Solid Low Density Polyethylene (LDPE) Waste Plastic. International Journal of Applied Chemistry. 2012;8:153-163.

[10] Clapp J, Swanston L. Doing away with plastic shopping bags: International patterns of norm emergence and policy implementation. Environmental Politics. 2009;18:315-332.

[11] Mader FW. Plastics waste management in Europe. Macromolecular Symposia: Wiley Online Library; 1992;57:15-31.

[12] Eriksen M, Lebreton LC, Carson HS, Thiel M, Moore CJ, Borerro JC, et al. Plastic pollution in the world's oceans: more than 5 trillion plastic pieces weighing over 250,000 tons afloat at sea. PloS one. 2014;9:20-30.

[13] Moore C. Plastic Pollution. Encyclopaedia Britannica. 2015, pp.76.

[14] Hammer J, Kraak MH, Parsons JR. Plastics in the marine environment: the dark side of a modern gift. Reviews of environmental contamination and toxicology: Springer, 2012, p. 1-44.

[15] Allen JI, Stewart JR, Readman J, Davidson K, Moore M. Marine Pollution and Human Health: Royal Society of Chemistry, 2011, p.1-24.

[16] Barnes DK, Galgani F, Thompson RC, Barlaz M. Accumulation and fragmentation of plastic debris in global environments. Philosophical Transactions of the Royal Society of London B: Biological Sciences. 2009;364:1985-1998.

[17] Fernández-Armesto F. Pathfinders: a global history of exploration: WW Norton & Company; 2007.

[18] André P. Hill, Marquita K., 1900. Understanding Environmental Pollution. Cambridge University Press,1999,415-430.

[19] Kumar A, Negi YS, Bhardwaj NK, Choudhary V. Synthesis and characterization of methylcellulose/PVA based porous composite, Carbohydrate Polymers 2012;88:1364-1372.

[20] Steller R, Meissner W. Structure and properties of degradable polyolefin-starch blends. Polymer Degradation and Stability. 1998;60:471-480.
[21] Ramis X, Cadenato A, Salla J, Morancho J, Valles A, Contat L, et al. Thermal degradation of polypropylene/starch-based materials with enhanced biodegradability. Polymer Degradation and Stability. 2004;86:483-491.
[22] Morancho J, Ramis X, Fernández X, Cadenato A, Salla J, Vallés A, et al. Calorimetric and thermogravimetric studies of UV-irradiated polypropylene/starch-based materials aged in soil. Polymer Degradation and Stability. 2006;91:44-51.
[23] Orhan Y, Hrenovic J, Buyukgungor H. Biodegradation of plastic compost bags under controlled soil conditions. Acta Chimica Slovenica. 2004;51:579-588.
[24] Jain K, Madhu G, Bhunia H, Bajpai PK, Reddy MS. Kinetics of biodegradation of polypropylene/polylactide blends. Journal of Polymer Materials. 2014;31:63-76.
[25] Jain K, Madhu G, Bhunia H, Bajpai PK, Nando GB, Reddy MS. Physico-mechanical characterization and biodegradability behavior of polypropylene/poly (L-lactide) polymer blends. Journal of Polymer Engineering. 2015;35:407-415.
[26] Rutkowska M, Jastrzębska M, Janik H. Biodegradation of polycaprolactone in sea water. Reactive and Functional Polymers. 1998;38:27-30.
[27] Roy P, Surekha P, Rajagopal C, Choudhary V. Degradation behavior of linear low-density polyethylene films containing pro-oxidants under accelerated test conditions. Journal of Applied Polymer Science. 2008;108:2726-33.
[28] Headifen R. Plastic Waste Solution. http://plasticwastesolutionscom/the-4rs-for-controlling-plastic-waste (accessed 06.02.2018)
[29] Lu Y, Ozcan S. Green nanomaterials: On track for a sustainable future. Nano Today. 2015;10:417-420.
[30] Kashyap PL, Xiang X, Heiden P. Chitosan nanoparticle based delivery systems for sustainable agriculture. International Journal of Biological Macromolecules. 2015;77:36-51.
[31] Kumar M, Mohanty S, Nayak S, Parvaiz MR. Effect of glycidyl methacrylate (GMA) on the thermal, mechanical and morphological property of biodegradable PLA/PBAT blend and its nanocomposites. Bioresource Technology. 2010;101:8406-84015.
[32] Mehta R, Kumar V, Bhunia H, Upadhyay S. Synthesis of poly (lactic acid): a review. Journal of Macromolecular Science, Part C: Polymer Reviews. 2005;45:325-349.
[33] Datta R, Henry M. Lactic acid: recent advances in products, processes and technologies—a review. Journal of Chemical Technology and Biotechnology. 2006;81:1119-1129.
[34] Saeidlou S, Huneault MA, Li H, Park CB. Poly (lactic acid) crystallization. Progress in Polymer Science. 2012;37:1657-1677.
[35] Abdelwahab MA, Flynn A, Chiou B-S, Imam S, Orts W, Chiellini E. Thermal, mechanical and morphological characterization of plasticized PLA–PHB blends. Polymer Degradation and Stability. 2012;97:1822-1828.
[36] Södergård A, Stolt M. Industrial production of high molecular weight poly (lactic acid). Poly (Lactic Acid): Synthesis, Structures, Properties, Processing, and Applications. 2010, p.27-41.
[37] Langer R, Tirrell DA. Designing materials for biology and medicine. Nature. 2004;428:487-492.

[38] Singh G, Kaur N, Bhunia H, Bajpai PK, Mandal UK. Degradation behaviors of linear low-density polyethylene and poly (L-lactic acid) blends. Journal of Applied Polymer Science. 2012;124:1993-1998.
[39] Tambe PB, Bhattacharyya AR, Kulkarni AR. The influence of melt-mixing process conditions on electrical conductivity of polypropylene/multiwall carbon nanotubes composites. Journal of Applied Polymer Science. 2013;127:1017-1026.
[40] Auras R, Harte B, Selke S. Effect of water on the oxygen barrier properties of poly (ethylene terephthalate) and polylactide films. Journal of Applied Polymer Science. 2004;92:1790-1803.
[41] Pospíšil J, Horák Z, Kruliš Z, Nešpůrek S. The origin and role of structural inhomogeneities and impurities in material recycling of plastics. Macromolecular Symposia: Wiley Online Library, 1998, p. 247-263.
[42] Benítez A, Sánchez JJ, Arnal ML, Müller AJ, Rodríguez O, Morales G. Abiotic degradation of LDPE and LLDPE formulated with a pro-oxidant additive. Polymer Degradation and Stability. 2013;98:490-501.
[43] Imre B, Pukánszky B. Compatibilization in bio-based and biodegradable polymer blends. European Polymer Journal. 2013;49:1215-1233.
[44] Singh B, Sharma N. Mechanistic implications of plastic degradation. Polymer Degradation and Stability. 2008;93:561-584.
[45] Fayolle B, Colin X, Audouin L, Verdu J. Mechanism of degradation induced embrittlement in polyethylene. Polymer Degradation and Stability. 2007;92:231-238.
[46] Celina MC. Review of polymer oxidation and its relationship with materials performance and lifetime prediction. Polymer Degradation and Stability. 2013;98:2419-2429.
[47] Ojeda T, Freitas A, Birck K, Dalmolin E, Jacques R, Bento F, et al. Degradability of linear polyolefins under natural weathering. Polymer Degradation and Stability. 2011;96:703-707.
[48] Wiles DM, Scott G. Polyolefins with controlled environmental degradability. Polymer Degradation and Stability. 2006;91:1581-1592.
[49] Nanda S, Sahu S, Abraham J. Studies on the biodegradation of natural and synthetic polyethylene by Pseudomonas spp. Journal of Applied Sciences and Environmental Management. 2010;14:57-60.
[50] Gerard T, Budtova T. Morphology and molten-state rheology of polylactide and polyhydroxyalkanoate blends. European Polymer Journal. 2012;48:1110-1117.
[51] Corradini E, Mattoso L, Guedes C, Rosa D. Mechanical, thermal and morphological properties of poly (ε-caprolactone)/zein blends. Polymers for Advanced Technologies. 2004;15:340-345.
[52] Briassoulis D. The effects of tensile stress and the agrochemical Vapam on the ageing of low density polyethylene (LDPE) agricultural films. Part I. Mechanical behaviour. Polymer Degradation and Stability. 2005;88:489-503.
[53] Busfield WK, Taba P. Photo-oxidative degradation of mechanically stressed polyolefins. Polymer Degradation and Stability. 1996;51:185-196.
[54] Ammala A, Bateman S, Dean K, Petinakis E, Sangwan P, Wong S, et al. An overview of degradable and biodegradable polyolefins. Progress in Polymer Science. 2011;36:1015-1049.

[55] Kodama Y, Lima NB, Machado LD, Nakayama K. Investigation of gamma irradiated PCL/PLLA blend by wide-angle x-ray diffraction. In: INAC conference on International Nuclear Atlantic, Brazil, Sep 30-Oct 30, 2007.
[56] Iovino R, Zullo R, Rao M, Cassar L, Gianfreda L. Biodegradation of poly (lactic acid)/starch/coir biocomposites under controlled composting conditions. Polymer Degradation and Stability. 2008;93:147-157.
[57] Husarova L, Machovsky M, Gerych P, Houser J, Koutny M. Aerobic biodegradation of calcium carbonate filled polyethylene film containing pro-oxidant additives. Polymer Degradation and Stability. 2010;95:1794-1799.
[58] Maiti P, Batt CA, Giannelis EP. Biodegradable polyester/layered silicate nanocomposites. MRS Online Proceedings Library Archive. 2002;740:54-67.
[59] Chiellini E, Corti A, Swift G. Biodegradation of thermally-oxidized, fragmented low-density polyethylenes. Polymer Degradation and Stability. 2003;81:341-351.
[60] Reddy RM, Vijaya CH. Impact of soil composting using municipal solid waste on biodegradation of plastics. Indian Journal of Biotechnology. 2008;7:235-239.
[61] Zheng Y, Yanful EK, Bassi AS. A review of plastic waste biodegradation. Critical Reviews in Biotechnology. 2005;25:243-250.
[62] Mallakpour S, Banihassan K, Sabzalian MR. Novel bioactive chiral poly (amide–imide) s containing different amino acids linkages: studies on synthesis, characterization and biodegradability. Journal of Polymers and the Environment. 2013;21:568-574.
[63] Bardi MA, Munhoz MM, Auras RA, Machado LD. Assessment of UV exposure and aerobic biodegradation of poly (butylene adipate-co-terephthalate)/starch blend films coated with radiation-curable print inks containing degradation-promoting additives. Industrial Crops and Products. 2014;60:326-334.
[64] OCED 208. Terrestial plant growth test: OECD guidelines for Testing of Chemicals,1984.
[65] Gong P, Wilke B-M, Strozzi E, Fleischmann S. Evaluation and refinement of a continuous seed germination and early seedling growth test for the use in the ecotoxicological assessment of soils. Chemosphere. 2001;44:491-500.
[66] Rani M, Agarwal A, Negi YS. Chitosan based hydrogel polymeric beads–As drug delivery system. BioResources. 2010;5:2765-2807.
[67] Arkatkar A, Arutchelvi J, Sudhakar M, Bhaduri S, Uppara PV, Doble M. Approaches to enhance the biodegradation of polyolefins. The Open Environmental Engineering Journal. 2009;2:68-80.
[68] Central Pollution Control Board (CPCB), 2004. Management of Municipal Solid Wastes. New Delhi, India.
[69] Misra V, Pandey S. Hazardous waste, impact on health and environment for development of better waste management strategies in future in India. Environment International. 2005;31:417-431.
[70] Hamad K, Kaseem M, Deri F. Rheological and mechanical characterization of poly (lactic acid)/polypropylene polymer blends. Journal of Polymer Research. 2011;18:1799-1806.
[71] Czechowska-Biskup R, Rokita B, Lotfy S, Ulanski P, Rosiak JM. Degradation of chitosan and starch by 360-kHz ultrasound. Carbohydrate Polymers. 2005;60:175-184.
[72] Rosa D, Grillo D, Bardi M, Calil M, Guedes C, Ramires E, et al. Mechanical, thermal and morphological characterization of polypropylene/biodegradable polyester blends with additives. Polymer Testing. 2009;28:836-842.

[73] Scott G, Wiles DM. Programmed-life plastics from polyolefins: a new look at sustainability. Biomacromolecules. 2001;2:615-622.
[74] Avérous L, Fringant C, Moro L. Plasticized starch–cellulose interactions in polysaccharide composites. Polymer. 2001;42:6565-6572.
[75] Yu L, Dean K, Li L. Polymer blends and composites from renewable resources. Progress in Polymer Science. 2006;31:576-602.
[76] Al-Salem SM, Sharma BK, Khan AR, Arnold JC, Alston SM, Chandrasekaran SR, et al. Thermal Degradation Kinetics of Virgin Polypropylene (PP) and PP with Starch Blends Exposed to Natural Weathering. Industrial & Engineering Chemistry Research. 2017;56:5210-5220.
[77] Saffar A, Carreau PJ, Ajji A, Kamal MR. Development of polypropylene microporous hydrophilic membranes by blending with PP-g-MA and PP-g-AA. Journal of Membrane Science. 2014;462:50-61.
[78] Obasi H, Igwe I. Effects of native cassava starch and compatibilizer on biodegradable and tensile properties of polypropylene. American Journal of Engineering Research. 2014;3:96-104.
[79] Vasile C, Darie RN, Cheaburu-Yilmaz CN, Pricope G-M, Bracic M, Pamfil D, et al. Low density polyethylene–chitosan composites. Composites Part B: Engineering. 2013;55:314-323.
[80] Martínez-Camacho A, Cortez-Rocha M, Graciano-Verdugo A, Rodriguez-Felix F, Castillo-Ortega M, Burgos-Hernández A, et al. Extruded films of blended chitosan, low density polyethylene and ethylene acrylic acid. Carbohydrate Polymers. 2013;91:666-674.
[81] Kurek M, Brachais C-H, Nguimjeu CM, Bonnotte A, Voilley A, Galić K, et al. Structure and thermal properties of a chitosan coated polyethylene bilayer film. Polymer Degradation and Stability. 2012;97:1232-1240.
[82] Ghosh S, Chowdhury R, Bhattacharya P. Sustainability of cereal straws for the fermentative production of second generation biofuels: a review of the efficiency and economics of biochemical pretreatment processes. Applied Energy. 2017;198:284-298.
[83] Amri F, Husseinsyah S, Hussin K. Mechanical, morphological and thermal properties of chitosan filled polypropylene composites: The effect of binary modifying agents. Composites Part A: Applied Science and Manufacturing. 2013;46:89-95.
[84] Sunilkumar M, Francis T, Thachil ET, Sujith A. Low density polyethylene–chitosan composites: a study based on biodegradation. Chemical Engineering Journal. 2012;204:114-124.
[85] Chiaramonti D. Bioethanol: role and production technologies. Improvement of crop plants for industrial end uses: Springer, 2007, p.209-251.
[86] Kaczmarek H, Ołdak D, Malanowski P, Chaberska H. Effect of short wavelength UV-irradiation on ageing of polypropylene/cellulose compositions. Polymer Degradation and Stability. 2005;88:189-198.
[87] Martin O, Averous L. Poly (lactic acid): plasticization and properties of biodegradable multiphase systems. Polymer. 2001;42:6209-6219.
[88] Reddy N, Nama D, Yang Y. Polylactic acid/polypropylene polyblend fibers for better resistance to degradation. Polymer Degradation and Stability. 2008;93:233-241.
[89] Ebadi-Dehaghani H, Khonakdar HA, Barikani M, Jafari SH. Experimental and theoretical analyses of mechanical properties of PP/PLA/clay nanocomposites. Composites Part B: Engineering. 2015;69:133-144.

[90] Ploypetchara N, Suppakul P, Atong D, Pechyen C. Blend of polypropylene/poly (lactic acid) for medical packaging application: physicochemical, thermal, mechanical, and barrier properties. Energy Procedia. 2014;56:201-210.
[91] Choudhary P, Mohanty S, Nayak SK, Unnikrishnan L. Poly (L-lactide)/polypropylene blends: Evaluation of mechanical, thermal, and morphological characteristics. Journal of Applied Polymer Science. 2011;121:3223-3237.
[92] Yoo TW, Yoon HG, Choi SJ, Kim MS, Kim YH, Kim WN. Effects of compatibilizers on the mechanical properties and interfacial tension of polypropylene and poly (lactic acid) blends. Macromolecular Research. 2010;18:583-588.
[93] Basu D, Datta C, Banerjee A. Biodegradability, mechanical properties, melt flow index, and morphology of polypropylene/amylose/amylose-ester blends. Journal of Applied Polymer Science. 2002;85:1434-1442.
[94] Anderson KS, Hillmyer MA. Melt preparation and nucleation efficiency of polylactide stereocomplex crystallites. Polymer. 2006;47:2030-2035.
[95] Liu B, Jiang L, Liu H, Zhang J. Synergetic effect of dual compatibilizers on in situ formed poly (lactic acid)/soy protein composites. Industrial & Engineering Chemistry Research. 2010;49:6399-6406.
[96] Soni S, Gupta H, Kumar N, Nishad DK, Mittal G, Bhatnagar A. Biodegradable Biomaterials. Recent Patents on Biomedical Engineering. 2010;3:30-40.
[97] Jakubowicz I. Evaluation of degradability of biodegradable polyethylene (PE). Polymer Degradation and Stability. 2003;80:39-43.
[98] Konduri MK, Koteswarareddy G, Rohini Kumar D, Venkata Reddy B, Lakshmi Narasu M. Effect of pro-oxidants on biodegradation of polyethylene (LDPE) by indigenous fungal isolate, Aspergillus oryzae. Journal of Applied Polymer Science. 2011;120:3536-3545.
[99] Roy P, Surekha P, Rajagopal C, Chatterjee S, Choudhary V. Effect of benzil and cobalt stearate on the aging of low-density polyethylene films. Polymer Degradation and Stability. 2005;90:577-585.
[100] Roy P, Surekha P, Rajagopal C, Raman R, Choudhary V. Study on the degradation of low-density polyethylene in the presence of cobalt stearate and benzil. Journal of Applied Polymer Science. 2006;99:236-243.
[101] Burman L, Albertsson AC. Evaluation of long-term performance of antioxidants using pro-oxidants instead of thermal acceleration. Journal of Polymer Science Part A: Polymer Chemistry. 2005;43:4537-4546.
[102] Belfiore LA, Pires AT, Wang Y, Graham H, Ueda E. Transition-metal coordination in polymer blends and model systems. Macromolecules. 1992;25:1411-1419.
[103] Reddy M, Deighton M, Gupta RK, Bhattacharya S, Parthasarathy R. Biodegradation of oxo-biodegradable polyethylene. Journal of Applied Polymer Science. 2009;111:1426-1432.
[104] Ulutan S, Gilbert M. Mechanical properties of HDPE/magnesium hydroxide composites. Journal of Materials Science. 2000;35:2115-2120.
[105] Sun Y, Olsen P, Waag T, Krueger A, Steinmuller-Nethl D, Albertsson AC, et al. Disaggregation and Anionic Activation of Nanodiamonds Mediated by Sodium Hydride—A New Route to Functional Aliphatic Polyester-Based Nanodiamond Materials. Particle & Particle Systems Characterization. 2015;32:35-42.

[106] Roy P, Surekha P, Raman R, Rajagopal C. Investigating the role of metal oxidation state on the degradation behaviour of LDPE. Polymer Degradation and Stability. 2009;94:1033-1039.
[107] Muthukumar T, Aravinthan A, Mukesh D. Effect of environment on the degradation of starch and pro-oxidant blended polyolefins. Polymer Degradation and Stability. 2010;95:1988-1993.
[108] Koutny M, Sancelme M, Dabin C, Pichon N, Delort A-M, Lemaire J. Acquired biodegradability of polyethylenes containing pro-oxidant additives. Polymer Degradation and Stability. 2006;91:1495-1503.
[109] Fontanella S, Bonhomme S, Koutny M, Husarova L, Brusson J-M, Courdavault J-P, et al. Comparison of the biodegradability of various polyethylene films containing pro-oxidant additives. Polymer Degradation and Stability. 2010;95:1011-1021.
[110] Tabari HZ, Nourbakhsh A, Ashori A. Effects of nanoclay and coupling agent on the physico-mechanical, morphological, and thermal properties of wood flour/polypropylene composites. Polymer Engineering & Science. 2011;51:272-277.
[111] Dintcheva NT, Al-Malaika S, La Mantia FP. Effect of extrusion and photo-oxidation on polyethylene/clay nanocomposites. Polymer Degradation and Stability. 2009;94:1571-1588.
[112] Hapuarachchi TD, Peijs T, Bilotti E. Thermal degradation and flammability behavior of polypropylene/clay/carbon nanotube composite systems. Polymers for Advanced Technologies. 2013;24:331-338.
[113] Kumanayaka T, Parthasarathy R, Jollands M. Accelerating effect of montmorillonite on oxidative degradation of polyethylene nanocomposites. Polymer Degradation and Stability. 2010;95:672-676.
[114] Kwon OH, Nho YC. Radiation-induced graft polymerization of methyl methacrylate onto ultrahigh molecular weight polyethylene in the presence of a metallic salt and acid. Journal of Applied Polymer Science. 2002;86:2348-2356.
[115] Guan R. Study on compatibility of PP–STC blends functionalized by ultraviolet irradiation. Journal of Applied Polymer Science. 2000;77:96-103.
[116] Chaudhari C, Dubey K, Goel N, Bhardwaj Y, Varshney L. Correlation between surface energy and uptake behavior of radiation-grafted methacrylic acid-g-LDPE. Polymer Bulletin. 2012;69:779-793.
[117] Zhao J, Geuskens G. Surface modification of polymers VI. Thermal and radiochemical grafting of acrylamide on polyethylene and polystyrene. European Polymer Journal. 1999;35:2115-2123.
[118] Nasef MM, Hegazy ESA. Preparation and applications of ion exchange membranes by radiation-induced graft copolymerization of polar monomers onto non-polar films. Progress in Polymer Science. 2004;29:499-561.
[119] Lopérgolo L, Catalani L, Machado L, Rela P, Lugao A. Development of reinforced hydrogels—I. Radiation induced graft copolymerization of methylmethacrylate on non-woven polypropylene fabric. Radiation Physics and Chemistry. 2000;57:451-454.
[120] Kaur I, Gupta N, Kumari V. Swelling, ion uptake and biodegradation studies of PE film modified through radiation induced graft copolymerization. Radiation Physics and Chemistry. 2011;80:947-956.

[121] El-Arnaouty M, Abdel Ghaffar A, El Shafey H. Radiation-induced graft copolymerization of acrylic acid/acrylonitrile onto LDPE and PET films and its biodegradability. Journal of Applied Polymer Science. 2008;107:744-754.
[122] Clesceri LSG, A. E.; Trussell, R. R. . (Eds.) Standard methods for the examination of water and wastewater; American Public Health Association (APHA), American Water Works Association (AWWA), Water Pollution Control Federation (WPCF),: 17th Ed. Washington, DC, 1989.
[123] Haji A, Shoushtari AM, Abdouss M. RSM optimization of plasma initiated grafting of acrylic acid onto polypropylene nonwoven. Journal of Macromolecular Science, Part A. 2014;51:76-87.
[124] Anjum N, Gupta B, Riquet AM. Surface designing of polypropylene by critical monitoring of the grafting conditions: Structural investigations. Journal of Applied Polymer Science. 2006;101:772-778.
[125] Friedman HL. Kinetics of thermal degradation of char-forming plastics from thermogravimetry. Application to a phenolic plastic. Journal of Polymer Science Part C: Polymer Symposia.1964;5:183-195.
[126] Kissinger HE. Reaction kinetics in differential thermal analysis. Analytical chemistry. 1957;29:1702-1706.
[127] Flynn JH, Wall LA. General treatment of the thermogravimetry of polymers. Journal of Research of the National Bureau of Standard. 1966;70:487-523.
[128] Paik P, Kar KK. Kinetics of thermal degradation and estimation of lifetime for polypropylene particles: Effects of particle size. Polymer Degradation and Stability. 2008;93:24-35.
[129] Madhu G, Mandal DK, Bhunia H, Bajpai PK. Thermal degradation kinetics and lifetime of HDPE/PLLA/pro-oxidant blends. Journal of Polymer Engineering. 2016;36:1-15.
[130] Coats A, Redfern J. Kinetic parameters from thermogravimetric data. Nature. 1964;201:68-69.
[131] Ozawa T. A new method of analyzing thermogravimetric data. Bulletin of the Chemical Society of Japan. 1965;38:1881-1886.
[132] Vyazovkin S, Wight CA. Model-free and model-fitting approaches to kinetic analysis of isothermal and nonisothermal data. Thermochimica Acta. 1999;340:53-68.
[133] Premkumar T, Govindarajan S, Coles AE, Wight CA. Thermal decomposition kinetics of hydrazinium cerium 2, 3-pyrazinedicarboxylate hydrate: a new precursor for CeO_2. The Journal of Physical Chemistry B. 2005;109:6126-6129.
[134] Yu Y, Wang M, Gan W, Tao Q, Li S. Polymerization-induced viscoelastic phase separation in polyethersulfone-modified epoxy systems. The Journal of Physical Chemistry B. 2004;108:6208-6215.
[135] Kim S, Park JK. Characterization of thermal reaction by peak temperature and height of DTG curves. Thermochimica Acta. 1995;264:137-156.
[136] Toop DJ. Theory of life testing and use of thermogravimetric analysis to predict the thermal life of wire enamels. IEEE Transactions on Electrical Insulation. 1971;6:2-14.
[137] Gupta Y, Chakraborty A, Pandey G, Setua D. Thermal and thermooxidative degradation of engineering thermoplastics and life estimation. Journal of Applied Polymer Science. 2004;92:1737-1748.

[138] ASTM D. 5338 Standard Test Method for Determining Aerobic Biodegradation of Plastic Materials under Controlled Composting Conditions, Incorporating Thermophilic Temperatures. 2011.
[139] Aneja K. A textbook of basic and applied microbiology: New Age International, 2008.
[140] Mallakpour S, Dehghani M, Sabzalian MR. Green step-grow polymerization of biodegradable amino acid based diacids with 3, 5-diamino-N-(thiazole-2-yl) benzamide: characterization and study on bioactivity. Journal of Polymer Research. 2013;20:80-85.
[141] Myers RH, Montgomery DC, Anderson-Cook CM. Response surface methodology: process and product optimization using designed experiments: John Wiley & Sons, 2016.
[142] Mehrabani J, Noaparast M, Mousavi S, Dehghan R, Ghorbani A. Process optimization and modelling of sphalerite flotation from a low-grade Zn-Pb ore using response surface methodology. Separation and Purification Technology. 2010;72:242-249.
[143] Khayet M, Seman MA, Hilal N. Response surface modeling and optimization of composite nanofiltration modified membranes. Journal of Membrane Science. 2010;349:113-122.
[144] Lin B-T, Jean M-D, Chou J-H. Using response surface methodology for optimizing deposited partially stabilized zirconia in plasma spraying. Applied Surface Science. 2007;253:3254-3262.
[145] Barani H, Broumand MN, Haji A, Kazemipur M. Optimization of dyeing wool fibers procedure with Isatis tinctoria by response surface methodology. Journal of Natural Fibers. 2012;9:73-86.
[146] Mandal DK, Bhunia H, Bajpai PK, Chaudhari C, Dubey K, Varshney L. Radiation-induced grafting of acrylic acid onto polypropylene film and its biodegradability. Radiation Physics and Chemistry. 2016;123:37-45.
[147] Uflex IL. Films for pakaging application. http://www.flexfilm.com/CPP%20Films.aspx (accessed 18.03.2016). 1983.
[148] Naguib H, Aly R, Sabaa M, Mokhtar S. Gamma radiation induced graft copolymerization of vinylimidazole-acrylic acid ont**o** polypropylene films. Polymer Testing. 2003;22:825-830.
[149] Kovacik D, Zahoranová A, Černák M, Mazúr M. Surface modification of polypropylene non-woven fabrics by atmospheric-pressure plasma activation followed by acrylic acid grafting. Plasma Chemistry and Plasma Processing. 2005;25:427-437.
[150] Dong Z, Liu Z, Han B, He J, Jiang T, Yang G. Modification of isotactic polypropylene film by grafting of acrylic acid using supercritical CO_2 as a swelling agent. Journal of Materials Chemistry. 2002;12:3565-3569.
[151] Huang H, Zhu C, Zhou Z, Liu N. Melt grafting of a long-chain unsaturated carboxylic acid onto polypropylene. Reactive and Functional Polymers. 2002;50:49-55.
[152] Rao GS, Choudhary M, Naqvi M, Rao K. Functionalization of isotactic polypropylene with acrylic acid in the melt: synthesis, characterization and evaluation of thermomechanical properties. European Polymer Journal. 1996;32:695-700.
[153] Bidaux J-E, Smith GD, Bernet N, Månson J-AE, Hilborn J. Fusion bonding of maleic anhydride grafted polypropylene to polyamide 6 via in situ block copolymer formation at the interface. Polymer. 1996;37:1129-1136.
[154] Zhang X, Yin Z, Li L, Yin J. Grafting of glycidyl methacrylate onto ethylene-propylene copolymer: Preparation and characterization. Journal of Applied Polymer Science. 1996;61:2253-2257.

[155] Flores-Gallardo S, Sánchez-Valdes S, Valle D, Ramos L. Polypropylene /polypropylene-grafted acrylic acid blends for multilayer films: Preparation and characterization. Journal of Applied Polymer Science. 2001;79:1497-1505.
[156] Chen S, Wu G, Liu Y, Long D. Preparation of poly (acrylic acid) grafted multiwalled carbon nanotubes by a two-step irradiation technique. Macromolecules. 2006;39:330-334.
[157] Francis S, Dhanawade B, Mitra D, Varshney L, Sabharwal S. Radiation-induced grafting of diallyldimethylammonium chloride onto acrylic acid grafted polyethylene. Radiation Physics and Chemistry. 2009;78:42-47.
[158] Dalia El-Sayed H. Selectivity of Acrylic Acid Radiation Grafted Non-Woven Polypropylene Sheets towards Some Heavy Metals Ions. Open Journal of Polymer Chemistry. 2012;02:6-13.
[159] Tang W, Li XG, Yan D. Thermal decomposition kinetics of thermotropic copolyesters made from trans-p-hydroxycinnamic acid and p-hydroxybenzoic acid. Journal of Applied Polymer Science. 2004;91:445-454.
[160] Kiran N, Ekinci E, Snape C. Recyling of plastic wastes via pyrolysis. Resources, Conservation and Recycling. 2000;29:273-283.
[161] Heikkinen J, Hordijk J, de Jong W, Spliethoff H. Thermogravimetry as a tool to classify waste components to be used for energy generation. Journal of Analytical and Applied Pyrolysis. 2004;71:883-900.
[162] McCoy BJ. Distribution kinetics for temperature-programmed pyrolysis. Industrial & Engineering Chemistry Research. 1999;38:4531-4537.
[163] Koutny M, Lemaire J, Delort A-M. Biodegradation of polyethylene films with pro-oxidant additives. Chemosphere. 2006;64:1243-1252.
[164] Riga A, Collins R, Mlachak G. Oxidative behavior of polymers by thermogravimetric analysis, differential thermal analysis and pressure differential scanning calorimetry. Thermochimica Acta. 1998;324:135-149.
[165] Kim YF, Choi CN, Kim YD, Lee KY, Lee MS. Compatibilization of immiscible poly (l-lactide) and low density polyethylene blends. Fibers and Polymers. 2004;5:270-274.
[166] Zhou S, Chen Y, Zou H, Liang M. Thermally conductive composites obtained by flake graphite filling immiscible polyamide 6/polycarbonate blends. Thermochimica Acta. 2013;566:84-91.
[167] Madhu G, Bhunia H, Bajpai PK, Nando GB. Physico-mechanical properties and biodegradation of oxo-degradable HDPE/PLA blends. Polymer Science Series A. 2016;58:57-75.
[168] Montagna LS, da Camargo Forte MM, Santana RMC. Induced degradation of polypropylene with an organic pro-degradant additive. Journal of Materials Science and Engineering A. 2013;3:118-123.
[169] Santhoskumar A, Palanivelu K. A new additive formulation to enhance photo and biodegradation characteristics of polypropylene. International Journal of Polymeric Materials. 2012;61:793-808.
[170] Nourbakhsh A, Ashori A. Influence of nanoclay and coupling agent on the physical and mechanical properties of polypropylene/bagasse nanocomposite. Journal of Applied Polymer Science. 2009;112:1386-1390.
[171] De Abreu DP, Losada PP, Angulo I, Cruz J. Development of new polyolefin films with nanoclays for application in food packaging. European Polymer Journal. 2007;43:2229-2243.

[172] Perrin-Sarazin F, Ton-That M-T, Bureau M, Denault J. Micro-and nano-structure in polypropylene/clay nanocomposites. Polymer. 2005;46:11624-11634.
[173] Peterson JD, Vyazovkin S, Wight CA. Kinetics of the thermal and thermo-oxidative degradation of polystyrene, polyethylene and poly (propylene). Macromolecular Chemistry and Physics. 2001;202:775-784.
[174] Singala K, Mungray A, Mungray A. Degradation behavior of polypropylene–organically modified clay nanocomposites. Industrial & Engineering Chemistry Research. 2012;51:10557-10564.
[175] Tsuchiya Y, Sumi K. Thermal decomposition products of polypropylene. Journal of Polymer Science Part A: Polymer Chemistry. 1969;7:1599-1607.
[176] Lattimer RP. Pyrolysis field ionization mass spectrometry of polyolefins. Journal of Analytical and Applied Pyrolysis. 1995;31:203-225.
[177] Stotzky G, Rem L. Influence of clay minerals on microorganisms: I. Montmorillonite and kaolinite on bacteria. Canadian Journal of Microbiology. 1966;12:547-563.
[178] Stotzky G. Influence of clay minerals on microorganisms: III. Effect of particle size, cation exchange capacity, and surface area on bacteria. Canadian Journal of Microbiology. 1966;12:1235-1246.
[179] Stotzky G. Influence of clay minerals on microorganisms. II. Effect of various clay species, homionic clays, and other particles on bacteria. Canadian Journal of Microbiology. 1966;12:831-848.
[180] Marschner H. Mineral nutrition of higher plants, 2nd ed. Academic Press: UK, 1995.

Publications

I. In Peer Reviewed (SCI) Journals

1.1 Publications Related to Ph.D. Work

1. **Dev K. Mandal**, Haripada Bhunia, Pramod K. Bajpai, C. V. Chaudhari, K. A. Dubey and L. Varshney "Radiation-induced grafting of acrylic acid into polypropylene film and its biodegradability" *Radiation Physics and Chemistry* 2016, 123, 37-45 (Impact Factor: 1.315).
2. **Dev K. Mandal,** Haripada Bhunia, Pramod K. Bajpai, J. P. Khuswaha, C. V. Chaudhari, K. A. Dubey and L. Varshney "Optimization of acrylic acid grafting onto polypropylene using response surface methodology and its biodegradability" *Radiation Physics and Chemistry*. 2017, 132, 71-81 (Impact Factor: 1.315).
3. **Dev K. Mandal,** Haripada Bhunia, Pramod K. Bajpai and Vinod Kumar Bhalla "Thermal degradation kinetics and estimation of lifetime of simultaneous radiation induced acrylic acid grafted polypropylene" *Radiation Physics and Chemistry*. 2017, 136, 1-8 (Impact Factor: 1.315).
4. **Dev K. Mandal,** Haripada Bhunia, Pramod K. Bajpai, Chandrasekhar V. Chaudhari, Kumar A. Dubey and Lalit Varshney "Morphology, Rheology and Biodegradation of Oxo-degradable Polypropylene/Poly (lactic acid) blends" *Journal of Polymer Engineering.* (Accepted, DOI: 10.1515/polyeng-2016-0380) (Impact Factor: 0.631).
5. **Dev K. Mandal,** Haripada Bhunia, Pramod K. Bajpai, Anil Kumar, Gaurav Madhu and Golok B. Nando "Biodegradation of pro-oxidant filled polypropylene films and evaluation of the ecotoxicological impact" *Journal of Polymers and Environment*. 2018, 26, 1061-1071 (Impact Factor: 1.969).

1.2 Other Publications in the Related Area

1. **Dev K. Mandal,** Haripada Bhunia, Pramod K. Bajpai, Kumar A. Dubey, Lalit Varshney and Gaurav Madhu "Thermo-oxidative degradation kinetics of grafted polypropylene films" *Radiation Effects and Defects in Solids* 2017,172,1-8 (Impact Factor: 0.50).

2. G Madhu, **Dev K. Mandal,** H Bhunia, PK Bajpai "Thermal degradation kinetics and lifetime of high-density polyethylene/poly (l-lactic acid) blends" *Journal of Thermoplastic Composite Materials* 2017, 30, 773-793 (Impact Factor: 1.13).
3. G Madhu, **Dev K. Mandal,** H Bhunia, PK Bajpai "Thermal degradation kinetics and lifetime of HDPE/PLLA/pro-oxidant blends" *Journal of Polymer Engineering* 2016, 36, 917-931(Impact Factor: 0.631).

1.3 Under Review/ Communicated

1. **Dev K. Mandal,** Haripada Bhunia, Pramod K. Bajpai, Kumar A. Dubey and Lalit Varshney "Rheology, Biodegradation and Ecotoxicological impact of PP/PLA/nanoclay composite" *Polymer Bulletin* (Manuscript ID POBU-D-17-00821) (Under review) (Impact Factor: 1.43).
2. **Dev K. Mandal,** Haripada Bhunia, Pramod K. Bajpai, Kumar A. Dubey and Lalit Varshney "Thermo-oxidative degradation kinetics of PP/PLA/nanoclay composite" *Journal of Thermoplastic Composite Materials* (Manuscript ID JTCM-17-0284) (Under review) (Impact Factor: 1.13).

II. In Conferences

2.1 International Conference

1. **Dev K. Mandal,** H. Bhunia, Pramod K. Bajpai, C.V. Chaudhari, K.A. Dubey and L. Varshney "Biodegradable polypropylene: Optimization, biodegradability and evaluation of eco-toxicological impact" *International Conference on Applications of Radiation Science and Technology*, Vienna, Austria, April 24-28, 2017, p. 388.

2.2 National Conference

1. **Dev K. Mandal,** Gaurav Madhu, H. Bhunia, Pramod K. Bajpai, "Radiation grafting of polyolefins" *Proceedings of National Conference on Technological Advance in Chemical, Petroleum & Natural Gas Engineering*, Chandigarh University, April 10-11, 2015, p. 30.

2. **Dev K. Mandal,** H. Bhunia, Pramod K. Bajpai, "Grafting of acrylic acid onto polypropylene films by high energy radiation" *Proceedings of 2nd Conference on Microscopy in Materials Science*, Thapar Institute of Engineering & Technology (Deemed to be University), Patiala, February 25-27, 2016, p. 95.

3. **Dev K. Mandal,** H. Bhunia, Pramod K. Bajpai, "Radiation grafting of acrylic acid onto polypropylene films and its biodegradability" *Proceedings of Symposium on Application of Radioisotopes and Radiation Technology in Industry, Healthcare and Agriculture*, Thapar Institute of Engineering & Technology (Deemed to be University), Patiala, November 28-29, 2016, p. 71.

Dev K. Mandal, Haripada Bhunia*, Pramod K. Bajpai, Chandrasekhar V. Chaudhari, Kumar A. Dubey and Lalit Varshney

Morphology, rheology and biodegradation of oxo-degradable polypropylene/polylactide blends

DOI 10.1515/polyeng-2016-0380
Received November 11, 2016; accepted April 1, 2017

Abstract: The blends of polypropylene (PP)/polylactide (PLA) with or without compatibilizer, and with pro-oxidant (cobalt stearate/calcium stearate) and pro-oxidant filled PP were prepared by using the melt blending technique. Films of these blends were prepared by compression molding. PP85PL15 and PP85PL15MA4 were the optimum blends from the tensile strength point of view. The improvement in the tensile strength of PP85PL15MA4 blend was achieved by addition of 4 phr compatibilizer. Cobalt stearate and calcium stearate were added separately to PP85PL15MA4 blend in 0.2% (w/w) ratio. The optimized blends were further characterized by differential scanning calorimetry, X-ray diffraction, rheological studies, scanning electron microscopy (SEM) and biodegradability test. Rheological studies confirmed the pseudoplastic nature of all the blend samples. SEM studies have revealed that the addition of PLA in PP85PL15 enhances the void and roughness on the blend. All the prepared blends have biodegraded in the composting environment and the blend containing pro-oxidant biodegraded to the maximum extent.

Keywords: biodegradability; polylactide; polypropylene; pro-oxidant; rheology.

1 Introduction

Plastics are widely used in packaging, medical, agricultural, electrical, automobile and manufacturing industries due to their low cost and desirable physical, chemical, mechanical, thermal and electrical properties. But they are a big source of environmental problems. After the short-term use, they are thrown to landfill sites. They get accumulated in the environment at the rate of 60 million metric tons per year worldwide [1]. In India particularly, the figure of plastic waste generation was approximately 5.6 million metric tons per year in 2012 [2]. It is estimated that the plastic waste generation would rise to approximately 16.5 million metric tons by 2030, trebling every 10 years. India is the third largest consumer market (behind USA and China) for plastic goods with a consumption of 12.5 million metric tons per annum. After polyethylene (PE), polypropylene (PP) is an extensively used plastic material in the packaging industries like trash bag, food packaging etc. The hydrophobic nature, unavailability of functional groups and long chain of PP molecules resist microorganism attack and make it non-biodegradable. Short-term use and long-term functionality of PP create huge waste management problems. Recycling is one of the important processes to reduce plastic waste, but it is not efficient and produces inferior quality products. In the last two decades, researchers have been working on the degradation and biodegradation of PP. Degradation was improved by (1) blending with biodegradable natural polymers such as cellulose [3], starch [4–7], poly(lactic) acid [8, 9], poly(ε-caprolactone) [10], etc., (2) blending with stearate of transition metals and (3) isolation and identification of microorganisms capable of biodegradation [11].

Polylactide (PLA), a linear aliphatic polyester derived from biomass through bioconversion and polymerization, can be degraded upon disposal in biotic environment such as bacteria, algae, fungi, etc. [12]. However, inherent brittleness characteristics, high cost and limited shelf life restrict its use as a replacement of commercial synthetic packaging polymer materials. Many researchers have reported blending of PLA with linear low density polyethylene (LLDPE) [13, 14], high density polyethylene (HDPE) [15], PP [8, 9, 16, 17] and with other aliphatic polyesters such as poly(ε-caprolactone) [10, 18–20] and poly(hydroxybutyrate) [21–23]. Most of the blends of these polymers with PLA are partially immiscible and have poor mechanical properties. Addition of suitable compatibilizer is helpful in improving the miscibility and mechanical properties of these blends. Over the past decades,

*Corresponding author: Haripada Bhunia, Department of Chemical Engineering, Thapar University, Patiala 147004, Punjab, India, e-mail: hbhunia@thapar.edu
Dev K. Mandal and Pramod K. Bajpai: Department of Chemical Engineering, Thapar University, Patiala 147004, Punjab, India
Chandrasekhar V. Chaudhari, Kumar A. Dubey and Lalit Varshney: Radiation Technology Development Division, Bhabha Atomic Research Centre, Trombay, Mumbai 400085, India

J Polym Environ
DOI 10.1007/s10924-017-1016-3

ORIGINAL PAPER

Biodegradation of Pro-oxidant Filled Polypropylene Films and Evaluation of the Ecotoxicological Impact

Dev K. Mandal[1] · Haripada Bhunia[1] · Pramod K. Bajpai[1] · Anil Kumar[2] · Gaurav Madhu[3] · Golok B. Nando[4]

Abstract The biodegradability of calcium stearate (CaSt) and cobalt stearate (CoSt) filled polypropylene (PP) films were investigated in this work. The PP films were prepared using melt blending technique followed by hot press moulding. On the basis of their tensile properties, the optimum amount of pro-oxidants was taken as 0.2 phr. Fourier transform infrared spectroscopy (FTIR), thermogravimetric analysis (TGA) and differential scanning calorimetry (DSC) were used for the characterization of optimized films. Presence of pro-oxidant in the PP was confirmed by the FTIR studies. Addition of pro-oxidants in the films decreased the thermal stability as revealed by TGA analysis. Crystallinity of the pro-oxidant filled PP decreased with addition of pro-oxidants as shown by DSC. The maximum biodegradation of CaSt and CoSt containing PP films was showen 7.65 and 8.34%, respectively with 0.2 phr. Both the microbial test and plant growth test (on corn and tomato) indicated that biodegradation intermediates were non toxic.

Keywords Polypropylene · Pro-oxidant · Physico-mechanical · Biodegradability · Ecotoxicological impact

Electronic supplementary material The online version of this article (doi:10.1007/s10924-017-1016-3) contains supplementary material, which is available to authorized users.

✉ Haripada Bhunia
hbhunia@thapar.edu

[1] Department of Chemical Engineering, Thapar University, Patiala, Punjab 147004, India

[2] Department of Biotechnology, Thapar University, Patiala, Punjab 147004, India

[3] Indian Institute of Packaging, Andheri (East), Mumbai 400093, India

[4] Rubber Technology Centre, Indian Institute of Technology, Kharagpur, West Bengal 721302, India

Introduction

Polypropylenes (PP) are extensively used as a flexible packaging material e.g. trash bags due to its low cost, good mechanical strength, hydrophobic nature, chemical resistance, effective water and gas barrier properties and ease of processability [1]. PP are petroleum derived products mainly combination of carbon and hydrogen. High molecular weight and hydrophobic nature make it water resistance, inhibit to microbial attack, increase self life and highly resistance to degradation. Therefore, accumulation of PP in different land sites leading to long term economical, environmental and waste management problem. Recycling of PP is one of the best solutions for this but it produces inferior quality products. The environmental problem should be reduced by producing harmles material and by proper management of PP waste materials. So, the searching and studying of new composition of materials, that can enhance the degradation of PP by various means has become very demanding to manage such environmental problems [2, 3].

Pro-oxidants are basically transition metal ion complexes. They are added in the PP in the form of either stearates or other organic ligand complexes including thermal or photo oxidation. Iron stearate (Fe^{3+}), megnasium stearate (Mn^{2+}) and cobalt stearate (Co^{2+}) [4, 5] are the most used pro-oxidnats in the polyolefins. Among them, Fe^{3+} initiates photo oxidative degradation. Mn^{2+} and Co^{2+} initiate thermo oxidative degradation process and decreasing the molecular mass of PP to a level where microorganisms attack is possible. Pro-oxidant containing PP has demonstrated that the use of suitable pro-oxidant on the conventional low density

Published online: 10 April 2017

Radiation Physics and Chemistry 136 (2017) 1–8

Contents lists available at ScienceDirect

Radiation Physics and Chemistry

journal homepage: www.elsevier.com/locate/radphyschem

Thermal degradation kinetics and estimation of lifetime of radiation grafted polypropylene films

Dev K. Mandal[a], Haripada Bhunia[a,*], Pramod K. Bajpai[a], Vinod Kumar Bhalla[b]

[a] Department of Chemical Engineering, Thapar University, Patiala 147004, Punjab, India
[b] Department of Computer Science and Engineering, Thapar University, Patiala 147004, Punjab, India

ARTICLE INFO

Keywords:
Polypropylene
Acrylic acid
Radiation grafting
Thermal kinetics
Lifetime estimation

ABSTRACT

In this research work, thermal stability and degradation behavior of acrylic acid grafted polypropylene (PP-g-PAAc) films were investigated by using thermogravimetric (TGA) analysis at four different heating rates 5, 10, 15 and 20 °C/min over a temperature range of 40–550 °C in nitrogen atmosphere. The kinetic parameters namely activation energy (E_a), reaction order (n) and frequency factor (Z) were calculated by three multiple heating rate methods. The thermal stability of PP-g-PAAc films is found to decrease with increase in degree of grafting. The TGA data and thermal kinetic parameters were also used to predict the lifetime of grafted PP films. The estimated lifetime of neat PP as well as grafted PP decreased with increase in temperature by all the three methods. Studies also indicated that E_a and lifetime of PP-g-PAAc films decreased with increase in degree of grafting, which may also be helpful in biodegradation of grafted PP films.

1. Introduction

Polypropylene (PP) is one of the most extensively used plastic materials in flexible packaging application due to its low cost, recalcitrant nature, chemical resistance, effective water and gas barrier properties (Briassoulis et al., 2004). PP is a petroleum derived product, highly stable and takes long time for degradation. High molecular weight synthetic polypropylene containing largely carbon-carbon bond are generally resistance to biodegradation due to microbes are not accessible to them because their hydrophobic in nature. After use, packaging films are dumped in open sites or different landfills, which produce huge waste management problem. Incineration and burning of packaging films is associated with serious health hazards. The waste management problem should be reduced by production of less harmful packaging materials.

Biodegradable packaging films provide an excellent solution for waste management problem. These films can be easily biodegraded into small byproducts and microorganisms will consume it as an energy source. In the degradation process, plastics are reduced to low molecular weight products due to the environmental effects such as heat, sunlight, etc. and latter they are utilized by microorganisms as carbon source. Degradable packaging films are produced by blending of two or more polymers such as linear low density polyethylene (LLDPE) (Singh et al., 2012a, 2011, 2012b), high density polyethylene (HDPE) (Madhu et al., 2014), and polypropylene (PP) (Choudhary et al., 2011; Jain et al., 2015, 2014; Ying-Chen et al., 2010) with poly lactic acid (PLA).

PP films are hydrophobic in nature due to lack of chemical functionalities and non-polarity. These drawbacks can be removed by inserting functionality to the backbone with hydrophilic monomers through grafting. Grafting polymerization is a well-known method for the modification of chemical and physical properties of polymeric materials (Chaudhari et al., 2012). Polymeric materials with high functionality can be achieved by the introduction of ions or components that enhance the hydrophilicity of grafted polymers. Grafting copolymerization can be achieved using several methods namely photoradiation, thermal, enzymatic, chemical and gamma-radiation grafting (Mandal et al., 2016). Among these methods, gamma-radiation grafting has particular advantage due to its extensive penetration in the polymer matrix and rapid radical production to initiate the grafting polymerization. From our previous work (Mandal et al., 2016), it was found that the biodegradability of acrylic acid grafted PP did not significantly improve beyond 35% degree of grafting due to cross-linking on the surface. Now, there is a need to know the thermal stability and lifetime estimation of different degrees of grafted PP films with the help of thermal degradation kinetics parameters.

TGA method is an excellent way to study the thermal degradation kinetics. It provides information on activation energy (E_a), reaction order (n) and frequency factor (Z) by using various kinetic models such as (Friedman, 1964), (Kissinger, 1957), (Flynn and Wall, 1966), (Paik

* Corresponding author.
E-mail address: hbhunia@thapar.edu (H. Bhunia).

http://dx.doi.org/10.1016/j.radphyschem.2017.03.036
Received 6 December 2016; Received in revised form 4 March 2017; Accepted 21 March 2017
Available online 22 March 2017
0969-806X/

Radiation Physics and Chemistry 132 (2017) 71–81

Contents lists available at ScienceDirect

Radiation Physics and Chemistry

journal homepage: www.elsevier.com/locate/radphyschem

Optimization of acrylic acid grafting onto polypropylene using response surface methodology and its biodegradability

Dev K. Mandal[a], Haripada Bhunia[a,*], Pramod K. Bajpai[a], Jai P. Kushwaha[a], Chandrasekhar V. Chaudhari[b], Kumar A. Dubey[b], Lalit Varshney[b]

[a] Department of Chemical Engineering, Thapar University, Patiala 147004, Punjab, India
[b] Radiation Technology Development Division, Bhabha Atomic Research Centre, Trombay, Mumbai 400085, India

ARTICLE INFO

Keywords:
Acrylic acid
Biodegradability
Design of experiments
Polypropylene films
Radiation grafting
Response surface methodology

ABSTRACT

Simultaneous radiation grafting was optimized to graft acrylic acid monomer on the polypropylene (PP) films to make them hydrophilic and enhance their biodegradability. Experiments were designed based on full factorial central composite design (response surface methodology) and influence of monomer concentration, radiation dose, inhibitor concentration, solvent concentration on degree of grafting was investigated. The extent of grafting was found to increase with increasing monomer concentration, inhibitor concentration and radiation dose. The targeted 35% grafting could be achieved at optimum condition viz. monomer concentration 12.09 wt %, radiation dose 12.40 kGy, inhibitor concentration 0.07 M and solvent concentration 0.12 M. The grafted PP films at different degrees of grafting were tested for tensile properties and characterized by swelling studies, fourier transform infrared spectroscopy (FTIR), thermogravimetric analysis (TGA), differential scanning calorimetry (DSC) and scanning electron microscopy (SEM). Successful grafting of acrylic acid onto polypropylene films was indicated by FTIR and confirmed quantitatively by determination of carboxylic groups on the film surface. Tensile strength of grafted PP films decreased with increase in degree of grafting. The crystallinity of the grafted PP films was lower than that of PP film as indicated by DSC studies. Grafting of acrylic acid increased the roughness on the surface of PP films indicated by SEM studies. The maximum biodegradability of the 34.55% grafted film was 5.5%.

1. Introduction

Polypropylene (PP) is a synthetic polymeric material widely used in flexible packaging applications. However, it is non biodegradable due to the hydrophobic nature and unavailability of functional groups. After the short term use, PP films reach at open dumps, landfills, or as simple litter. Incineration of polypropylene wastes are not free from toxic compounds such as furan and recycling of plastic waste is not reducing the waste disposal problems. The waste disposal problems should be reduced by proper waste management of packaging waste and production of less harmful packaging films. Searching and studying of new alternative materials, which can be used for environment friendly packaging application (Kaczmarek et al., 2005).

Great hopes for the packaging industries are connected with biodegradable packaging films. Biodegradable polymers are disintegrate due to the hydrolysis of polymer chains by the action of microbes into monomers or water and carbon dioxide (Yoo et al., 2010). There have been many researches on the preparation of partially degradable polymer blends by blending of poly(lactic acid) with conventional polymers such as linear low density polyethylene (LLDPE) (Singh et al., 2012), high density polyethylene (HDPE) (Madhu et al., 2014), and polypropylene (PP) (Jain et al., 2015). However, there has been very little effort on the degradability study of polymers produced by grafting polymerization methods. Polyethylene film grafted acrylamide/methacrylic acid (AAm)/(MAAc) showed degradability up to 47% within 50 days in soil burial test (Kaur et al., 2011). Soil burial test was confirmed that the degradability of acrylic acid/acrylonitrile grafted low density polyethylene (LDPE-*g*-AAc/AN) due to the high concentration of AAc (El-Arnaouty et al., 2008).

Grafting polymerization is highly popular method for the modification of shape, size and structure of polymeric materials. Grafting copolymerization can be achieved by various methods, viz. chemical means (Kwon and Nho, 2002), photoradiation (Guan, 2000), γ-radiation (Chaudhari et al., 2012), and thermal (Zhao and Geuskens, 1999). Among these techniques, γ-radiation grafting copolymerization is one of the most important techniques due to its rapid formation of free

* Corresponding author.
E-mail address: hbhunia@thapar.edu (H. Bhunia).

http://dx.doi.org/10.1016/j.radphyschem.2016.12.003
Received 21 March 2016; Received in revised form 1 December 2016; Accepted 3 December 2016
Available online 08 December 2016
0969-806X/

Radiation Physics and Chemistry 123 (2016) 37–45

Contents lists available at ScienceDirect

Radiation Physics and Chemistry

journal homepage: www.elsevier.com/locate/radphyschem

Radiation-induced grafting of acrylic acid onto polypropylene film and its biodegradability

Dev K. Mandal [a], Haripada Bhunia [a,*], Pramod K. Bajpai [a], C.V. Chaudhari [b], K.A. Dubey [b], L. Varshney [b]

[a] Chemical Engineering Department, Thapar University, Patiala 147004, Punjab, India
[b] Radiation Technology Development Division, Bhabha Atomic Research Centre, Trombay, Mumbai 400085, India

HIGHLIGHTS

- Partially biodegradable polymer films from AAc-g-PP were prepared.
- Swelling behavior, FTIR, DSC, TGA, SEM and XRD studied.
- Effect of monomer concentration, inhibitor concentration, doses and dose rate on the degree of grafting studied.
- Biodegradability of the original and grafted PP samples was calculated by ASTM D 5338-11 standard.

ARTICLE INFO

Article history:
Received 31 July 2015
Received in revised form
22 November 2015
Accepted 6 February 2016
Available online 10 February 2016

Keywords:
Polypropylene
Acrylic acid
Radiation grafting
Biodegradability

ABSTRACT

Polypropylene based commodity polyolefins are widely used in packaging, manufacturing, electrical, pharmaceutical and other applications. The aim of the present work is to study the effect of grafting of acrylic acid on the biodegradability of acrylic acid grafted polypropylene. The effect of different conditions showed that grafting percentage increased with increase in monomer concentration, radiation dose and inhibitor concentration but decreased with increase in radiation dose rate. The maximum grafting of 159.4% could be achieved at optimum conditions. The structure of grafted polypropylene films at different degree of grafting was characterized by EDS, FTIR, TGA, DSC, SEM and XRD. EDS studies showed that the increase in acrylic acid grafting percentage increased the hydrophilicity of the grafted films. FTIR studies indicated the presence of acrylic acid on the surface of polypropylene film. TGA studies revealed that thermal stability decreased with increase in grafting percentage. DSC studies showed that melting temperature and crystallinity of the grafted polypropylene films lower than polypropylene film. SEM studies indicated that increase in acrylic acid grafting percentage increased the wrinkles in the grafted films. The maximum biodegradability could be achieved to 6.85% for 90.5% grafting. This suggested that microorganisms present in the compost could biodegrade acrylic acid grafted polypropylene.

1. Introduction

Polyolefins include low-density polyethylene (LDPE), high density polyethylene (HDPE), and polypropylenes (PP). They are long chains of carbon and hydrogen, petrochemical derived products and used in the application of automobile, electrical, agricultural, pharmaceutical, medical, packaging, etc. Polypropylenes are used in commercial applications due to their high molecular weight, low cost, good mechanical properties and ease of processability. High molecular weight and hydrophobic nature of polypropylene increases its resistance to microorganisms activity, hence non-biodegradability. Polypropylenes are highly stable to the environmental affects and have long life, it take several decades for the degradation (Montagna et al., 2013). Recycling of polyolefins is the one important solution but it produces inferior quality materials. So, the degradation of these polyolefins is in demand to control plastic waste problem (Madhu et al., 2014).

Degradability of polyolefins is improved by mixing of biodegradable polymers such as cellulose, starch and vegetable oil (Islam et al., 2011), or addition of pro-oxidants like stearate (St) complexes of transition metals such as iron stearate (FeSt), magnesium stearate (MnSt) and cobalt stearate (CoSt) (Konduri et al., 2011), which accelerate the degradation process. There were

* Corresponding author.
E-mail address: hbhunia@thapar.edu (H. Bhunia).

http://dx.doi.org/10.1016/j.radphyschem.2016.02.011
0969-806X/